ISSN 1916-6117 [online]
ISBN 978-1-4249-6867-1 [PDF]

ISSN 0826-9580 [print]
ISBN 978-1-4249-6866-4 [print]

THESE TERMS GOVERN YOUR USE OF THIS DOCUMENT

Your use of this Ontario Geological Survey document (the "Content") is governed by the terms set out on this page ("Terms of Use"). By downloading this Content, you (the "User") have accepted, and have agreed to be bound by, the Terms of Use.

Content: This Content is offered by the Province of Ontario's *Ministry of Northern Development and Mines* (MNDM) as a public service, on an "as-is" basis. Recommendations and statements of opinion expressed in the Content are those of the author or authors and are not to be construed as statement of government policy. You are solely responsible for your use of the Content. You should not rely on the Content for legal advice nor as authoritative in your particular circumstances. Users should verify the accuracy and applicability of any Content before acting on it. MNDM does not guarantee, or make any warranty express or implied, that the Content is current, accurate, complete or reliable. MNDM is not responsible for any damage however caused, which results, directly or indirectly, from your use of the Content. MNDM assumes no legal liability or responsibility for the Content whatsoever.

Links to Other Web Sites: This Content may contain links, to Web sites that are not operated by MNDM. Linked Web sites may not be available in French. MNDM neither endorses nor assumes any responsibility for the safety, accuracy or availability of linked Web sites or the information contained on them. The linked Web sites, their operation and content are the responsibility of the person or entity for which they were created or maintained (the "Owner"). Both your use of a linked Web site, and your right to use or reproduce information or materials from a linked Web site, are subject to the terms of use governing that particular Web site. Any comments or inquiries regarding a linked Web site must be directed to its Owner.

Copyright: Canadian and international intellectual property laws protect the Content. Unless otherwise indicated, copyright is held by the Queen's Printer for Ontario.

It is recommended that reference to the Content be made in the following form:

Houlé, M.G., Ayer, J.A., Baldwin, G., Berger, B.R., Dinel, E., Fowler, A.D., Moulton, B., Saumur, B.-M. and Thurston, P.C. 2008. Field trip guidebook to the stratigraphy and volcanology of supracrustal assemblages hosting base metal and gold mineralization in the Abitibi greenstone belt, Timmins, Ontario; Ontario Geological Survey, Open File Report 6225, 84p.

Use and Reproduction of Content: The Content may be used and reproduced only in accordance with applicable intellectual property laws. *Non-commercial* use of unsubstantial excerpts of the Content is permitted provided that appropriate credit is given and Crown copyright is acknowledged. Any substantial reproduction of the Content or any *commercial* use of all or part of the Content is prohibited without the prior written permission of MNDM. Substantial reproduction includes the reproduction of any illustration or figure, such as, but not limited to graphs, charts and maps. Commercial use includes commercial distribution of the Content, the reproduction of multiple copies of the Content for any purpose whether or not commercial, use of the Content in commercial publications, and the creation of value-added products using the Content.

Contact:

FOR FURTHER INFORMATION ON	PLEASE CONTACT:	BY TELEPHONE:	BY E-MAIL:
The Reproduction of Content	MNDM Publication Services	Local: (705) 670-5691 Toll Free: 1-888-415-9845, ext. 5691 (inside Canada, United States)	pubsales.ndm@ontario.ca
The Purchase of MNDM Publications	MNDM Publication Sales	Local: (705) 670-5691 Toll Free: 1-888-415-9845, ext. 5691 (inside Canada, United States)	pubsales.ndm@ontario.ca
Crown Copyright	Queen's Printer	Local: (416) 326-2678 Toll Free: 1-800-668-9938 (inside Canada, United States)	copyright@gov.on.ca

Ontario

Ontario Geological Survey
Open File Report 6225

Field Trip Guidebook to the Stratigraphy and Volcanology of Supracrustal Assemblages Hosting Base Metal and Gold Mineralization in the Abitibi Greenstone Belt, Timmins, Ontario

2008

Ontario

ONTARIO GEOLOGICAL SURVEY

Open File Report 6225

Field Trip Guidebook to the Stratigraphy and Volcanology of Supracrustal Assemblages Hosting Base Metal and Gold Mineralization in the Abitibi Greenstone Belt, Timmins, Ontario

by

M.G. Houlé, J.A. Ayer, G. Baldwin, B.R. Berger, E. Dinel, A.D. Fowler, B. Moulton, B.-M. Saumur and P.C. Thurston

2008

Houlé, M.G., Ayer, J.A., Baldwin, G., Berger, B.R., Dinel, E., Fowler, A.D., Moulton, B., Saumur, B.-M. and Thurston, P.C. 2008. Field trip guidebook to the stratigraphy and volcanology of supracrustal assemblages hosting base metal and gold mineralization in the Abitibi greenstone belt, Timmins, Ontario; Ontario Geological Survey, Open File Report 6225, 84p.

This product was produced as part of the Targeted Geoscience Initiative-3 (TGI-3) Abitibi Project of Natural Resources Canada and is a contribution to the TGI-3 Program of the Earth Sciences Sector.

Ce produit s'inscrit dans le cadre du projet IGC-3 Abitibi de Ressources naturelles Canada et est une contribution au programme de l'Initiative géoscientifique ciblée (IGC-3) du secteur des sciences de la Terre.

Natural Resources Canada | Ressources naturelles Canada

Open File Reports of the Ontario Geological Survey are available for viewing at the John B. Gammon Geoscience Library in Sudbury, at the Mines and Minerals Information Centre in Toronto, and at the regional Mines and Minerals office whose district includes the area covered by the report (see below). Free downloads are available at MNDM's *GeologyOntario* Web site.

Copies can be purchased at Publication Sales and the office whose district includes the area covered by the report. Although a particular report may not be in stock at locations other than the Publication Sales office in Sudbury, they can generally be obtained within 3 working days. All telephone, fax, mail and e-mail orders should be directed to the Publication Sales office in Sudbury. Use of VISA or MasterCard ensures the fastest possible service. Cheques or money orders should be made payable to the *Minister of Finance.*

Mines and Minerals Information Centre (MMIC) Macdonald Block, Room M2-17 900 Bay St. Toronto, Ontario M7A 1C3	Tel:	(416) 314-3800
John B. Gammon Geoscience Library 933 Ramsey Lake Road, Level A3 Sudbury, Ontario P3E 6B5	Tel:	(705) 670-5615
Publication Sales 933 Ramsey Lake Rd., Level A3 Sudbury, Ontario P3E 6B5	Tel: Fax: E-mail:	(705) 670-5691(local) 1-888-415-9845(toll-free) (705) 670-5770 pubsales.ndm@ontario.ca

Regional Mines and Minerals Offices:

Kenora - Suite 104, 810 Robertson St., Kenora P9N 4J2
Kirkland Lake - 10 Government Rd. E., Kirkland Lake P2N 1A8
Red Lake - Box 324, Ontario Government Building, Red Lake P0V 2M0
Sault Ste. Marie - 70 Foster Dr., Ste. 200, Sault Ste. Marie P6A 6V8
Southern Ontario - P.O. Bag Service 43, 126 Old Troy Rd., Tweed K0K 3J0
Sudbury - Level A3, 933 Ramsey Lake Rd., Sudbury P3E 6B5
Thunder Bay - Suite B002, 435 James St. S., Thunder Bay P7E 6S7
Timmins - Ontario Government Complex, P.O. Bag 3060, Hwy. 101 East, South Porcupine P0N 1H0
Toronto - MMIC, Macdonald Block, Room M2-17, 900 Bay St., Toronto M7A 1C3

Cette publication est disponible en anglais seulement.

Parts of this report may be quoted if credit is given. It is recommended that reference to the entire report be made in the following form:

Houlé, M.G., Ayer, J.A., Baldwin, G., Berger, B.R., Dinel, E., Fowler, A.D., Moulton, B., Saumur, B.-M. and Thurston, P.C. 2008. Field trip guidebook to the stratigraphy and volcanology of supracrustal assemblages hosting base metal and gold mineralization in the Abitibi greenstone belt, Timmins, Ontario; Ontario Geological Survey, Open File Report 6225, 84p.

To reference parts of the report, the following is recommended:

Houlé, M.G., Baldwin, G. and Thurston, P.C. 2008. Day 3: Physical volcanology of the Bartlett dome; *in* Field Trip Guidebook to the Stratigraphy and Volcanology of Supracrustal Assemblages Hosting Base Metal and Gold Mineralization in the Abitibi Greenstone Belt, Timmins, Ontario, Ontario Geological Survey, Open File Report 6225, p.59-73.

Contents

FIGURES

PHOTOS

TABLES

Abstract

This contribution provides an update and summarizes recent advances on the physical volcanology, stratigraphy, geochronology and host rocks controls on metallic mineralization within the Abitibi greenstone belt (AGB) in Ontario. The work was done in collaboration between the Ontario Geological Survey (OGS) and the Geological Survey of Canada (GSC) as part of Abitibi Targeted Geoscience Initiative III (TGI-3) program.

The trip provides new insights on the stratigraphic framework and the physical volcanology of the Deloro (2730-2724 Ma), Kidd–Munro (2719-2711 Ma) and Tisdale (2710-2704 Ma) assemblages based on new regional and detailed geological mapping, geophysical surveys, and recent geochronology within three areas in the Timmins region. It provides an update on the geology and stratigraphy, and field descriptions of: 1) the Porcupine gold camp and the Shaw Dome area; 2) the Munro Township area; and 3) the Bartlett Dome area.

The first transect (Day 1) is focused on Archean stratigraphy and physical volcanology on both sides of the Porcupine–Destor deformation zone (PDDZ) around Timmins. The V10B and V8 units of the Vipond formation, part of the Tisdale assemblage north of the PDDZ, will be examined for their volcanological features and possible influence on localizing gold mineralization within the well-known Porcupine gold camp. The physical volcanology and stratigraphic framework for komatiites within the Tisdale assemblage and their important relationships to the genesis and location of magmatic Ni-Cu-(PGE) deposits in the Shaw Dome area will be examined south of the PDDZ.

The second transect (Day 2) is focused on Munro Township approximately 100 km east of Timmins. This transect will highlight our new understanding of the Kidd–Munro stratigraphy from Kidd Creek to the Québec border. The upper stratigraphic part of the Kidd–Munro assemblage will be examined around the Potter Mine to better understand this unique VMS-style Cu-Zn deposit. The Potter Mine is hosted within a thick komatiitic-basaltic volcanic succession with numerous well exposed volcanological features in the units spatially associated with the deposit. The lower stratigraphic part of the Kidd–Munro assemblage will also be examined in southern Munro Township where felsic and mafic volcanic units with interesting volcanological features will be examined and discussed in regard to the base metal potential of this part of the stratigraphy.

The third transect (Day 3) is focused on Archean stratigraphy and physical volcanology within the Bartlett Dome (~35 km south of Timmins), an area of transition from the Deloro assemblage (2730-2724 Ma) into the unconformably overlying Tisdale assemblage (2710-2704 Ma). The upper Deloro is characterized by sedimentary interface zones (SIZ) that consist of sedimentary-dominated intervals composed of extensive chemical sediments (i.e., iron formations), minor clastic sedimentary rocks and intercalated volcanic rocks. The base of the Tisdale will also be examined where komatiite flows host Ni-Cu-(PGE) mineralization at the Texmont Mine immediately overlying the uppermost iron formation of the Deloro assemblage.

Field Trip Guidebook to the Stratigraphy and Volcanology of Supracrustal Assemblages Hosting Base Metal and Gold Mineralization in the Abitibi Greenstone Belt, Timmins, Ontario

M.G. Houlé[1], J.A. Ayer[1], G. Baldwin[2], B.R. Berger[1], E. Dinel[3,4,5], A.D. Fowler[3], B. Moulton[3], B.-M. Saumur[3] and P.C. Thurston[2]

Ontario Geological Survey
Open File Report 6225
2008

---

[1] Precambrian Geoscience Section, Ontario Geological Survey, Sudbury, Ontario
[2] Department of Earth Sciences, Laurentian University, Sudbury, Ontario
[3] Department of Earth Sciences, University of Ottawa, Ottawa, Ontario
[4] Natural Resources Canada, Geological Survey of Canada, Ottawa, Ontario
[5] Department of Geology, University of Toronto, Toronto, Ontario

Introduction

by J.A. Ayer, M.G. Houlé and P.C. Thurston

The Abitibi greenstone belt (AGB), located within the southern part of the Superior Province (Figure 1), is one of the largest Archean granite-greenstone belts in the world with prolific mineral endowment including world-class orogenic lode gold deposits, world-class volcanic-associated Cu-Zn-(Pb) massive sulphide deposits (VMS), and economically significant magmatic Ni-Cu-(PGE) deposits. Supracrustal successions within the AGB are complex associations of volcanic rocks, clastic and chemical sedimentary rocks intruded by multiple phases of tonalite-trondhjemite-granodiorite suites (TTG).

This guidebook was prepared initially for use with Field Trip B4 held in conjunction with the Geological Association of Canada–Mineralogical Association of Canada joint annual meeting in Québec City, May 26 to 28, 2008. This contribution provides an update and summarizes recent advances on the physical volcanology, stratigraphy, and host rock controls on metallic mineralization acquired in collaboration between the Precambrian Geoscience Section (PGS) of the Ontario Geological Survey (OGS) and the Geological Survey of Canada (GSC) as part of Abitibi project under the Targeted Geoscience Initiative III (TGI-3) program. It also benefits from previous collaboration between the PGS-OGS, Laurentian University (LU) as part of the Greenstone Architecture project of Discover Abitibi and more recently as graduate research projects on komatiites (M. Houlé's PhD at University of Ottawa [UO] and LU), on iron formation (G. Baldwin's MSc at LU) and on rhyolites (B. Moulton's MSc at UO).

Stratigraphic models of the physical volcanology of Abitibi greenstone belt units have evolved over the years based on numerous detailed and regional geological mapping projects, geophysical surveys, and extensive geochronology throughout the belt. The stratigraphy and volcanology is presented during this field trip via three main transects through the Kidd–Munro (2719-2711 Ma) and Tisdale (2710-2704 Ma) assemblages (Figure 2):

- Stratigraphy and volcanology of the Timmins area (Day 1)
- Stratigraphy and volcanology of Munro Township (Day 2)
- Stratigraphy and volcanology of the Bartlett Dome area (Day 3)

New insights on Archean stratigraphy and volcanology of the AGB presented herein emphasise the relationship of volcanic rocks and mineral deposits such as komatiite-associated Ni-Cu-(PGE), Cu-Zn VMS and lode gold deposits within the Kidd–Munro and Tisdale assemblages, two metallogenically important lithostratigraphic assemblages within the Ontario portion of the Abitibi greenstone belt. Despite the fact that komatiites, variolitic basalts, pillow-lobe dacites and rhyolites represent minor components of these assemblages, they are important hosts for many of these deposits and thus represent stratigraphic markers useful as an exploration tool for identifying prospective areas. The physical volcanology and sea-floor processes in these assemblages is assessed within an overall stratigraphic framework derived from a combination of detailed geological mapping and over 200 highly precise U-Pb zircon ages conducted over several decades.

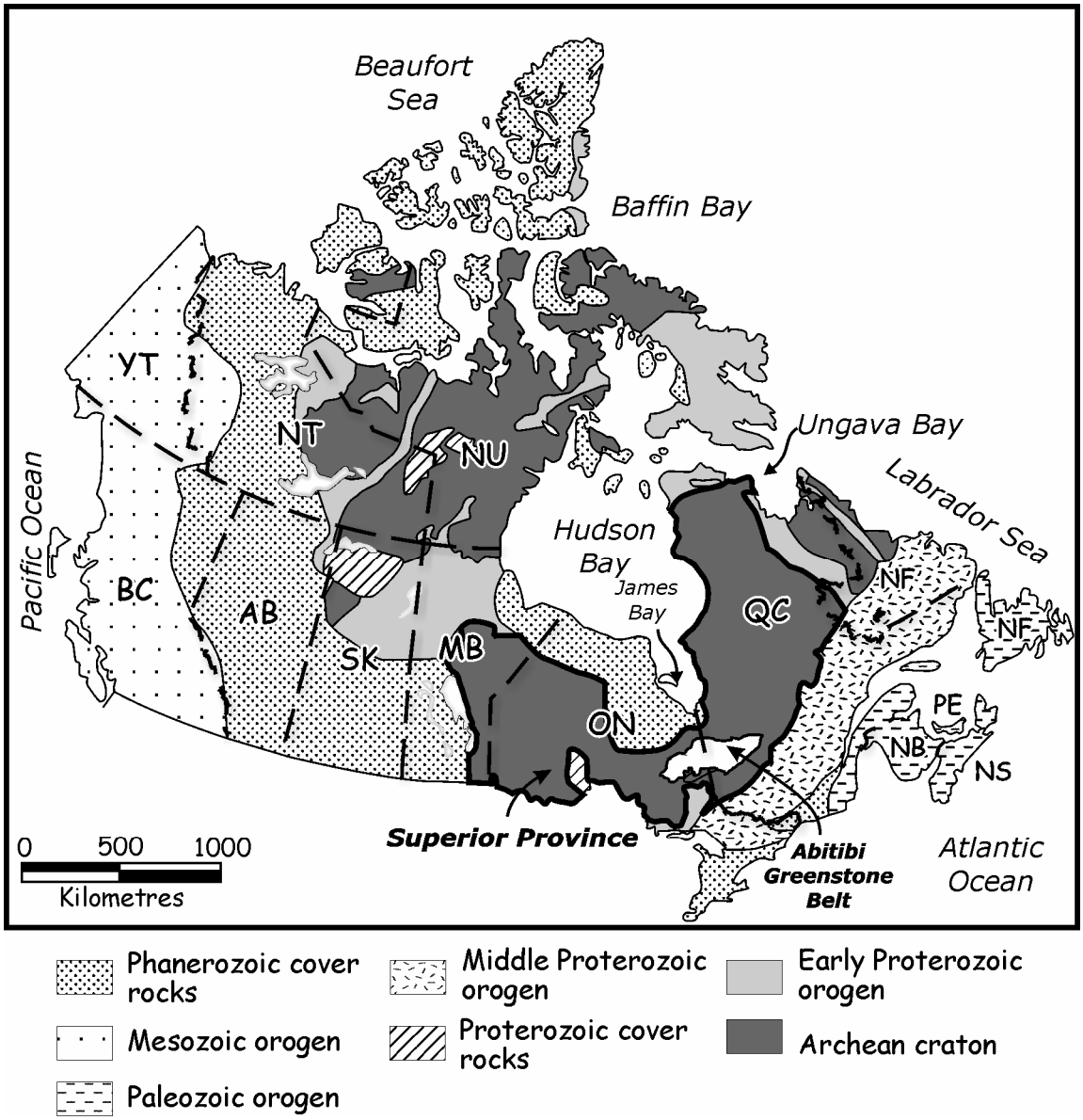

Figure 1. Tectonic map of Canada showing the location of the Abitibi greenstone belt within the Superior Province. Abbreviations: NF = Newfoundland and Labrador; PE = Prince Edward Island; NS = Nova Scotia; NB = New Brunswick; QC = Québec; ON = Ontario; MB = Manitoba; SK = Saskatchewan; AB = Alberta; BC = British Columbia; NU = Nunavut; NT = Northwest Territories; YT = Yukon.

SAFETY

For users of this guidebook, please bear in mind that some of the stops listed in this guidebook involve hiking in the bush. Therefore, standard bush safety practices should be followed. Such practices include wearing appropriate footwear; travelling with a group or in pairs; advising others of your starting time, location and expected return time; carrying sufficient water for the trip; being prepared for sudden changes in the weather; and carrying the appropriate emergency and safety gear. Most of the trip routes are on Crown land, but access is on or near private property for some routes. As in all such situations, please respect the property rights of others, so that future access for other geologists is not adversely affected.

Table 1. Agenda and itinerary for Field Trip B4, held in conjunction with the Geological Association of Canada–Mineralogical Association of Canada joint annual meeting in Québec City, May 26 to 28, 2008.

Thursday May 29th		Participant arrivals in Timmins, Ontario
Friday May 30th	***AM***	Physical volcanology of the Timmins area
		Trip Leader: A.D. Fowler
		Physical volcanology of the Shaw Dome area
		Trip Leader: M.G. Houlé
	PM	Physical volcanology of the Shaw Dome area (cont'd)
		Trip Leader: M.G. Houlé
	Evening	Talks – various topics related to the focus of the trip
Saturday May 31st	***AM***	Physical volcanology of Munro Township
		Trip Leaders: M.G. Houlé and A.D. Fowler
	Lunch	Core layout with Dave Gamble (Millstream Mines Ltd.) and M. Houlé
	PM	Physical volcanology of Munro Township (cont'd)
		Trip Leaders: A.D. Fowler and B. Moulton
Sunday June 1st	***AM***	Physical volcanology of the Bartlett Dome (McArthur Township)
		Trip Leaders: M.G. Houlé, G. Baldwin and P.C. Thurston
	PM	Physical volcanology of the Bartlett Dome (Bartlett and English townships)
		Trip Leaders: G. Baldwin, M.G. Houlé, and P.C. Thurston
	Evening	End of the trip

ACKNOWLEDGMENTS

Brian Atkinson, the Timmins Regional Resident Geologist with the Ontario Geological Survey, is thanked for helping with logistics and accompanying the trip as a co-leader. The authors would like to acknowledge work conducted under the Greenstone Architecture Project of the Discover Abitibi Initiative (H. Gibson, B. Hathway, S. Hocker, P. MacDonald, S. Péloquin, and S. Piercey) and currently being conducted under the Abitibi Targeted Geoscience Initiative phase III (W. Bleeker, B. Dubé, J. Goutier, V. McNicoll, P. Mercier-Langevin and O. van Breemen) for providing scientific input, new geological information and geochronology. The authors acknowledge the contributions by Liberty Mines Inc. (W. Randall, T. Dunnett), Millstream Mines Ltd. (E. Harrison, D. Gamble), and Fletcher Nickel Inc. (D. Beilhartz, E. Giguère) for access to, and information on, the geology and mineralization of the Hart Nickel Deposit, the Potter Mine, and the Texmont Mine, respectively. The authors thank J. Chartrand for drafting assistance with the figures in this guidebook.

ABITIBI GREENSTONE BELT

The Abitibi greenstone belt (AGB) lies in the eastern part of the Wawa–Abitibi Subprovince of the southern Superior Province (Figure 1). The belt has long been central to understanding greenstone belt mineral deposits (e.g., Goodwin 1965). The AGB has had a total mineral production of approximately $120 billion, derived from world-class and smaller sized deposits such as volcanogenic massive sulphide (VMS) deposits, gold-rich VMS deposits, Ni-Cu-(PGE) deposits, and epigenetic gold deposits (Table 2).

Table 2. Distribution of the main camps, mines or deposits throughout the Abitibi greenstone belt.

Deposit Type	Camp/Mine/Deposit	Ass.-Aged	General References
VMS			
	Gemini-Turgeon (12)	Pacaud	Franklin et al. 2005
	Shunsby (1)	Deloro	Heather 1998
	Normetal (13)	Deloro	Franklin et al. 2005
	Selbaie (16)	Deloro	Franklin et al. 2005
	Joutel (20)	Deloro	Franklin et al. 2005
	Matagami (22)	Deloro	Franklin et al. 2005
	Kidd Creek (4)	Kidd–Munro	Hannington et al. 1999
	Potter (10)	Kidd–Munro	Gibson and Gamble 2000
	Langlois (26)	Kidd–Munro	Franklin et al. 2005
	Louvicourt (24)	Tisdale	Franklin et al. 2005
	Kam-kotia (3)	Blake River	Franklin et al. 2005
	Noranda (14)	Blake River	Gibson and Watkinson 1990
Au-rich VMS			
	Estrades (17)	Stoughton–Roquemaure	Franklin et al. 2005
	Lemoine (25)	Kidd–Munro	Franklin et al. 2005
	Horne (15)	Blake River	
	La Ronde–Penna (19)	Blake River	Mercier-Langevin et al. 2007a, 2007b; Dubé et al. 2007
Ni-Cu-(PGE)			
Komatiite-Associated			
	Kanichee	Stoughton–Roquemaure?	Hawke 1982; Good 1989
	Dundonald (9)	Kidd–Munro	Houlé et al., in press; Barrie et al. 1999
	Dumont (18)	Kidd–Munro?	Duke 1986
	Marbridge (21)	Kidd–Munro	Giovenazzo 2000
	Sothman (6)	Tisdale	Coad 1979
	Texmont (7)	Tisdale	Coad 1979
	Shaw Dome (8)	Tisdale	Coad 1979
Gabbro-Associated			
	Temagami Island Copper	Pacaud	Simony 1964
	Montcalm (2)	Blake River	Barrie et al. 1990
Epigenetic Au			
	Timmins (5)		Bateman et al. 2005
	Kirkland Lake (11)		Ispolatov et al. 2005
	Sigma–Lamaque (23)		Robert and Brown 1986

(1): refers to number on Figure 2; ***bold italic*** refers to world-class deposits in the Abitibi greenstone belt; Ass.-Aged: refers to the age of the assemblage hosting the deposit(s).

This mineral endowment led to considerable amounts of mapping and geoscientific research, conducted at multiple scales, resulting in the AGB being an important belt worldwide for development of genetic models for VMS, Ni-Cu-PGE and gold deposits, and for evolutionary models of greenstone belt development (Goodwin 1979; Dimroth et al. 1982, 1983; Jensen and Langford 1985; Jackson et al. 1994; Ayer et al. 2002).

The AGB is composed of east-trending synclines of largely volcanic rocks (felsic to ultramafic in composition) and intervening domes cored by synvolcanic and/or syntectonic plutonic rocks (gabbro-diorite, tonalite and granite), alternating with east-trending bands of turbiditic wackes (Ayer et al. 2002; Daigneault et al. 2004; Goutier and Melançon 2007; MER–OGS 1984). Most of the volcanic and sedimentary strata dip vertically and are generally separated by abrupt, east-trending faults with variable dip. Some of these faults, such as the Porcupine–Destor deformation zone, display evidence for overprinting deformation events, including early thrusting with later strike-slip and extension events (Goutier 1997; Benn and Peschler 2005; Bateman et al. 2005). Two ages of unconformable successor basins occur: early, widely distributed "Porcupine-style" basins of fine-grained clastic rocks and minor calc-alkaline volcanic rocks; followed by "Timiskaming-style" basins of coarser clastic and minor alkaline volcanic rocks which are largely proximal to major strike-slip faults (Porcupine–Destor, Larder–Cadillac and similar faults in the northern AGB: Ayer et al. 2002, 2005; Goutier and Melançon 2007). In addition, the AGB is cut by numerous late-tectonic plutons (from syenite and gabbro to granite, with lesser dikes of lamprophyre and carbonatite).

Field and geochronological data indicates that the AGB developed autochthonously, based on preserved in-situ stratigraphy and widespread evidence of isotopic inheritance of older zircons found in younger episodes and feeder dikes and mafic to ultramafic sills cutting older units but with similar ages of overlying volcanic units (Ayer et al. 2005; Thurston et al., in press). The recent revisions to the stratigraphy of the AGB presented in Thurston et al. (in press) (*see* Figure 2) has implications for autochthonous development of the volcanic stratigraphy and for exploration models for syngenetic mineralization. In Ontario, we have subdivided the AGB into six early volcanic stratigraphic episodes (i.e., assemblages) on the basis of groupings of numerous U-Pb zircon ages:

- 2770-2735 Ma Pacaud assemblage;
- 2730-2724 Ma Deloro assemblage;
- 2723-2720 Ma Stoughton–Roquemaure assemblage;
- 2719-2711 Ma Kidd–Munro assemblage;
- 2710-2704 Ma Tisdale assemblage; and
- 2704-2696 Ma Blake River assemblage;

unconformably overlain by two late sedimentary assemblages:

- 2690-2685 Ma Porcupine assemblage; and
- 2676-2670 Ma Timiskaming assemblage.

Given the continuous nature of deposition of the volcanic rocks within the early volcanic-dominated assemblages, it is striking to observe that there are depositional gaps in representative stratigraphic sections including:

1. the central part of the Swayze area, southwest of Timmins, where Heather (2001) and van Breemen et al. (2006) noted a depositional gap between the 2735 +6/-4 Ma Marion Group and the 2705 ± 2 Ma Trailbreaker Group (*see also* Heather et al. 1995);
2. south of Timmins, where rocks of the 2730-2724 Ma Deloro assemblage are overlain by the 2710-2704 Ma Tisdale assemblage (Ayer et al. 2002);
3. the Shining Tree area, south of Timmins, where the 2770-2735 Ma Pacaud assemblage is overlain by the 2730-2724 Ma Deloro assemblage (Ayer et al. 2002);

4. south of Kirkland Lake and in the Temagami area, where the 2770-2735 Pacaud assemblage is overlain by the 2723-2720 Stoughton–Roquemaure assemblage (Ayer et al. 2005, 2006);
5. the Matagami area, where rocks of the 2725-2723 Ma Lac Watson Group are overlain by rocks of the 2720 ± 1 Ma Dussieux Formation (Goutier et al. 2004);
6. the Chibougamau area, where ca. 2730 Ma rocks of cycle 1 are overlain by 2718 ± 2 Ma volcanic rocks of cycle 2 (Mortensen 1993; Pilote 2006).

In light of these age gaps and a lack of evidence for large-scale thrusting, we propose these depositional gaps in the AGB are related to sedimentary interface zones (SIZ) associated with localized time gaps, which are also potentially related to episodes of syngenetic mineralization (Thurston et al., in press). Worldwide, SIZ have been identified at the top of mafic to felsic volcanic cycles and at geochemical transitions within volcanic successions of greenstone belts in the Pilbara Supergroup of the Pilbara Craton (van Kranendonk 2006); the Belingwe greenstone belt of the Zimbabwe Craton (Bickle et al. 1994); the Barberton greenstone belt of the Kaapvaal Craton (Lowe et al. 1999); and the Red Lake greenstone belt of the western part of the Superior Province (Sanborn-Barrie et al. 2001).

The SIZ units consist of sedimentary-dominated intervals composed of extensive chemical sediments, minor clastic sedimentary rocks and intercalated volcanic rocks at the top, as well as within, the major volcanic assemblages. They could include numerous lithologies such as iron formations, chert, chert breccia units, heterolithic debris flows, conglomerates, and graphitic argillites.

Iron formation units within the SIZ generally consist of alternating layers of oxides, sulphides, silicates, carbonates, and cherts. However, they are dominated by oxide facies, with lesser sulphide facies iron formations. Two main mechanisms could be involved in the genesis of those iron formations (e.g., van den Boorn et al. 2007): 1) chert units directly precipitated from sea water; and 2) iron formation produced by silicification of precursor rock types such as wackes or felsic ash. Most of the iron formation within SIZ is thin bedded (<5 cm), silt-grade wacke, felsic ash or cherty turbidites grading up to oxide-rich upper units.

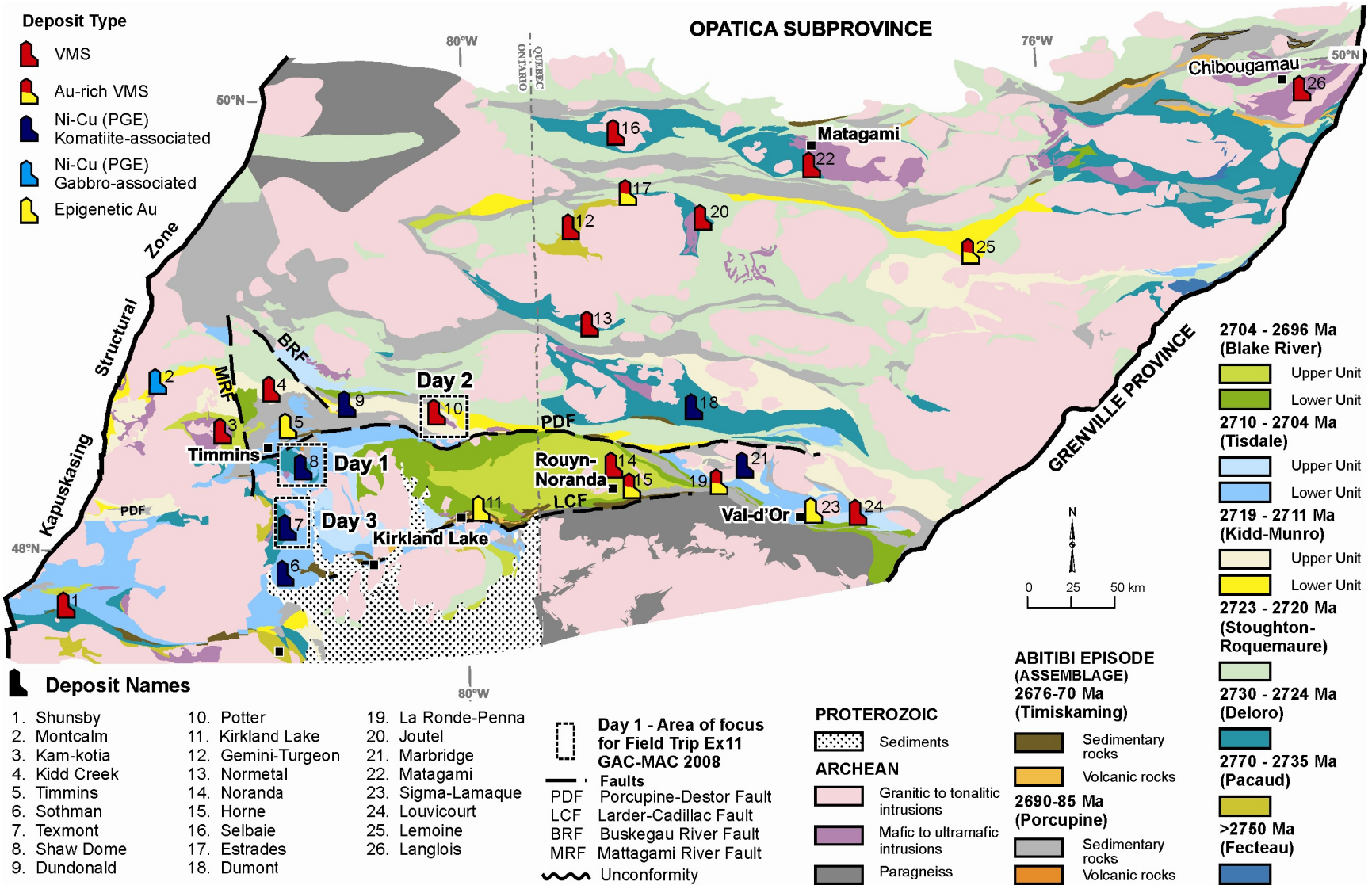

Figure 2. Stratigraphic map of the Abitibi greenstone belt (AGB) (*modified after* Thurston et al., in press). The southern AGB is based on Ayer et al. 2005 and the Québec portion on Goutier and Melançon 2007.

Two types of chert breccia are recognized within the AGB SIZ: 1) hydrothermal breccia cemented by iron carbonate, which cross-cuts thinly laminated iron formation beds; and 2) stratabound, stratiform units of chert fragments cemented by iron oxide, biotite and quartzo-feldspathic material, bounded by bedded chert, iron formation, or heterolithic debris flows. The intercalation of the chert breccia units with undisturbed, finely laminated chert at the top of the Deloro assemblage suggests the stratiform breccia units are syn-sedimentary and represent either episodic down-slope movement of iron formation from its formative environment (Heather 2001), products of hydrothermal circulation (van Kranendonk 2006), and/or dewatering structures (Krapez et al. 2003).

Iron formation conglomerate consists of metre-scale thicknesses of unbedded, ungraded conglomerate containing clasts of oxide-facies iron formation, arkose, and shale. The conglomerates represent multiple generations of down-slope movement of iron formation. Early, angular breccias of dismembered chert beds are incorporated into iron formation clasts, suggesting the iron formation conglomerate units represent multiple episodes of re-sedimentation of partially to wholly consolidated banded iron formation (e.g., Heather 2001; Pickard et al. 2003).

Graphitic argillite units within SIZ are centimetre- to metre-scale thicknesses of graphitic argillite, commonly with framboidal pyrite, which display thin, A-E laminations typical of distal turbidites, and contain very little terrigenous, quartzo-feldspathic material. They commonly occur at geochemical discontinuities in volcanic stratigraphy and are interpreted to represent very low rates of sedimentation in a basinal setting.

Thus, SIZ within and capping major volcanic successions of the AGB provide some evidence for the existence of depositional gaps represented by: 1) condensed sections typified by iron formation and chert breccia/conglomerate; 2) sections with low sedimentation rates accompanied by hydrothermal circulation and deposition of chert breccias; and 3) sections with no sedimentation and early diagenetic replacement by chert (Thurston et al., in press). Recent sequence-stratigraphic interpretive models (Catuneanu 2003; Miall 1994) equate condensed sections, low sedimentation rates, and periods of no sedimentation with so-called correlative conformities. Mitchum (1977) defined a correlative conformity as the seaward continuation of an unconformity surface nearer shore. The surface is marked by parallel strata in the basin. While we lack near-shore units with mappable unconformities, we suggest that the top of the major volcanic episodes may represent correlative conformities; more conservatively, we prefer the term submarine disconformity. Some of the characteristics of these submarine disconformities will be observed on Day 3 of the field trip.

Pacaud Assemblage

The 2770-2735 Ma Pacaud assemblage is the oldest outcropping supracrustal unit identified in the southern Abitibi greenstone belt (Ayer et al. 2002). It consists predominantly of tholeiitic volcanic rocks with calc-alkalic intermediate to felsic volcanic rocks and minor komatiites outcropping on the flanks of the Round Lake and Ramsey–Algoma batholiths (*see* Figure 2) and the Chambers batholith in the Temagami area (not shown on Figure 2). We have recently extended the lower age limit for the Pacaud assemblage to ca. 2770 Ma based on a new age of 2766.9 ± 1.1 Ma from a mafic to felsic volcanic succession on the northern margin of the Temagami greenstone belt capped by an SIZ iron formation unit hosting the Sherman Iron Mine (Ayer et al. 2006).

The base of the Pacaud assemblage is everywhere cut by batholiths and thus its relationship to older volcanic units such as the 2790 Ma Fecteau Formation, southwest of Chibougamau

(Bandyayera et al. 2004) in the northern Abitibi, is unknown. Recently discovered 2860 to 2800 Ma xenocrystic zircons in isolated volcanic units (Ayer et al. 2005), in conjunction with similar aged xenocrysts in isolated synvolcanic batholith samples in the western part of the AGB (Ketchum et al., in press), indicates that older crust was locally sampled by the Abitibi-aged magmas. However, the precise nature of the relationship to the older basement remains elusive, as other radiogenic isotopic systems, such as Nd and Hf, display signatures that typically indicate these magmas were derived from juvenile depleted mantle. There are also some isolated samples indicating minor contamination by ancient crust (e.g., Corfu and Noble 1992; Ayer et al. 2002; Sproule et al. 2004; Ketchum et al., in press).

The age of the Pacaud assemblage compared to the overlying Deloro assemblage in the southern AGB in Ontario suggests a local age gap or depositional hiatus of 2 to 5 million years between the two assemblages. The thickest remnants of the Pacaud assemblage occur in the Shining Tree and Temagami areas, where they are represented largely by tholeiitic mafic volcanic rocks in the lower part, with lesser komatiite and calc-alkalic intermediate to felsic volcanic rocks in the upper parts. In the southern Swayze greenstone belt, there is a depositional gap of approximately 8 million years between the 2739±1 Ma Chester Group and the 2731±2 Ma Marion Group (van Breemen et al. 2006), whereas in the Temagami area there is a gap of about 15 million years with the overlying Stoughton–Roquemaure assemblage.

Deloro Assemblage

In the southern AGB, units of the 2730-2724 Ma Deloro assemblage (Ayer et al. 2005) occur as homoclinal panels underlain by the Pacaud assemblage, on the southwestern flank of the Kenogamissi batholith, and on the northern flank of the Ramsey–Algoma batholith in the Shining Tree and Swayze areas (*see* Figure 2). The Deloro assemblage also occurs in the core of the Shaw Dome, south of Timmins, and north of the Porcupine–Destor deformation zone, west of Timmins. The Deloro is composed largely of calc-alkalic volcanic rocks and regionally extensive iron formation units; however, tholeiitic mafic volcanics of this age are widespread in the northern Abitibi and locally evident at the base of the assemblage in the southern Abitibi (e.g., east of the Kenogamissi batholith). In most instances, the assemblage is underlain by rocks of the Pacaud assemblage with a depositional gap of about 5 Ma.

Stoughton–Roquemaure Assemblage

The 2723 to 2720 Ma Stoughton–Roquemaure assemblage consists of mafic volcanic rocks with subordinate intermediate to felsic volcanic rocks and komatiites. It is a very widespread assemblage in the northern part of the AGB (*see* Figure 2). However, within the Timmins–Kirkland Lake region it is restricted to north and south of the the Porcupine–Destor (PDDZ) and Larder Lake–Cadillac (LLCDZ) deformation zones, respectively (*see* Figure 2). North of the PDDZ, the assemblage is conformably underlain by the Hunter Mine group of the Deloro assemblage east of the Lake Abitibi batholith in Québec, without any evidence of a significant stratigraphic gap (Mueller and Mortensen 2002). South of the LLCDZ, the assemblage is underlain by the Pacaud assemblage, with a depositional gap of approximately 12 million years, on the eastern and southern flanks of the Round Lake batholith and in the central part of the Temagami belt (Ayer et al. 2005, 2006).

Kidd–Munro Assemblage

The most widespread part of the Kidd–Munro assemblage extends about 450 km across the AGB, from fault-bounded contact with the Kapuskasing Structural Zone in the west, to fault-bounded contact with the Grenville Province in the east (*see* Figure 2). Most of the eastern portion occurs along the north margin of the PDDZ. Other smaller parts of this assemblage are also preserved in the southern Swayze and Shining Tree areas and southwest of Chibougamau.

The Kidd–Munro assemblage, formerly a single stratigraphic unit with an age range of 2719-2711 Ma (Ayer et al. 2002; Bleeker et al. 1999), is now subdivided (Ayer et al. 2005) into lower and upper parts. The lower part (2719-2717 Ma) includes dominantly intermediate to felsic calc-alkalic volcanic rocks including: 1) the former Coulson–Rand assemblage of Jackson and Fyon (1991) south of Lake Abitibi; 2) in the central part of the western AGB where it is complexly infolded with upper Kidd–Munro assemblage rocks in Dundonald and Clergue townships; and 3) west of Timmins in Thornburn and Loveland townships, where 2719.5 ± 1.7 Ma (Ayer et al. 2002) calc-alkalic rocks are in tectonic contact with a northeast-facing unit of the upper part of the Kidd–Munro assemblage to the south (Hathway et al. 2005). The upper part of the Kidd–Munro assemblage (2717-2711 Ma: Ayer et al. 2005) extends across the AGB, north of the PDDZ in Ontario (*see* Figure 2). It consists of tholeiitic and komatiitic units with minor centimetre- to metre-scale graphitic metasedimentary rocks and localized felsic volcanic centres. At the eastern end of the assemblage, its southern limit is the PDDZ. To the west, the southern contact is with Porcupine assemblage metasedimentary rocks across the Pipestone deformation zone, whereas west of the Buskegau River Fault, the southern contact is poorly known. West of the Mattagami River Fault, the assemblage is northeast facing, and is in tectonic contact with the upper part of the Blake River assemblage in Jamieson Township (Hathway et al. 2005).

South of the Kamiskotia area, the base of the upper part of the Kidd–Munro assemblage is in contact with pillow basalts of the Deloro assemblage. Here the basal contact represents a roughly 13 million year gap between the Deloro assemblage and the 2712.2 ± 0.9 Ma Kidd–Munro felsic tuffs in Carscallen Township (Hall and Smith 2002). Oxide facies iron formation containing chert breccia clasts, chert replacement of iron formation and erosional features at this basal contact indicate the basal contact is marked by an SIZ (Thurston et al., in press).

In the upper Kidd–Munro assemblage between the Buskegau River Fault (*see* Figure 2) and the Québec border, relationships are complex. The Kidd–Munro assemblage is tectonically juxtaposed with the younger Porcupine assemblage, and parts of the Kidd–Munro stratigraphy have been removed by thrusting (Berger et al. 2007).

Tisdale Assemblage

The most widespread part of the Tisdale assemblage extends about 300 km from fault-bounded contact with the Kapuskasing Structural Zone in the west to the Larder Lake area in the east. Here, it is bounded to the north by the PDDZ and to the south by the LLCDZ (*see* Figure 2). Smaller portions of this assemblage occur north of the Porcupine–Destor deformation zone in Ontario (e.g., the Porcupine gold camp) and in Québec.

The Tisdale assemblage has also been subdivided into a lower part and an upper part (Ayer et al. 2005). The lower part of the Tisdale assemblage ranges in age from 2710-2706 Ma and consists of tholeiitic mafic flows with locally developed komatiites and intermediate to felsic calc-alkalic volcanic rocks and iron formation. The most extensive part of the assemblage lies between the Porcupine–Destor and Larder Lake–Ridout fault systems and extends over 250 km from the Kapuskasing structure to the Québec border (*see* Figure 2). Throughout this part of the

assemblage, the lower Tisdale directly overlies the Deloro assemblage, marking a profound stratigraphic gap of ca. 15 million years (Ayer et al. 2002).

The upper part of the Tisdale assemblage, the "Marker Horizon" of Corfu and Noble (1992), is characterized by 2706-2704 Ma calc-alkalic felsic to intermediate volcanic rocks. They include amygdaloidal flows, heterolithic debris flows and volcaniclastic units. The Marker Horizon forms the core of three east-trending synclines on the west flank of the Watabeag batholith southeast of Timmins. The presence of iron formation toward the top of the unit in this area indicates a possible SIZ, marking a volcanic hiatus of approximately 2 million years between the upper part of the Tisdale assemblage and the overlying lower part of the Blake River assemblage.

In the Kirkland Lake area, on the north flank of the Spectacle Lake Anticline, the upper part of the Tisdale assemblage volcanic rocks are overlain by reworked pyroclastic units above which are, in ascending order: 10 to 20 m of tuff; a chert-basalt conglomerate; a laminated chert; and pillowed flows of the lower Blake River assemblage (Roberts and Morris 1982). This interval is another example of a volcanic hiatus represented by a SIZ between the Upper Tisdale and Blake River assemblages.

Northeast of Timmins, the upper Tisdale assemblage occurs as an east-trending unit between the Kidd–Munro and Stoughton–Roquemaure assemblages. While the southern contact with the Kidd–Munro appears to be tectonic, the contact with Stoughton–Roquemaure to the north appears to be transected by a 2704 ± 5 Ma (i.e., Tisdale-aged) mafic to ultramafic intrusive complex (Barrie 1999) suggesting a conformable contact marked by a roughly 15 million year depositional gap.

Blake River Assemblage

The most extensive part of the Blake River assemblage occurs immediately overlying the Tisdale assemblage between the PDDZ and LLCDZ (*see* Figure 2). Smaller portions of the assemblage occur southeast of Kirkland Lake (Skead group), in the Kamiskotia volcanic complex, west of Timmins, and in the central part of the Swayze belt.

The Blake River assemblage has also been subdivided into a lower stratigraphic part ranging from 2704 to 2702 Ma, and an upper part ranging from 2701 to 2696 Ma (Ayer et al. 2005). The lower Blake River represents new nomenclature for the former Kinojevis assemblage of Ayer et al. (2002) in order to remove confusion with the 2718 ± 2 Ma (Zhang et al. 1993) Kinojévis Group in Québec, which correlates with the Stoughton–Roquemaure and the Kidd–Munro assemblages in Ontario. In Québec, the stratigraphic equivalent to the lower Blake River assemblage is a unit of tholeiitic basalts beneath the Blake River Group assigned to the Hébécourt Formation (Goutier 1997). In Ontario, the lower Blake River assemblage occupies the north and south margins of the Blake River synclinorium; and along the west flank of the Nat River batholith in the Kamiskotia area, where it is underlain by the Kidd–Munro assemblage. In the former area, the assemblage consists of high Fe and high Mg basalts with minor felsic volcanic units and turbiditic metasediments. In the latter area tholeiitic basalts and minor rhyolite flows and pyroclastic units occur.

The upper Blake River assemblage ranges in age from 2701 to 2696 Ma and consists predominantly of flows of calc-alkalic basalt and andesite, locally with bimodal tholeiitic basalt and rhyolite. It occurs in a number of areas: 1) in the core of the Blake River synclinorium extending eastward from Ontario into Québec; 2) in the Kamiskotia area as an east-facing homoclinal succession on the eastern flank of the Nat River batholith; 3) in the Skead Formation southeast of the Kirkland Lake area, where it consists of calc-alkalic intermediate to felsic volcanic rocks with an age of 2701 Ma (Ayer et al. 2005) overlying the Stoughton–Roquemaure

assemblage on the eastern and southern flanks of the Round Lake batholith; and 4) in the Swayze Group in the central part of the Swayze greenstone belt, where it overlies the Tisdale assemblage (Ayer et al. 2002).

Successor Basins: Porcupine and Timiskaming Assemblages

Two ages of unconformable successor basins occur in the AGB: early, widely distributed Porcupine assemblage basins of fine-grained clastic rocks and minor volcanic rocks; followed by Timiskaming assemblage basins of coarser clastic and minor volcanic rocks, which are largely proximal to major strike-slip faults, such as the PDDZ, LLCDZ and other faults in the northern AGB (Ayer et al. 2002; Goutier and Melançon 2007) (*see* Figure 2).

The early turbidite-dominated Porcupine assemblage forms laterally extensive basins succeeded by the Timiskaming assemblage in more restricted alluvial-fluvial basins (Ayer et al. 2002). The Porcupine-type sedimentary basins form wacke-dominated, kilometre-scale sequences unconformably overlying the metavolcanic assemblages and are transitional into much more extensive basins such, as the wacke-dominated Quetico Subprovince to the north and the Pontiac Subprovince to the south. In the southern AGB the Porcupine-type successor basin is 2690-2685 Ma in age, based on the crystallization age of the basal Krist volcanic unit and detrital zircons in the overlying wackes in the Timmins area (Ayer et al. 2005). The basal contact of this assemblage in the Timmins area is a low-angle unconformity (Bateman et al. 2005). In the Timmins area, the contact typically lacks regoliths or paleosol (Ayer et al. 2002) and is therefore interpreted as submarine.

The Timiskaming assemblage represents the youngest supracrustal unit in the AGB. The rocks include alluvial-fluvial conglomerates, sandstones, turbidites and alkalic to calc-alkalic volcanic rocks that unconformably overlie metavolcanic rocks and/or Porcupine assemblage units with numerous examples of erosional discordance and development of paleosols (Jackson and Fyon 1991; Mueller 1991; Chown et al. 1992). East of Timmins, the lower contact of the Timiskaming assemblage is a sharp erosional angular unconformity with the underlying Porcupine assemblage, with no evidence of subaerial weathering (Born 1995). In the Timmins and Kirkland Lake area, the Timiskaming assemblage ranges in age from 2676 to 2670 Ma, based on twelve U-Pb detrital zircon age determinations (Ayer et al. 2005).

METALLOGENIC EVENTS

The Abitibi greenstone belt is recognized for its prolific mineral endowment that includes world-class volcanic-associated Cu-Zn-(Pb) massive sulphide deposits (VMS), magmatic Ni-Cu-(PGE) deposits, and world-class orogenic lode gold deposits. The entire volcano-sedimentary stratigraphy of the AGB has potential to host one or more of these distinct types of deposits. However, specific stratigraphic intervals are more prospective for specific types (Figure 3). VMS-style mineralization occurs throughout volcanic-dominated assemblages such as Pacaud, Deloro, Stoughton–Roquemaure, Kidd–Munro, Tisdale, and Blake River. Gold-rich VMS-style mineralization appears to be only associated with the youngest volcanic-dominated assemblage (i.e., Blake River). Thus far, Ni-Cu-(PGE) mineralization is limited to the Pacaud, Stoughton–Roquemaure, Kidd–Munro, and Tisdale assemblages. However, komatiite-associated Ni-Cu-(PGE) deposits appeared to be restricted only within the younger volcanic-dominated assemblages such as the Kidd–Munro and the Tisdale assemblages. Orogenic gold mineralization is structurally controlled mineralization that occurs within numerous assemblages. However, world-class lode gold deposits are spatially and genetically associated with the Porcupine–Destor

and Larder Lake–Cadillac faults systems. The Timiskaming assemblage is also spatially associated with these fault systems and temporally with orogenic gold (*see* Figure 3).

VMS-STYLE MINERALIZATION

In the AGB, VMS-style mineralization occurs within six volcanic assemblages, with the early VMS epochs (Pacaud, Deloro, and Stoughton–Roquemaure assemblages) temporally correlative with regional iron formations (*see* Figure 3). Spatially, VMS deposits are commonly associated with tholeiitic rhyolites in bimodal basalt-rhyolite successions (Lesher et al. 1986; Hart et al. 2004).

The oldest known VMS deposit in the AGB is the Gemeni–Turgeon, with an age of 2736 Ma, associated with an SIZ at the top of the Pacaud assemblage in northern Québec (Goutier and Melançon 2007). This age is correlative with the iron formation hosting the Sherman Iron Mine at the top of the Pacaud in the Temagami area (Ayer et al. 2006).

VMS mineralization within the Deloro assemblage occurs in two main rock associations: 1) massive sulphide deposits in mafic to felsic calc-alkalic volcanic rocks spatially associated with tholeiitic rhyolites; and 2) base metal mineralization in sulphide facies iron formations representing proximal exhalative mineralization localized within regional-scale oxide facies iron formations. Almost all significant VMS deposits that have been found to date in the northern AGB in Québec are associated with mafic to felsic volcanic rocks and include the Matagami, Joutel and Normetal mines. The Shunsby deposit within the Swayze belt is one example of Cu-Zn VMS deposits associated with iron formation (Heather 1998).

The Stoughton–Roquemaure assemblage is host to the Estrades VMS deposit in northern Québec, and is also correlative with a regional iron formation that occurs in the Temagami area. Numerous iron formations of this age occur in the northern Abitibi (Ayer et al. 2007) and such areas should be further considered for exploration for VMS-style mineralization.

The upper Kidd–Munro assemblage is host to the giant Kidd Creek Mine, associated with high-silica rhyolites and ultramafic volcanic rocks, and smaller deposits such as the Potter Mine and Potterdoal in Munro Township, associated with ultramafic and mafic volcanic rocks. Stratigraphy established at the Kidd Creek Mine (Bleeker 1999) and at the North Rhyolite (De Wolfe 2004) has recently been extended approximately 15 km to the northeast into Prosser Township (Berger et al. 2007). A key point apparent in the simplified stratigraphic columns (Figure 4) is that high-silica rhyolites with similar geochemistry, volcanic facies and ages of 2716 Ma (which are the host to the Kidd Creek deposit) have been identified up to 15 km to the northeast of the Kidd Creek Mine and thus serve as a time–stratigraphic marker unit in this part of the assemblage. These easily recognized felsic volcanic rocks occur in other places throughout the assemblage, and may be useful reference units for stratigraphic correlations and to help focus exploration. Calc-alkalic metavolcanic rocks in Prosser Township, correlated with the lower part of the Kidd–Munro assemblage based on their age and stratigraphic facings, consistently underlie the tholeiitic rocks (*see* Figure 4). Stringer zinc and copper mineralization, accompanied by widespread hydrothermal alteration in Prosser Township, indicates that these rocks are also prospective hosts for base metal mineralization.

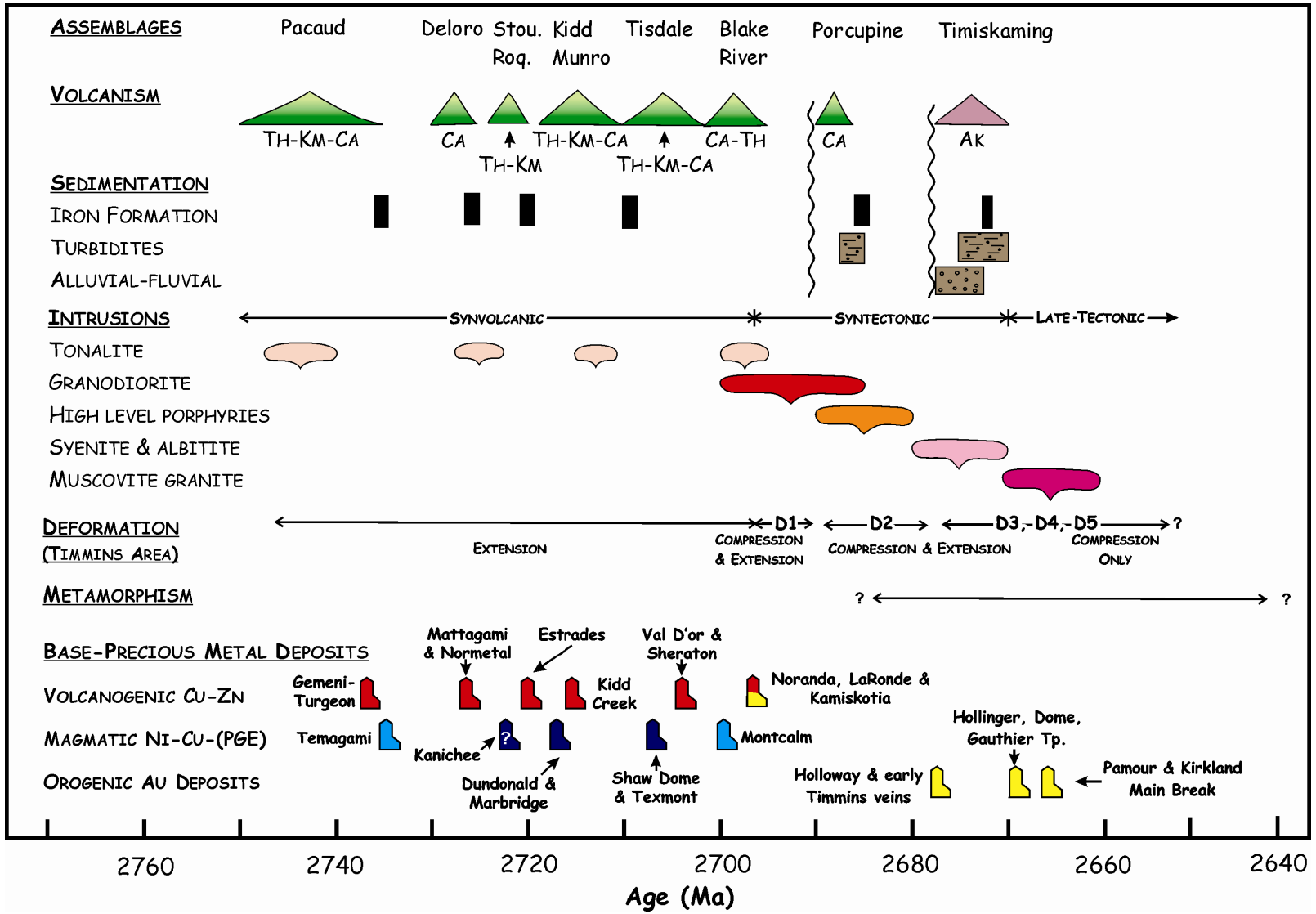

Figure 3. Timeline (*modified from* Bateman et al. 2005) for the evolution of the western Abitibi greenstone belt including the volcanic and sedimentary assemblages, intrusions, deformation, metamorphism and mineralization episodes. Color, within the mineralization episodes, represents different types of mineralization: red = base metals associated with VMS-style mineralization; yellow = gold deposits; pale blue = gabbro-associated base metals (Ni); and dark blue = komatiite-associated base metals (Ni).

A number of VMS deposits are known to occur in upper Tisdale-aged units in Québec. These deposits, which include the Louvicourt Mine, occur in the 2704 ± 2 Ma Val d'Or formation, which consists of calc-alkalic intermediate to felsic volcanic rocks (Scott et al. 2002). There are large areas underlain by calc-alkalic rocks of the upper Tisdale (*see* Figure 2). The recently discovered Zn-Cu-Pb mineralization in Sheraton Township (roughly 40 km east-southeast of Timmins) with an age of 2703.7 ± 1.5 Ma (Ayer et al. 2002), and the Cu-Zn-Au mineralization found along strike to the east in Currie Township, indicate the presence of VMS-style mineralization. These occurrences represent an area worthy of focus for VMS exploration similar to the Val d'Or formation in Québec.

The VMS deposits at Kamiskotia were previously believed to be part of the Tisdale assemblage, based on an age of 2705 ± 2 Ma from Godfrey Township (Barrie and Davis 1990). However, new geochronology indicates they are associated with bimodal tholeiitic basalts and rhyolites and occur within a single stratigraphic horizon that has an age of 2700 Ma. This indicates similarity in age and chemical affinity to the Blake River assemblage that hosts VMS deposits in the Noranda camp in Québec. Unconformable juxtaposition of VMS-bearing assemblages in the Kamiskotia area, such as the Kidd–Munro and Blake River assemblages, indicates a long history of formation of significant VMS deposits, and thus represents an area that is worthy of focused exploration for new Cu-Zn deposits (Hathway et al. 2005).

The youngest VMS episode occurs in the upper Blake River assemblage. The Noranda cauldron sequence of the Noranda subgroup hosts the majority of VMS deposits in the Blake River Group (Gibson 1989; Gibson and Watkinson 1990). However, pyroclastic rocks form an important part of the post-cauldron volcanism (Trudel 1978; Goutier 1997; Lafrance et al. 2003). The abundance of base metals associated with highly elevated precious metals in deposits such as the Horne Mine in Noranda and the gold deposits to the east, led Robert and Poulsen (1997) to suggest that some of the gold mineralization in the Blake River Group was related to volcanism. The gold-rich VMS deposits that were formed before the main deformation event include the LaRonde Penna deposit and the Doyon mine, located between Noranda and Val d'Or in the Doyon–Bousquet–LaRonde gold camp (Dubé et al. 2004; Mercier-Langevin et al. 2004). LaRonde is a giant pre-deformation gold-rich synvolcanic volcanogenic massive sulphide deposit (Mercier-Langevin et al. 2004; Dubé et al. 2004), whereas Doyon is a world-class Au-Cu sulphide-rich vein-type deposit. The gold-bearing stockwork and sheeted veins at Doyon are deformed by the main foliation, and mineralized veins in the West Zone are cut by pre-D2 deformation diorite dykes. These features suggest that the mineralization is pre- or early main-stage deformation. The Doyon deposit may be associated with the emplacement of a late magmatic phase (tonalite) of the multistage Mooshla pluton (Galley et al. 2003).

Cu-Zn VMS-style mineralization also occurs within the upper part of the Blake River assemblage in the Ben Nevis area, which has a U-Pb age of 2696.6 ±1.3 Ma. This is younger than the pre-cauldron phase of the Noranda subgroup (2701 ±1 Ma: Mortensen 1993b), younger than the Misema subgroup in Pontiac township (2701 ± 2 Ma: Corfu et al. 1989), and of the same age as the post-cauldron phase of the Noranda subgroup (the Reneault-Dufresnoy formation: 2697.9 +1.3/-0.7: Mortensen 1993b and 2696 ± 1.1 Ma: Lafrance et al. 2005, and the Bousquet formation: 2698.6 ± 1.5 Ma, 2698.0 ± 1.5 Ma and 2694 ± 2 Ma: Lafrance et al. 2005). Thus, the Ben Nevis–Clifford volcanic complex formed late in the Blake River Group volcanic event, and is an area in which gold-rich VMS deposits may also be present.

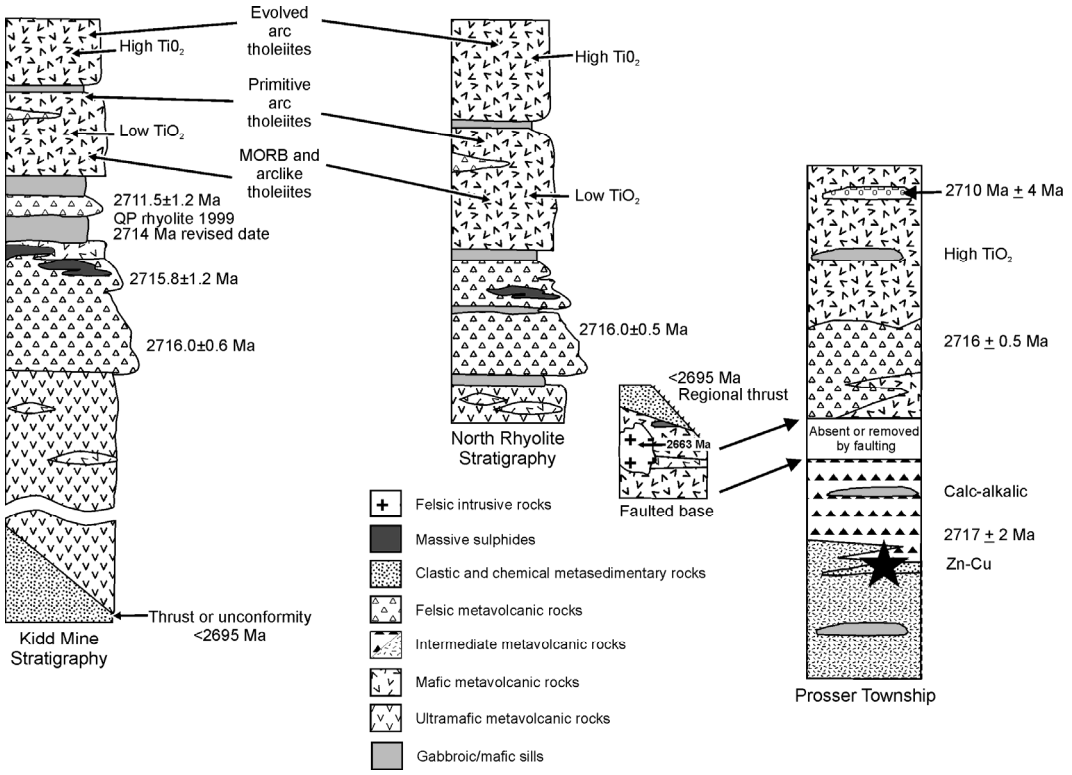

Figure 4. Stratigraphic column from the Kidd Creek Mine, the north rhyolite, and Prosser Township (*from* Berger et al. 2007).

NI-CU-(PGE) MINERALIZATION

Magmatic sulphide Ni-Cu-(PGE) deposits within the AGB are associated with a wide range of mafic to ultramafic magmas. Four main lithological/compositional associations are evident: komatiite; ferropicrite; layered intrusion; and gabbro-associated mineralization. Thus far, mineralization hosted by these main associations appear to be restricted to specific time intervals in the Abitibi greenstone belt (*see* Figure 3).

Only limited Ni-Cu-(PGE) mineralization is known to be associated with the Pacaud assemblage. However, recent work (Ayer et al. 2006) highlights some gabbro-associated Ni-Cu-(PGE) in the Temagami greentone belt (located south of Figure 2). The Temagami Island copper mine Ni-Cu-(PGE) mineralization occurs regionally as disseminated sulphides at the base of a gabbro sill, with higher grade mineralization locally occurring as remobilized footwall veins (Simony 1964).

Only limited Ni-Cu-(PGE) mineralization is reported within the Stoughton–Roquemaure assemblage. Subeconomic platinum-group element mineralization is known to occur within the Boston Creek sill ferropicrite in the Round Lake Dome area near Kirkland Lake (Stone et al. 1996). This mineralization is a "reef" style mineralization that occurs close to the transition zone between the ultramafic and mafic portion of the sill. A recent compilation map and geochronology within the Temagami greentone belt (Ayer et al. 2006) highlights the possibility that the Stoughton–Roquemaure assemblage could host komatiite-associated mineralization in this part of the AGB. The Kanichee intrusion is a komatiitic ultramafic to mafic layered body that hosts disseminated to net-textured sulphide mineralization at the base of the intrusion and some disseminated sulphide mineralization in the olivine-rich peridotite at the base of each cycle throughout the intrusion (Hawke 1982; Good 1989). The timing of this komatiitic intrusion is poorly constrained but may be coeval with komatiites in the overlying Stoughton–Roquemaure

assemblage and highlights the potential for Ni-Cu-(PGE) mineralization associated with komatiitic magmas outside of the well-known and highly prospective Kidd–Munro and Tisdale assemblages (discussed below).

Ni-Cu-(PGE) mineralization is well-known to occur within the Kidd–Munro and the Tisdale assemblages as komatiite-associated Ni-Cu-(PGE). The komatiites in the Kidd–Munro assemblage are considered to be highly prospective for magmatic Ni-Cu-(PGE) mineralization, with deposits such as the Alexo Mine, Dundonald South, and Dundeal deposits in Dundonald Township (Houlé et al., in press), and the past-producing Marbridge Mine in Québec.

The Tisdale assemblage is also highly prospective, with a number of past producers as well as currently producing komatiite-associated Ni-Cu-(PGE) mines (e.g., Redstone, McWatters, Langmuir #1 and #2). Geochronological results also suggest the lower Tisdale assemblage is a very widespread unit in the study area (*see* Figure 2) and that much of this area may have good potential for Ni-Cu-(PGE) discoveries associated with komatiites. Examples include the past-producing Texmont Mine in Bartlett and Geikie townships, and undeveloped deposits in Sothman and Bannockburn townships. Furthermore, a review of chalcophile element data (PGE, Ni, Cu, Co) of barren komatiitic rocks throughout the Abitibi greenstone belt reveals that all komatiitic rocks, regardless of age, display the same overall unfractionated trends (Sproule et al. 2005). Thus, the komatiitic magmas that generated these rocks were sulphide-undersaturated when they were erupted and did not lose their sulphide minerals or PGEs during ascent through the crust. Thus, all komatiitic rocks, regardless of assemblage, represent potentially favourable magma sources for Ni-Cu-PGE mineralization. Magmatic platinum-group element mineralization is also known to occur within the Tisdale assemblage as "reef" style mineralization that occurs close to the transition zone between the ultramafic and mafic portions of the intrusions. Examples of this type of mineralization occur in the Dundonald Sill (Dundonald Township), the Centre Hill Complex (Munro Township) and the Mann mafic to ultramafic intrusive complex (Mann Township: Good and Crocket 1999).

Younger gabbro-associated Ni-Cu mineralization is also present within the Montcalm gabbroic complex. This gabbroic intrusion with subordinate ultramafic phases, hosts the Montcalm Ni-Cu deposit. Gabbro from this complex has an age of 2702 ± 2 Ma and is cut by a granodiorite dike with an age of 2700 +5/-4 Ma (Barrie et al. 1990). These ages suggest the Ni-Cu mineralization in the Montcalm complex is coeval with Blake River assemblage volcanism in the Kamiskotia area to the east (Figure 2). Furthermore, the large size of a number of these mafic to ultramafic intrusions throughout the AGB (*see* Figure 2) suggests they should be considered as attractive targets for magmatic Ni-Cu mineralization.

EPIGENETIC GOLD MINERALIZATION

The Porcupine gold camp is the outstanding lode gold camp in Archean greenstone belts where its numerous deposits are dispersed over 35 km and together produced 63.7 million ounces of gold (Robert 2003). These deposits lie as pearls on a string along the northern margin of an originally south-dipping PDF (Bateman et al. 2005). Herein lies one of the structural anomalies to be resolved: how is it that the gold deposits apparently lie in the footwall of this shear zone, contrary to the experience in other Archean gold camps, such as Val d'Or and Kalgoorlie? Other uncertainties concerning these gold deposits include the kinematics and timing of deformations; the presence or absence of foliation predating the deposition of the Timiskaming assemblage; the relative timing of the several vein generations and styles that have long been known (at least in general terms) in this camp; and the way in which an evolving orogenesis determines the geometry and kinematics of coeval gold mineralization.

Several distinct phases of gold mineralization in the Porcupine gold camp occurred as early replacement- and later quartz-carbonate vein-style deposits. For example, clasts of colloform-crustiform ankerite vein in conglomerate of the Dome Formation at the Dome Mine (Dubé et al. 2003) demonstrate early hydrothermal low-grade replacement-style mineralization. Also, ankerite veining and minor replacement mineralization in Dome and Aunor mines predate the Timiskaming unconformity, and may be related to D2 thrusting (*see* Figure 5). Cu-Au-Ag-Mo mineralization in the Pearl Lake porphyry predates main-stage quartz-gold veins in the Hollinger Mine and is post-Timiskaming sedimentation. This replacement-style gold mineralization may be coeval with Lightning zone replacement-style gold mineralization at the Holloway Mine, which overprints a Timiskaming-aged volcanic unit (Ayer et al. 2005), is itself cut by an inter-mineral dyke with an age of 2671.5 ± 1.9 Ma, which is in turn overprinted by a later auriferous quartz-carbonate veining event (Ropchan et al. 2002). The bulk of the gold mineralization in Timmins however, corresponds to auriferous quartz veining in extensional fracture arrays interpreted as syn- to late-S3 foliation. Consequently, this main-stage gold-quartz mineralization at Hollinger-McIntyre, and Dome mines, and in other deposits, was late D3. The geometry of a significant proportion of quartz veins is structurally compatible with oblique (right-lateral, south-block-up) shear. Regionally, D3 was left lateral, so these vein systems may represent antithetic R' shear arrays. The extensional network of quartz-gold veins at Pamour crosscut S4 foliation with a minimum of deformation, and formed during north-south shortening, dip-slip fault movement (D4). D5 constriction generated local quartz ladder veins, but probably no new stage of gold mineralization was introduced.

This protracted history of deformation and alteration indicates a long-lived or multistage auriferous hydrothermal system (*see* Figure 3), and a plumbing system geometrically stable for long enough to feed gold into a relatively small volume of rock. Variability in timing is reflected in diverse styles of gold mineralization (vein type, disseminated, sulphide-rich mineralization), alteration mineralogy (massive ankerite, albite, sericite), sulphide and ore minerals (pyrite, tellurides) and metals (Au, Ag, Cu, Mo, W). Syn-deformation quartz-carbonate vein deposits are commonly spatially associated at the regional scale with Timiskaming-like regional unconformities and suggest an empirical relationship between large-scale greenstone quartz-carbonate gold deposits, deformation opening of these basins, and regional unconformities (Hodgson 1983; Robert 2000; Dubé et al. 2003, 2005). This is similar to the deformation-mineralization history recorded in the Archean Kalgoorlie gold camp in southwestern Australia (Bateman and Bierlein 2006).

Day 1: Physical Volcanology of the Timmins Area

by M.G. Houlé, E. Dinel, B. Saumur, A.D. Fowler and J.A. Ayer

GEOLOGY AND STRUCTURAL EVOLUTION OF THE TIMMINS AREA

Of specific relevance to this guidebook, the Timmins area north of the Porcupine–Destor deformation zone (PDDZ) is referred to as the Porcupine gold camp, whereas it is referred to as the Shaw Dome area, south of the PDDZ. The Porcupine gold camp consists of volcanic rocks of the Tisdale assemblage unconformably overlain by younger sedimentary rocks of the Porcupine and Timiskaming assemblages, all affected by numerous deformational episodes. The Shaw Dome area is an outward-facing domal structure with a core of Deloro assemblage overlain by the Tisdale assemblage. In detail, this structure represents an early southeast-plunging anticline modified by subsequent folding along the PDDZ corridor in the northwest.

Porcupine Gold Camp Stratigraphy

The stratigraphic nomenclature of the Porcupine gold camp has evolved over the past century. The reader is referred to Ferguson et al. (1968) and Brisbin (1997) for a historical review and more exhaustive descriptions of the stratigraphy than is shown in Figures 5 and 6.

The stratigraphy in the Porcupine gold camp has been subdivided into two main volcanic assemblages, the Deloro and the Tisdale assemblages, which are most relevant to this field trip. In the following sections we briefly describe these assemblages and their internal subdivisions.

DELORO ASSEMBLAGE

The Deloro assemblage is the lowermost stratigraphic unit observed in the vicinity of the Timmins gold camp (*see* Figure 5). It ranges in age from 2730 to 2724 Ma (Ayer et al. 2002) and is restricted to the area south of the PDDZ (*see* Figure 5). Here, it consists of mafic to felsic calc-alkalic volcanic rocks. The uppermost part of the assemblage also contains regionally extensive oxide iron formation units (banded iron formation-BIF). The assemblage thickness is estimated to be up to about 5 km, and is disconformably or unconformably overlain by volcanic rocks of the Tisdale assemblage, with an age gap of about 15 million years.

TISDALE ASSEMBLAGE

The Tisdale assemblage is mainly composed of a tholeiitic mafic volcanic rock suite, with some komatiitic and locally intermediate to felsic volcanic rocks. It ranges in age from 2710 to 2704 Ma (Ayer et al. 2005). The maximum apparent thickness of the Tisdale assemblage in the Porcupine camp is 3440 m (Brisbin 1997), measured in northeastern Tisdale Township, between the axis of the North Tisdale anticline and the upper contact with the Krist formation. Some authors have reported that the Porcupine–Destor fault is located at the base of the Tisdale assemblage (Pyke 1982). However, field mapping by Vaillancourt et al. (2000) and Hall et al. (2003) show that the location of the Porcupine–Destor fault is neither restricted to the base of the Tisdale assemblage nor is it a unique fault surface. Instead it is a large (100 to 500 m wide) corridor of ductile deformation overprinting the contact. The Tisdale assemblage was subdivided into several formations by Ferguson (1968), such as (from base to top): Hersey Lake formation; Central formation; Vipond formation; and the Gold Centre formation (*see* Figures 5 and 6). Some

of these formations were further subdivided into units, such as the V8 and V10B members of the Vipond formation (visited in this trip). The Tisdale assemblage is an important assemblage for gold exploration (Dunbar 1948), because the majority of gold extracted from the Porcupine camp has been from Tisdale assemblage host rocks, particularly within the Central and Vipond formations.

Hersey Lake Formation

At the base of the Tisdale assemblage, the Hersey Lake formation is composed of mainly Mg-rich mafic volcanic (high-Mg tholeiitic basalts) and komatiite lava flows. The estimated thickness is approximately 600 m (Brisbin 1997), measured on the south limb of the North Tisdale anticline. This formation is dominantly composed of intercalated polysutured ultramafic and pillowed mafic flows along the north side of the PDF in northern Deloro Township (Pyke 1982; Brisbin 1997) and southeastern Tisdale Township.

Central Formation

The Central formation is approximately 450 m thick (Brisbin 1997) and is mainly composed of mafic volcanic flows, intercalated massive, pillowed and pillow-breccia flows. The rocks of the Central formation are high-Mg tholeiites very similar to the Hersey Lake Formation rocks, except they do not have intercalated ultramafic volcanic rocks. Some variolitic rocks are present locally, and the upper contacts of some of the variolitic flows are characterized by beds of black argillites or cherty clasts.

Vipond Formation

The Vipond formation varies from approximately 300 m to 700 m in thickness and is characterized by very distinctive high-Fe tholeiitic variolitic pillowed mafic volcanic flows and variolitic hyaloclastic mafic flows, which are intercalated with massive mafic flows and carbonaceous argillite (Ferguson et al. 1968; Brisbin 1997). It contains two distinctive marker horizons, the V8 and the V10 units, the subjects of this part of the excursion. Volcanic rocks of the Vipond formation have been traced over a strike length of greater than 25 km (Dinel et al., in press).

The Vipond formation has been subdivided into several units, including (from base to top): the 99 flow (leucoxene-bearing massive mafic flows with an age of 2707 ± 3 Ma: Ayer et al. 2002); the V7 (laminated argillites and greywackes); the V8 (high-Fe tholeiites); the V9 (grey to black argillite); and the V10 (fragmental intermediate flows). The V8 and V10 are an integral part of this excursion and are addressed in more detail below.

V8 UNIT

The V8 is the most prominent rock unit on Ferguson's (1968) geological map that contains variolitic pillow flows. The unit is dominantly high Fe-tholeiites, with various textures, from massive flows to spherulitic pillow flows. The spherulites can vary from chloritic to albite and are concentrated in pillow rims.

V10 UNIT

The V10 unit has been subdivided into several subunits, such as (from base to top): V10A; V10B; V10C; and V10D. Brisbin (1997) documented the V10A unit at the former McIntyre Mine as being a fine-grained massive flow that is 12 to 35 m thick and locally underlain and overlain by

carbonaceous interflow sediments. At the Dome Mine this unit is called the "Andesite" flow. Overlying it at the McIntyre Mine is the V10B, which is described as a 20 to 40 m thick unit with a characteristic "chicken-feed" texture, which at Dome Mine forms the upper portion of the Andesite flow. The V10C at McIntyre is described as a massive flow identical to the V10A. It is approximately 5 to 20 m thick and correlative with the base of the "Dacite" flow at the Dome Mine. The V10D has the same "chicken-feed" texture as the V10B and is known as the upper Dacite flow at Dome Mine. Here it has also been described as having a "ropey flow top". It appears (Holmes 1968, *referenced in* Ferguson et al. 1968; Brisbin 1997) that at the Dome Mine the Dacite flow comprises two facies of the same lava and that the Andesite flow is composed of "several flows, which lens out along strike" (Holmes 1968). At Hollinger, the V10A and B were apparent but neither the V10C nor the V10D were recognized (Jones 1968, *referenced in* Ferguson et al. 1968). The V10B rocks are distinctive, being characterized as having a texture reminiscent of chicken feed. Graton et al. (1933) stipulates that "chicken-feed" is a local name applied to "…granulated glassy material filling spaces between the pillows and are more rarely found within the pillows themselves", i.e., hyaloclastite. Others have described it as consisting of broken spherulites or varioles (Ferguson et al. 1968; Brisbin 1997) or as consisting of "…brecciated spherules and angular porcelanic fragments or shards" (Griffis 1962).

Because of their distinctive texture, the association of Vipond rocks with gold mineralization, and the fact that the unit has been variously identified as a either dacite or andesite flow (e.g., Ferguson et al. 1968), or "chicken-feed" (e.g., Brisbin 1997), or pillow basalt (Pyke 1982), Dinel et al. (in press) investigated this unit further in the context of its volcanology and suitability as a host for ore.

Gold Centre Formation

The Gold Centre formation (*see* Figures 5 and 6) is the uppermost volcanic sequence of the Tisdale assemblage and is dominated by massive leucoxene-bearing flows and associated pillowed and pillow breccia (Brisbin 1997).

PORCUPINE ASSEMBLAGE

The Porcupine assemblage ranges in age from 2690 to 2685 Ma. It is mainly composed of wackes, local polymictic conglomerate, siltstone and mudstone locally with a basal unit of felsic volcanics (Ayer et al. 2005). In the Timmins area, it has been subdivided into units such as the Krist, Beatty, Hoyle, and Whitney formations. The reader is referred to Born (1995) for a more complete description of these formations.

TIMISKAMING ASSEMBLAGE

The Timiskaming assemblage in the Timmins area is mainly confined to narrow units of polymictic conglomerate and sandstone ranging in depositional age from 2676 to 2670 Ma. It has been subdivided into the a lower Dome formation and upper Three Nations formation. The reader is referred to Born (1995) for a more complete description.

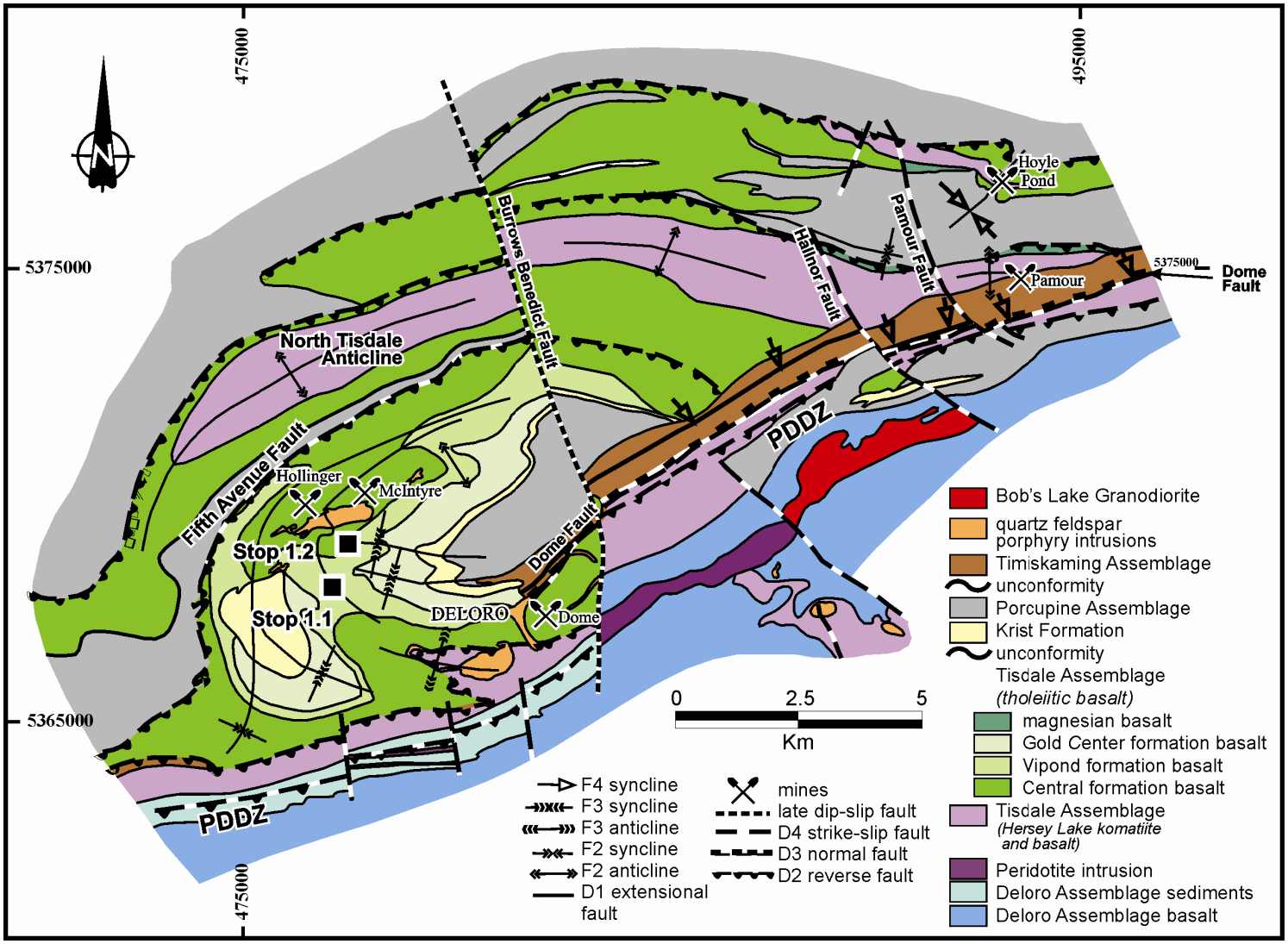

Figure 5. Geology of the Timmins gold camp (from Bateman et al. 2005), with stop locations for Day 1. Notice the distribution of the volcano-sedimentary rock assemblages, and the folding complexity of the area. Four deformation events are illustrated, which resulted in four different generations of folds, as interpreted by Bateman et al. (2005).

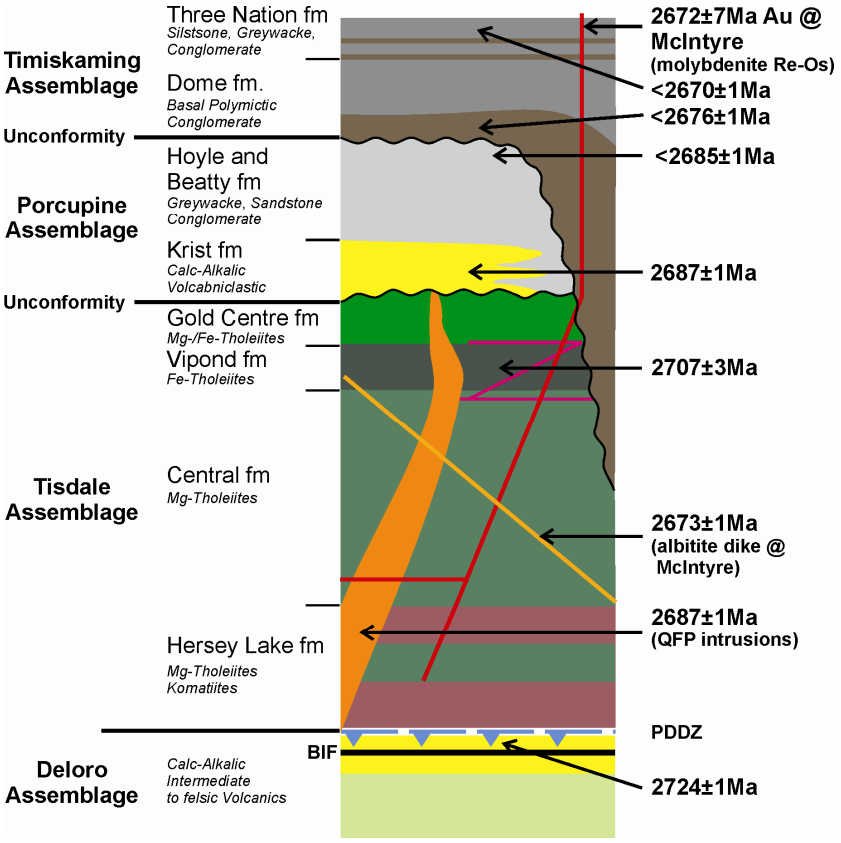

Figure 6. Schematic stratigraphic column north of the Porcupine–Destor deformation zone (PDDZ), illustrating the main volcano-sedimentary formations (*modified from* Barr 2005 and Dinel 2007). Age constraints are U-Pb ages from Ayer et al. (2005).

Structural Evolution

The following summary of the structural evolution of the Porcupine gold camp (*see* Figure 5 and Table 3) is based on research carried out during the Discover Abitibi project from 2003 to 2005. This work involved structural mapping and geochemical analysis of samples north of the Porcupine–Destor deformation zone (PDDZ), principally in Tisdale, Hoyle and Whitney townships (Bateman et al. 2005). It is also based on the PhD thesis of E. Dinel (2007). A structural scheme, with refinements to the stratigraphic column and geochronology, has been constructed for the Timmins–Porcupine gold camp in order to develop the constraints (*see* Figure 5). Bateman et al (2005) indicates initial deformation in the area was a regional uplift-extension event, producing a low-angle unconformity between the Tisdale and Porcupine assemblages, with partial excision of upper Tisdale stratigraphy. An early D2 dip-slip, south-over-north thrusting event produced a stacked set of south-over-north thrust sheets. These roots penetrated into the PDDZ, as shown by its C-S fabrics. The opening of the Timiskaming basin is interpreted in terms of opening of dilatational jogs in the curvilinear trace of the PDDZ. The Dome fault may represent the faulted margin of a half-graben formed in this manner. D3 folds along the northern flank of the PDDZ can be interpreted as a set of en-echelon folds resulting from left-lateral strike-slip movement along this zone, continuing from before, to after Timiskaming sedimentation. The S4 foliation formed during right-lateral strike-slip movement and folding of S3 foliation, making a compressional jog in the trace of the PDDZ overprinting the earlier dilatational jog that resulted in formation of the Timiskaming depositional basin. These represent the main deformation phases of an overall transpressional regime.

Rhys (2003) interpretation					Bateman et al. (2005)	Dinel 2007
Age (Ma)	Lithologies	Deformation events	Age (Ma)	Lithologies	Deformation events	Deformation events
2730-2725	Deposition of the Deloro assemblage		2730-2723	Deposition of the Deloro assemblage		
2708-2700	Deposition of the Tisdale assemblage		2708-2703	Deposition of the Tisdale assemblage		
2700- ~2690		**D1a** : Northwest trending folds, no foliation developed or preserved.			**D1**: extensional-uplift event, no foliation associated. Tisdale-Porcupine unconformity.	**D1** : No fabric observed at the mine.
~2691- ~2680	Deposition of the Porcupine assemblage		2691- ~2682	Deposition of the Porcupine assemblage	**D2**: Isoclinal folds (e.g. North Tisdale Anticline, Porcupine Syncline) and late thrust event (Tisdale thrust over Porcupine). Early dip-slip faulting in the Destor-Porcupine deformation zone.	**D2**: No fabric observed at the mine (based on Rhys, 2003, internal company report).
~ 2680- ~2675		**D1b**: West-northwest trending isoclinal folds lacking axial planar cleavage, modification of D1a folds.				**D3**: East-west isoclinal folds with axial planar cleavage parallel to bedding, possible late gold mineralization (2687>D3>2684). Late D3 thrust, Tisdale on Porcupine.
~2675- ~2672		Destor-Porcupine fault system, early faulting, >10km sinistral strike slip displacement, north side down.	2678-2669	Deposition of the Timiskaming assemblage + albitite dyke at McIntyre Mine (~2672Ma)	**D3**: folding (e.g. South Tisdale anticline) and axial planar cleavage S3 dominant penetrative fabric in Timmins (oriented 281°) post 2677 Ma, result of oblique-slip movement along major deformation zones. Gold mineralization associated with D3.	
~2674- ~2672	Deposition of the Timiskaming assemblage + albitite dyke		> 2669		Formation of the Dome Fault. **D4**: Isoclinal folding and S4 axial planar cleavage oriented 070° strong, restricted to the Timiskaming syncline. Dip-slip movement associated to D4 faults. Associated to gold mineralization.	**D4**: penetrative S4 fabric oriented 070°, axial planar to isoclinal folds and gold mineralization associated with D4.
~2672-?2643		**D2** + regional metamorphism: penetrative S2. east-southeast cleavage. Late gold mineralization.			**D5**: constrictional strain, observed west of Porcupine syncline, forming very stretched pillows, prominent where the Destor-Porcupine fault deflects. **D6**: Flat-lying crenulation cleavage.	**D5**: Northeast crenulation cleavage associated to small scale Z-folds and conjugate kinks. **D6**: sub-horizontal crenulation cleavage axial planar to broad open fold (vertical displacement along S4).
		D3: Spaced S3 foliation east-southeast cleavage, continuation of sinistral displacement. **D4**: late retrograde deformation, north-northeast crenulation cleavage and conjugate kinks. **D5**: shallow southwest dipping crenulation cleavage.			**D7**: north-northeast striking kink and chevron folds, steeply dipping axial planar cleavage.	

Table 3. Summary of the structural evolution of the Porcupine gold camp (*after* Dinel 2007).

AM: Physical Volcanology of the Vipond Formation

STOP 1.1: PILLOW-LOBE DACITE, VIPOND FORMATION, V10B

This outcrop is located in Timmins (Stop 1.1 on Figure 5; UTM 5368120mN, 0477580mE, Zone 17, NAD 83) at the "Fire Tower" hill just northeast of the junction of Vipond road and the Moneta or "Back" road. Vehicles can be parked by the power line, leaving the gate to the access road clear. Today the hill is used for radio antenna, and the outcrops can be found by ascending the dirt access road to its top, and then proceeding a few metres to the west-northwest of the white telecommunications shed. The outcrops are within a few hundred metres of the former Vipond Mine, part of the McIntyre system. Initial work at this locality was conducted by Saumur (2005) as part of his BSc thesis and subsequently by Dinel (2007) as part of his PhD thesis, at the University of Ottawa.

In essence, the outcrops contain decimetre- to metre-scale, contorted, lobate, flow-banded, green- to buff-coloured pillow-lobes with abundant breccia (Figure 7). The rocks are composed of chlorite, albite and carbonate (calcite and ankerite), typical of the low degree of metamorphism in the area. Moreover, they were subjected to a penetrative deformation that produced a nearly vertical stretching lineation. Nonetheless their original textures are still well preserved. The characteristic feature of the outcrops, pillow-lobes, can be divided into three types, described below, that are related to their size, and therefore their cooling and alteration features. All pillow-lobes are surrounded by approximately 5 cm thick, dark-green-colored margins composed of extremely fine-grained altered glass composed of chlorite and carbonate. Note that the margins are aphyric and they have a "crumbled" look, resulting from in-situ primary brecciation as a result of shear during flow. In common with the remainder of the pillow-lobes, the margins have been complexly deformed while still plastic. All pillow-lobes are aphyric.

"Spherulite-core" pillow-lobes

In the largest pillow-lobes (≥ 1 m long), the margin gives way to a breccia zone of variable thickness (10 to 50 cm) consisting of millimetre-scale brecciated homogeneous or flow-banded aphyric chloritized and ankeritized glass. The fragments are blocky and angular with sharp boundaries and rotated clasts. In some places jigsaw-fit breccias can be observed. Perlitic fractures are evident in some clasts. Pore spaces between the clasts are filled with quartz, albite and calcite. Chloritized breccia appears massive on weathered surfaces, whereas ankeritized material shows a distinct mottled, porous texture, where clasts appear brownish-white because of carbonate dissolution. The latter is the material that was named "chicken-feed" by Graton et al. (1933), Griffis (1962), Ferguson et al. (1968) and Brisbin (1997). Flow banding defined by varioles (spherulites) is commonly observed in the brecciated zones and shows complex flow history and rotation. Also, a wrinkled or "ropey" structure is evident on some of the thinner extremities of the more contorted pillow-lobes.

The cores of these large pillow-lobes are of variable size (50 cm to 4 m long) and composed of altered aphyric glass containing abundant plagioclase spherulites. The spherulites weather white, and form millimetre-scale positive-relief mounds. In places, generally toward the centre of a particular pillow, the spherulites have impinged and form centimetre- to decimetre-scale white weathering amoeboid patches of rock. The spherulites are composed of fine radiating fibers of plagioclase in a matrix of chloritized former glass. Rarely, they have nucleated on the margins of gas bubbles. The cores of the pillows are evidently less brecciated and therefore were likely less

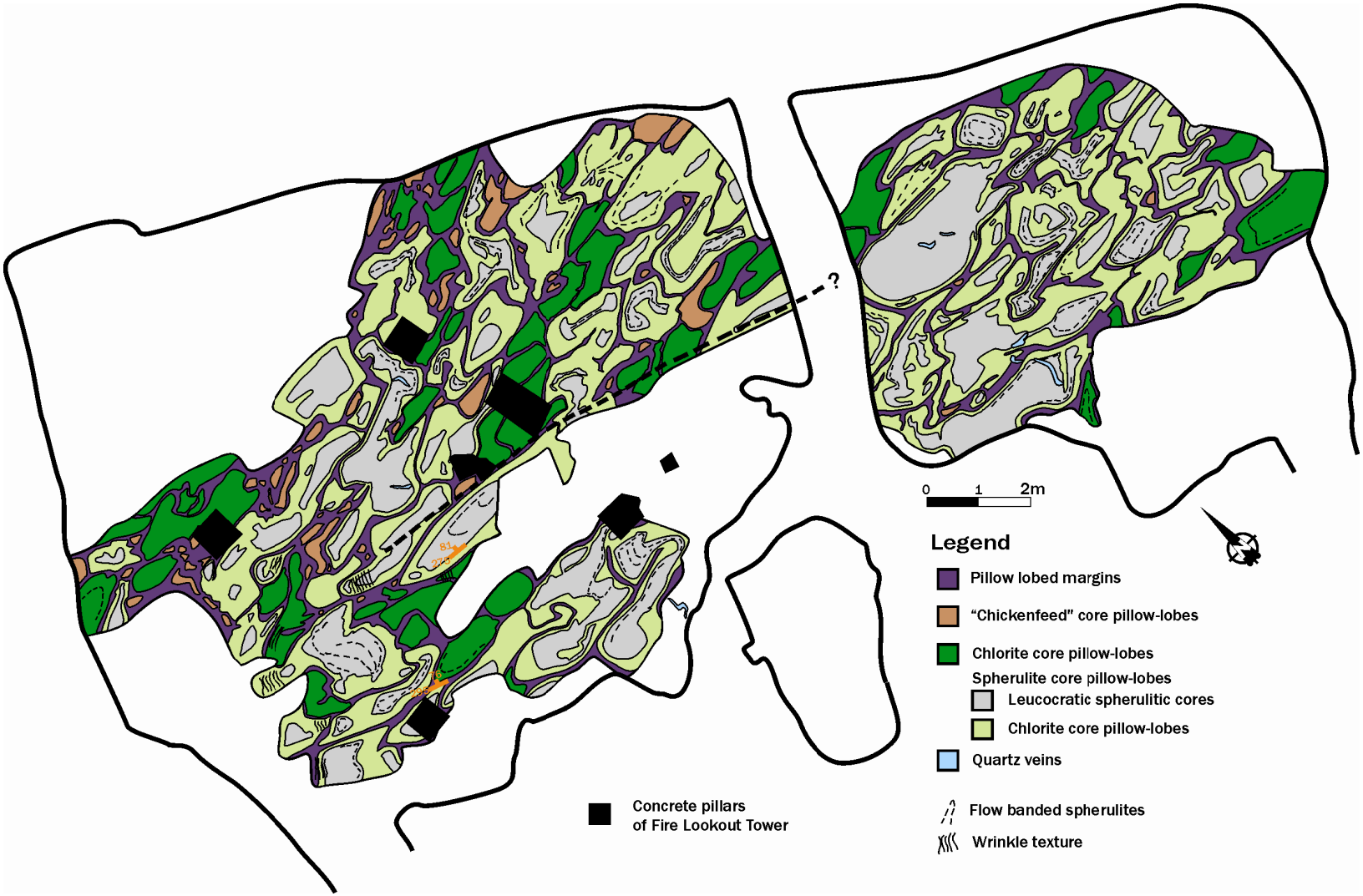

Figure 7. Geological map of the Fire Tower Hill outcrop, Stop 1.1 (*after* Saumur 2005).

permeable than their exteriors. Flow banding can commonly be traced within spherulitic cores. Figure 8 illustrates a section of an idealized spherulitic core pillow-lobe.

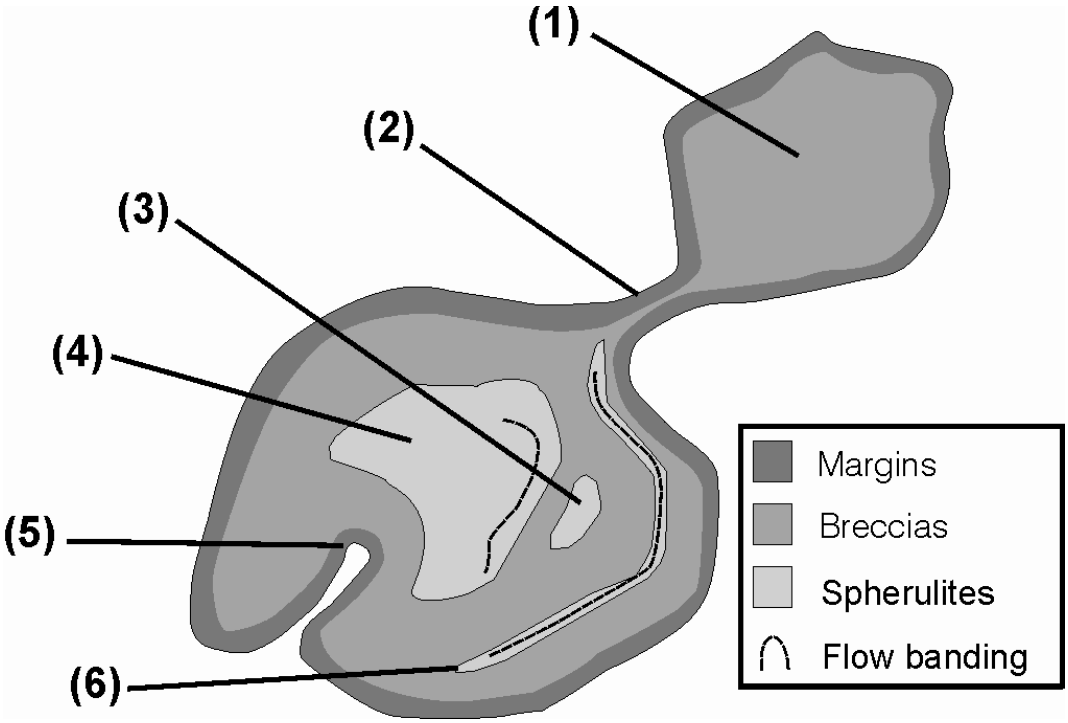

Figure 8. Idealized sketch of dacite pillow-lobe (*from* Dinel 2007). (1) Pillow-lobe containing no spherulites, constituent breccia may have a "chicken-feed" appearance. (2) Primary contortion and connection between two breccia zones as defined by margins (necking). (3) Observation of more than one spherulite-rich area in a pillow-lobe is common. (4) The boundary between spherulitic cores and breccia is generally diffuse: the spherulites are discrete at the core's edge and impinge on one another at the core's interior. Spherulite-defined flow banding is common. (5) Margins are generally severely contorted and can be in-folded (6) There is commonly flow banding in the brecciated material defined by spherulites.

Breccia-core pillow-lobes

Smaller pillow-lobes do not have the full range of features observed in the larger ones. Pillow-lobes ranging from approximately 40 cm to 1 m in size lack a spherulitic core and have chlorite breccia identical to that of the breccia zone of spherulitic pillow-lobes. There is usually a zone of ankerite rich "chicken-feed" surrounding these chloritic cores. The outer chicken-feed zone has more primary porosity than the chlorite breccia in the cores. Chlorite-core pillows commonly contain flow-banding defined by spherulites. Hence a distinction is made between spherulites concentrated in pillow-lobe cores and spherulites defining flow banding. Only the largest of these pillow-lobes are contorted in a similar fashion to spherulite-core ones.

Chlorite-core and ankerite "chicken-feed" core pillow-lobes

The smallest pillow-lobes are typically decimetre-scale brownish pods completely filled with "chicken-feed", and it is in these pillow-lobes that this texture is best developed as millimetre- to centimetre-scale void spaces related to primary brecciation. The perimeter walls of the void spaces are quasi-planar, stand out in relief, and meet at well-defined corners. However, the carbonate within the voids is recessively weathered forming conspicuous hemi-spherical pits,

giving the false impression that the texture is composed of broken spherical fragments (i.e., spherulites).

Both these pillow-lobe types are similar in the sense that they are both almost entirely composed of breccia, are smaller than, and not as deformed as, spherulite-core type pillow-lobes. We interpret both pillow-lobe types as having had the same primary volcanic origin, but alteration played a major role in determining their appearance on weathered surfaces. Penetrative chloritization is associated with regional metamorphism (Thompson 2005), whereas ankeritization overprints it. The ankeritization is later, and related to hydrothermal fluids, and was evidently dependent on permeability as only the smallest of pillow lobes are completely ankeritized.

Geochemistry of the V10B unit

The REE patterns for the V10B unit in the Fire Tower Hill area (Figure 9) are "flat", roughly 40 to 70 times chondrites, and have no conspicuous Eu anomalies. The flat patterns are typical of rocks of the tholeiitic suite in the area, wherein basalts have roughly 10 times chondrites and rhyolites approximately 100 times chondrites. The REE analyses and other geochemical analyses we have undertaken, plus the observations of flow banding, contorted geometry and abundant breccia, are all consistent with the rocks being intermediate (dacite) in composition.

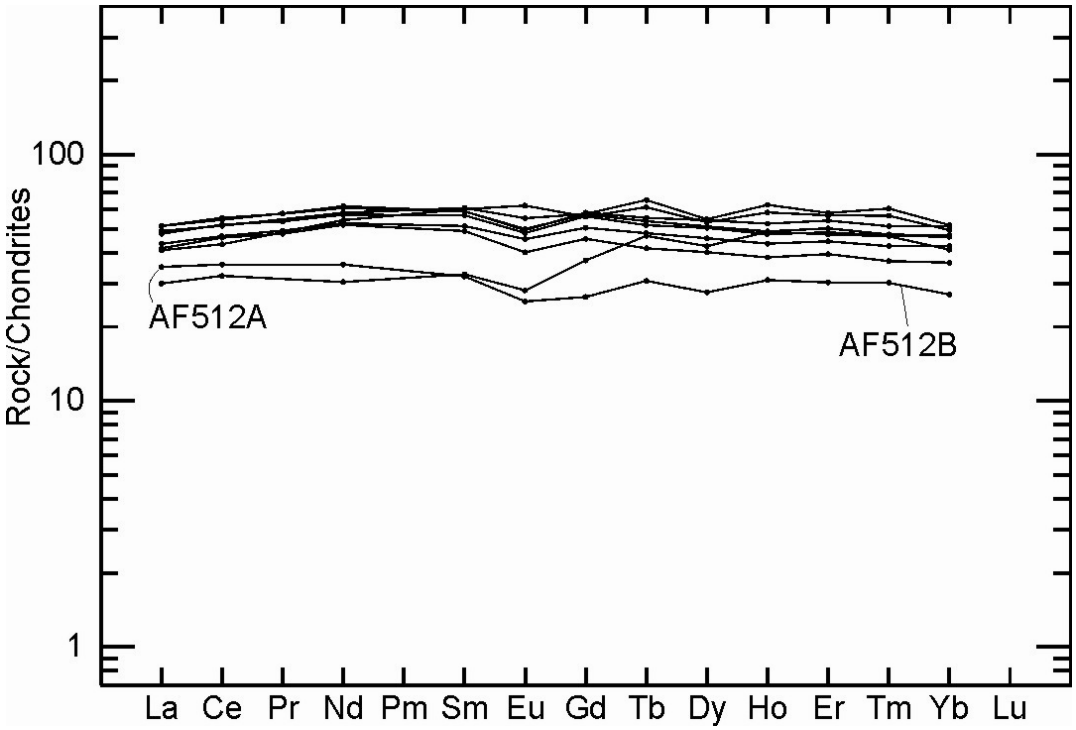

Figure 9. Chondrite-normalized REE plot of V10B rocks of the Fire Tower Hill outcrops and two other V10B localities in Timmins (AF512A and B) (*from* Dinel 2007).

Interpreted formation of pillow-lobes

We interpret the pillow-lobes to represent tubes and lobes formed during subaqueous flow, with some brecciation and flow-banding having been caused by movement during emplacement. Further brecciation was caused by thermally driven granulation.

Large pillow-lobes are characterized by a thin margin that gives way to a breccia zone and finally to a spherulitic core. We interpret the zones to be related to the thermal history of the melt as it cooled. The contorted nature, banding and tortuous outline of many of the pillow margins is evidence that the lava was viscous in comparison to basaltic melts, and that it most likely flowed down a reasonably steep gradient once it was erupted. It would appear that the exterior of the lava lobes cooled quickly below the glass transition, stiffened and brecciated. Only in the very large pillow-lobes was there sufficient time for crystallization to take place, rather than quenching to glass. Even so, the crystals that formed are spherulites, indicative of the viscous nature of the melt and its superheated or crystal-free state at the time of nucleation and crystallization. Small pillow-lobes are far less folded and more intensely brecciated because they were quenched quickly to glass. The fact that the rocks are aphyric means that they were erupted in a superheated state. Therefore, the melt viscosity was reduced at time of eruption, thus explaining why the dacites formed pillow-lobe flows, rather than the more typical dome facies.

Economic significance

The V10B rocks are good hosts for both the abundant vein and disseminated gold mineralization of the Porcupine camp. They have a rheological contrast with more ductile mafic rocks that would have allowed for the opening of space and vein formation during deformation. They are also good hosts for disseminated mineralization found at the camp (e.g., Hurst 1935) because they are permeable, were largely composed of reactive glass, and have high Fe/Mg ratios. Hurst (1935) reported a correlation between the Fe content of the wall rocks and gold content in the camp, and Ropchan et al. (2002) noted a similar relationship at the Holloway Mine further to the east. Bohlke's experimental work (1988) demonstrated that an elevated Fe/Mg ratio favors the formation of pyrite from gold thio-complexes and the scavenging of gold from solution, whereas low Fe/Mg rocks tend to form carbonate rather than pyrite. The common link between variolitic rocks and gold mineralization may in part lie in the fact that spherulites (varioles) are more common in the Fe-enriched tholeiitic suite than in the calc-alkalic rocks.

STOP 1.2: VARIOLITIC BASALTS, VIPOND FORMATION, V8 UNIT

This outcrop is located in the Schumacher part of Timmins, south of Highway 101 (Stop 1.2 on Figure 5; UTM 5368950mN, 0478180mE, Zone 17, NAD 83). Variolitic flows are an integral part of Archean metavolcanic assemblages in the Timmins area and occur within several assemblages within the Abitibi greentone belt. Ferguson et al. (1968) show that the V8 unit is dominated by effusive flows and composed of a number of different subunits. In general, the salient characteristics of the V8 unit are that it is composed of large pillows, approximately 3 to 20 m in diameter, thick hyaloclastite and locally abundant varioles. Unfortunately we are unaware of any well-preserved outcrops of variolitic pillow-basalt in the Timmins area. The V8 unit at this locality occurs as stretched and sheared pillows in which the spherulites can no longer be identified by their fibro-radial habit. These variolitic pillowed flows are part of the V8 unit of the Tisdale assemblage and were used as marker units by Ferguson et al. (1968) to map stratigraphy in the area, and our stop at this locality is designed to show the general morphology of the variolitic flows.

Varioles are centimetre-sized globules within fine-grained mafic rocks. Fowler et al. (1986) have shown that within Archean pillow basalts they are spherulites, chiefly plagioclase in composition, and grown directly from the melt above the glass transition, not through subsequent devitrification. Typically, they form in aphyric basaltic lavas of the tholeiite suite that were superheated (i.e., crystal free). Quenching during eruption causes a predictable progression of crystal morphologies from the cooling margin to the pillow core, from crystal-free in-situ brecciated glass, to glass containing small fine spherulites, to glass containing large coarse

spherulites, to completely spherulitic material, to dendritic plagioclase crystals. Typically the varioles are found as roughly 20 cm thick bands of cream-coloured ovoids within a fine-grained green chloritized matrix near the pillow margin, though in some cases the spherulites may be concentrated in the pillow cores.

COMPARISON BETWEEN V10B AND V8 UNITS

The V10B unit of the Vipond formation is a pillow-lobe dacite having abundant breccia, flow-banding, and a distinctive zonation, which serve to distinguish it from basalts of the V8 unit, though field discrimination can be difficult. The dacites formed as flows rather than domes because they were superheated and therefore relatively inviscid. The association of gold mineralization with spherulitic rocks is likely related to the high iron content of the tholeiitic suite with which spherulitic rocks are associated. Based on work at the Holloway Mine wherein the gold content is correlative with the Fe/Mg ratio of the host rocks, pillow-lobe dacites may be better hosts to mineralization than pillow basalts, making the need for distinguishing between the two important.

Lunch

Geology and Stratigraphy of the Shaw Dome

The main structural feature in the Shaw Dome is a southeast-trending antiform with a shallow southeast plunge centred in Shaw Township (Figures 10 and 11). The volcano-sedimentary strata young outward from the centre of this structure with a moderate northeast dip on the northeast limb, and a steep northwest dip on the northwest limb. With the exception of a few dike swarms (Matachewan and Abitibi) and minor Proterozoic sedimentary rocks in the southeast part of the map area, all the bedrock is Archean in age. Intrusions within the supracrustal rocks are dominantly felsic intrusions with subordinate feldspar and quartz porphyry, and ultramafic to mafic intrusions.

A highly strained deformation zone, approximately 100 m wide, is located in northern Deloro Township and is interpreted as the the locus of the Porcupine–Destor deformation zone (PDDZ). Here, the stratigraphy is highly complicated by the presence of a number of facing reversals related to this deformation zone. Numerous north-northwest-trending faults traverse the map area. South-dipping normal faults also occur in the southeast part of the Shaw Dome. This fault is affected by the main folding event in the Shaw Dome, supporting its early nature, and has resulted in tectonic superposition of Deloro assemblage strata over the younger Tisdale assemblage in the southern margin of the Dome.

Establishment of a stratigraphic distribution of the main lithological units has evolved over the years. Almost all previous stratigraphic schemes in the Shaw Dome subdivided the volcano-sedimentary succession in the Shaw Dome area south of the PDDZ into two main entities, currently identified from oldest to youngest as the Deloro and the Tisdale assemblages. In this contribution, based on new geochronology, we refine stratigraphic subdivision in the Shaw Dome into *Middle*, and *Upper Parts* of the Deloro assemblage, and into *Lower* and *Upper Sections* within the Lower Part of the Tisdale assemblage (Figure 12).

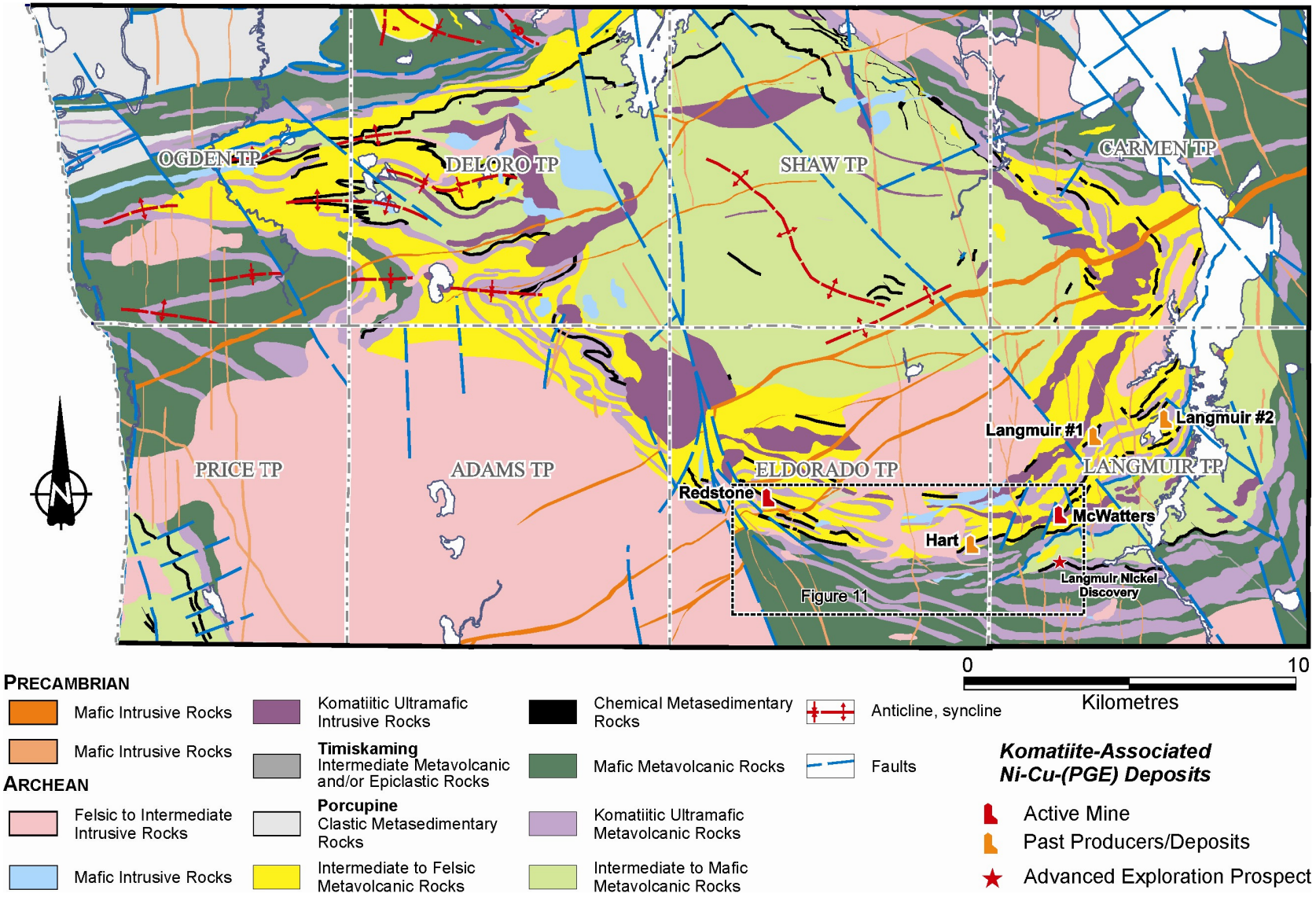

Figure 10. Simplified geological map of the Shaw Dome area showing main komatiite-associated Ni-Cu-(PGE) deposits in this area (*modified from* Houlé and Hall 2007).

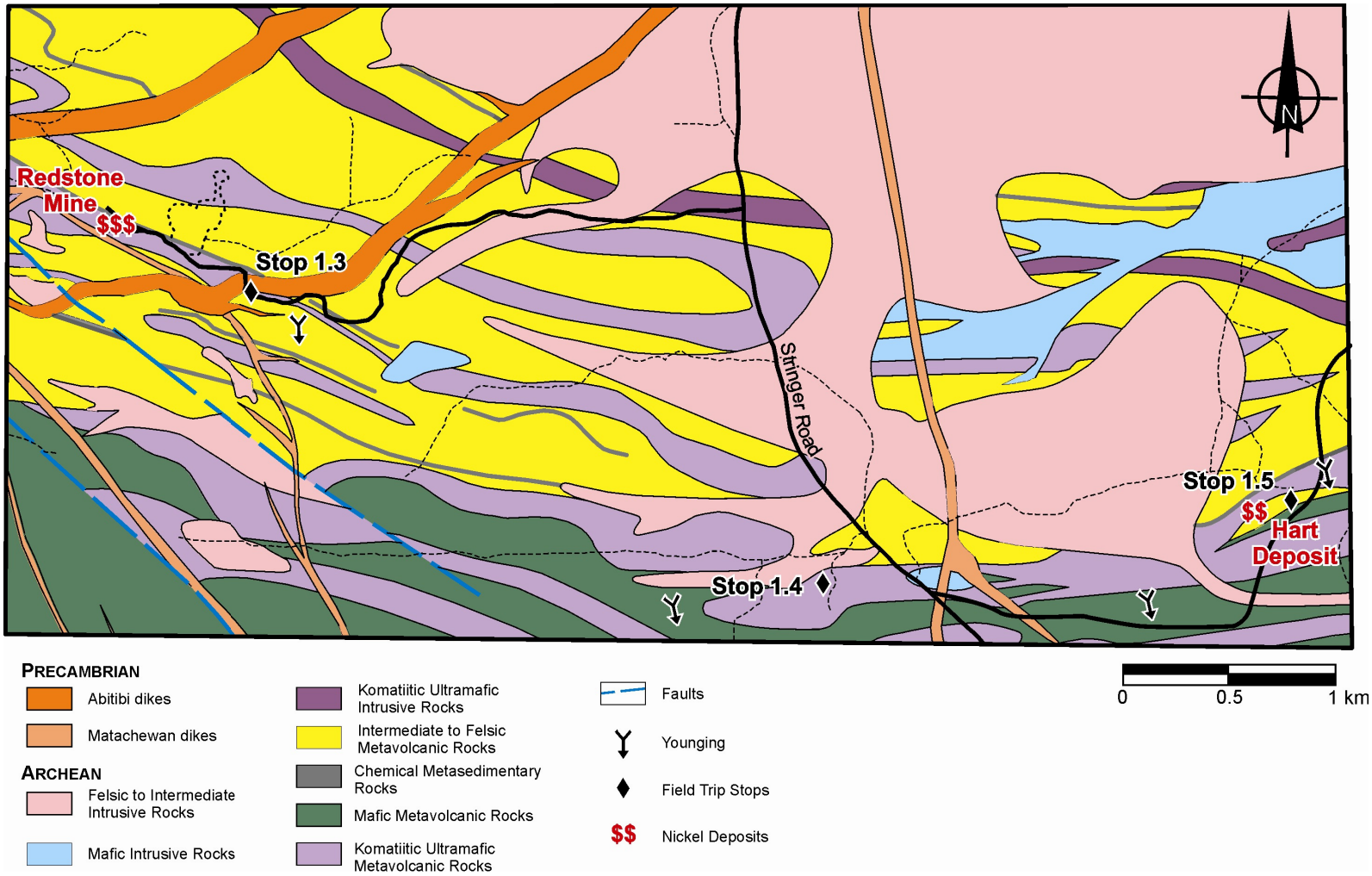

Figure 11. Close-up view of the geology in the area of stops 1.3 to 1.5, Shaw Dome area (*modified from* Houlé et al. 2004).

DELORO ASSEMBLAGE

Middle Section

The *Middle Section* of the Deloro assemblage is located in the central portion of the Shaw Dome structure and is composed dominantly of a coherent facies of calc-alkalic intermediate to mafic metavolcanic rocks with lesser intermediate volcaniclastic rocks. Flows are pillowed to massive, commonly amygdaloidal and plagioclase-phyric. Several horizons of iron formation occur throughout much of the *Middle Section*. They occur as small and discontinuous oxide-bearing iron formation horizons within, and as three thick, largely parallel and relatively continuous oxide-bearing iron formation horizons near the top of the *Middle Section* along the northeast flank of the Shaw Dome (Shaw Township). Small discontinuous units of felsic volcanic rocks also occur near the top of the *Middle Section* near the contact with the Tisdale assemblage rocks. Those units yielded an imprecise U-Pb age of 2727±12 Ma (Ayer et al. 2005). However, it is unclear if this represents the uppermost part of the *Middle Section* or constitutes the base of the Upper Section, because regionally extensive iron formation horizons occur in both sections.

Upper Section

The *Upper Section* is located exclusively in the northern part of Deloro Township within a 100 m wide highly strained zone, interpreted as the Porcupine–Destor deformation zone (L.A.F. Hall, OGS, personal communication, 2003). This package is composed of felsic fragmental metavolcanic rocks, with abundant lapilli-size fragments, including some "fuchsitic" or green mica fragments and rare quartz eyes. Felsic lapilli tuff from this package yielded a U-Pb age of 2724.1±3.7 Ma (Ayer et al. 2005). Several iron formation horizons also occur within the *Upper Section* of the Deloro assemblage. However, one thick and relatively continuous oxide-bearing iron formation horizon appears to occur near the base of the *Upper Section*.

TISDALE ASSEMBLAGE

Lower Section of the Lower Part

The *Lower Section* of the Lower Part of the Tisdale assemblage is located in the southeastern margin of the Shaw Dome structure. It consists of intermediate to felsic fragmental metavolcanic rocks (lesser coherent facies), iron formation, and ultramafic flows and intrusions. This package is interpreted as part of theTisdale assemblage (Houlé and Hall 2007) based on geological relationships and geochronology. A felsic volcanic rock, footwall to Langmuir Mine #2, yielded a U-Pb age of 2708±2 Ma (Barrie and Corfu 1999). This is the lowermost part of the Lower Tisdale and appears to be absent north of the PDDZ (see above). Several horizons of iron formation occur at different stratigraphic levels within this sequence.

Upper Section of the Lower Part

The *Upper Section* of the Lower Part of the Tisdale assemblage is located around the outer margins of the Shaw Dome structure. This supracrustal package consists of a coherent facies (pillowed to massive) of tholeiitic mafic metavolcanic rocks intercalated with a coherent facies (massive to organized flows) of komatiitic basalt and komatiite metavolcanic rocks. This part of the Shaw Dome stratigraphy is most likely correlative with the Hersey Lake formation in the Porcupine camp.

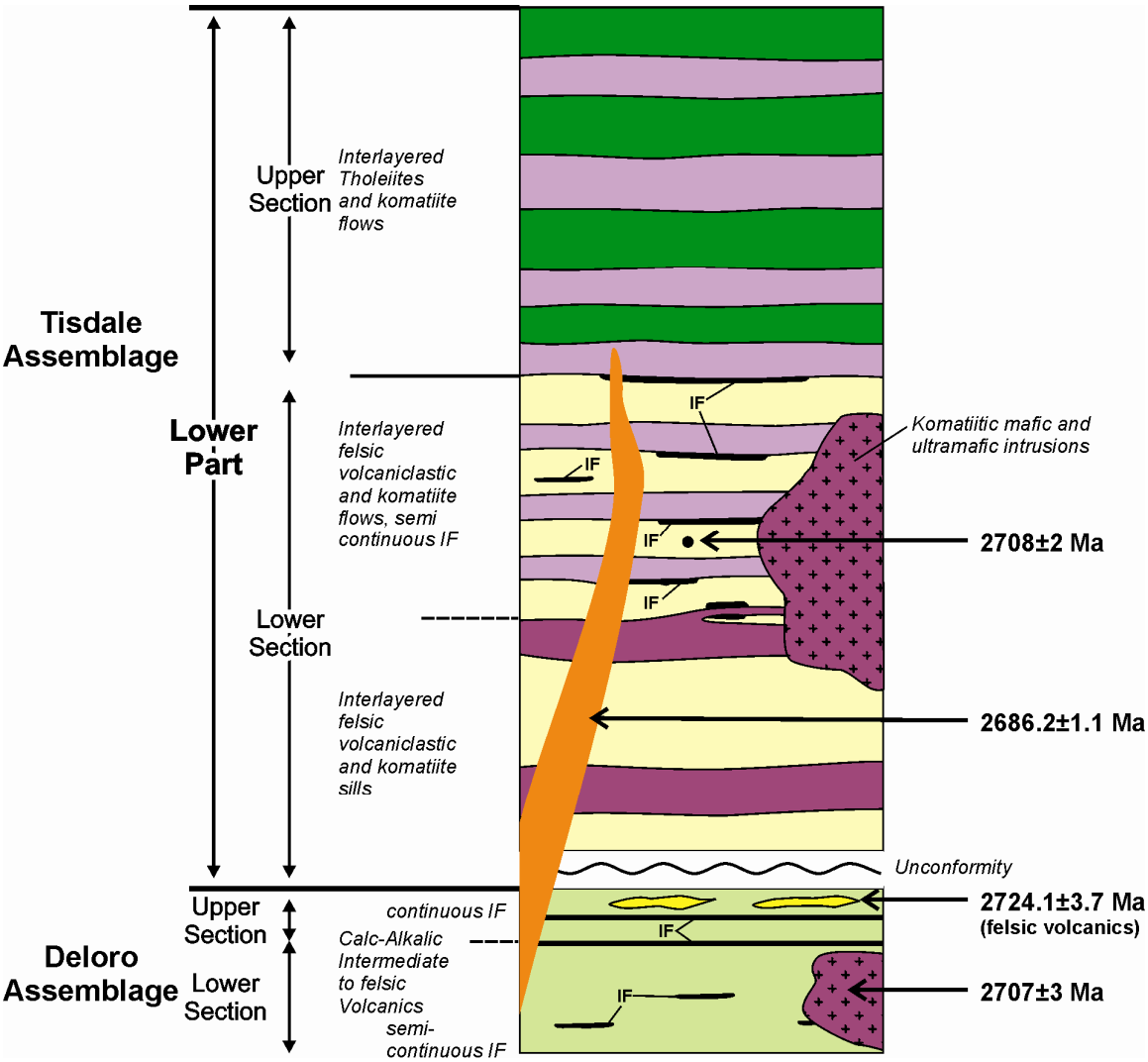

Figure 12. Schematic stratigraphic column of the Shaw Dome area south of the Porcupine–Destor deformation zone, illustrating the main volcano-sedimentary formations. Age constraints are U-Pb ages from Ayer et al. (2005) and unpublished data from Houlé.

PM: KOMATIITE VOLCANOLOGY IN THE SHAW DOME AREA

STOP 1.3: REDSTONE POWER LINE – KOMATIITE

The Redstone Power Line outcrop (Stop 1.3; UTM 5351174mN, 0488565mE, Zone 17, NAD 83) is located in the central part of Eldorado Township and is accessible via Redstone Mine road leading westward from Springer Road. This outcrop is located on the north side of the old mine access road under the power line.

The Redstone Mine is a Type I (basal contact), komatiite-associated Ni-Cu-(PGE) deposit. It was discovered in 1977, where the main ore zone (R Zone) was historically delineated over a strike length of 274.3 m, to a depth of 335 m with widths up 15.5 m. The nickel sulphide mineralization occurs as vein-like massive sulphides with associated stringer and blebby sulphides. Historically, 276 700 tonnes grading 2.4% Ni was mined from the upper 213 m of the deposit between between 1989-92 and 1995-96. When mining ceased, an inferred resource of 182 000 tonnes grading 3.28% Ni remained above the 335 m level. Since then, Liberty Mines Inc. has brought the Redstone Mine back into full production as of July 2007. At July 2007, the mineral resources were 274 000 tonnes grading 2.67% Ni measured, 145 000 tonnes grading 1.70% Ni indicated, and 148 000 tonnes grading 3.44% Ni inferred (Cole 2007).

The Redstone Power Line outcrop (Figure 13) is located along strike from the main ore zone of the Redstone Mine, less than 1000 m from the mine site. It consists of several flows exhibiting both lower and upper contacts. Most of them are relatively thin komatiite flows with a lower olivine cumulate zone and poorly-differentiated upper spinifex-textured zone. The facing direction on this outcrop is to the south, based on the distribution of the B Zones/A Zones. The lower cumulate zones of most of the flows are relatively well-preserved and exhibit polysutured jointing, whereas the upper spinifex zones of these flows are intensely deformed. The uppermost flow is composed essentially of olivine mesocumulate with some spinifex-textured clasts in the western part of the exposure. The presence of clasts is important because they suggest a moderate to high dynamic environment, one of the critical factors for the genesis of nickel sulphide mineralization in komatiite lava flows.

STOP 1.4: REDSTONE PAVEMENT I – KOMATIITE

The Redstone Pavement I outcrop (Stop 1.4; UTM 5349700mN, 491580mE, Zone 17, NAD 83) is located in the central part of Eldorado Township and is accessed by a trail leading westward from the Springer Road approximately 1.5 km after the turn-off for the Redstone Mine.

The Redstone Pavement I outcrop (Figure 14) is located along strike from the main ore zone of the Hart Deposit, less than 2.5 km from the new trenches that expose the basal footwall contact (see Stop 1.5). Three flows are exposed in the outcrop, but only the middle one is completely exposed, with both lower and upper contacts visible. Two of these have relatively thick (~20 m) lower cumulate “B” zones, which are locally intensely polysutured. These zones are composed mainly of texturally well-preserved meso- to orthocumulate komatiite containing serpentine pseudomorphs after medium-grained (1-2 mm) euhedral olivine. The lower and middle flows have relatively thin (~4 m) upper “A” zones composed of very coarse-grained olivine crescumulate komatiite and coarse- to medium-grained random olivine spinifex-textured komatiite, but no fine-grained random spinifex-textured komatiite or flow-top breccia. The contacts with the overlying flows are very sharp and wavy (contact between the lower and the middle flows) or very sharp and jigsaw-textured with small dikes of fine-grained komatiite

injected into the overlying cumulate rock (contact between the middle and the upper flows). The cumulate zones of the thickest two flows contain small (5 cm) subrounded pods of fine- to medium-grained olivine spinifex-textured rock with very sharp margins that may represent xenoliths or less likely pockets of trapped liquid. These pods are common in the lower parts of the cumulate zones and are absent in the upper parts of the cumulate zones. These lower cumulate portions that contain spinifex-textured clasts are similar to what was observed on the previous stop (Stop 1.3), but more abundant. Furthermore, a similar horizon is also present within the Galata showing, another nickel deposit associated with komatiites in the Shaw Dome.

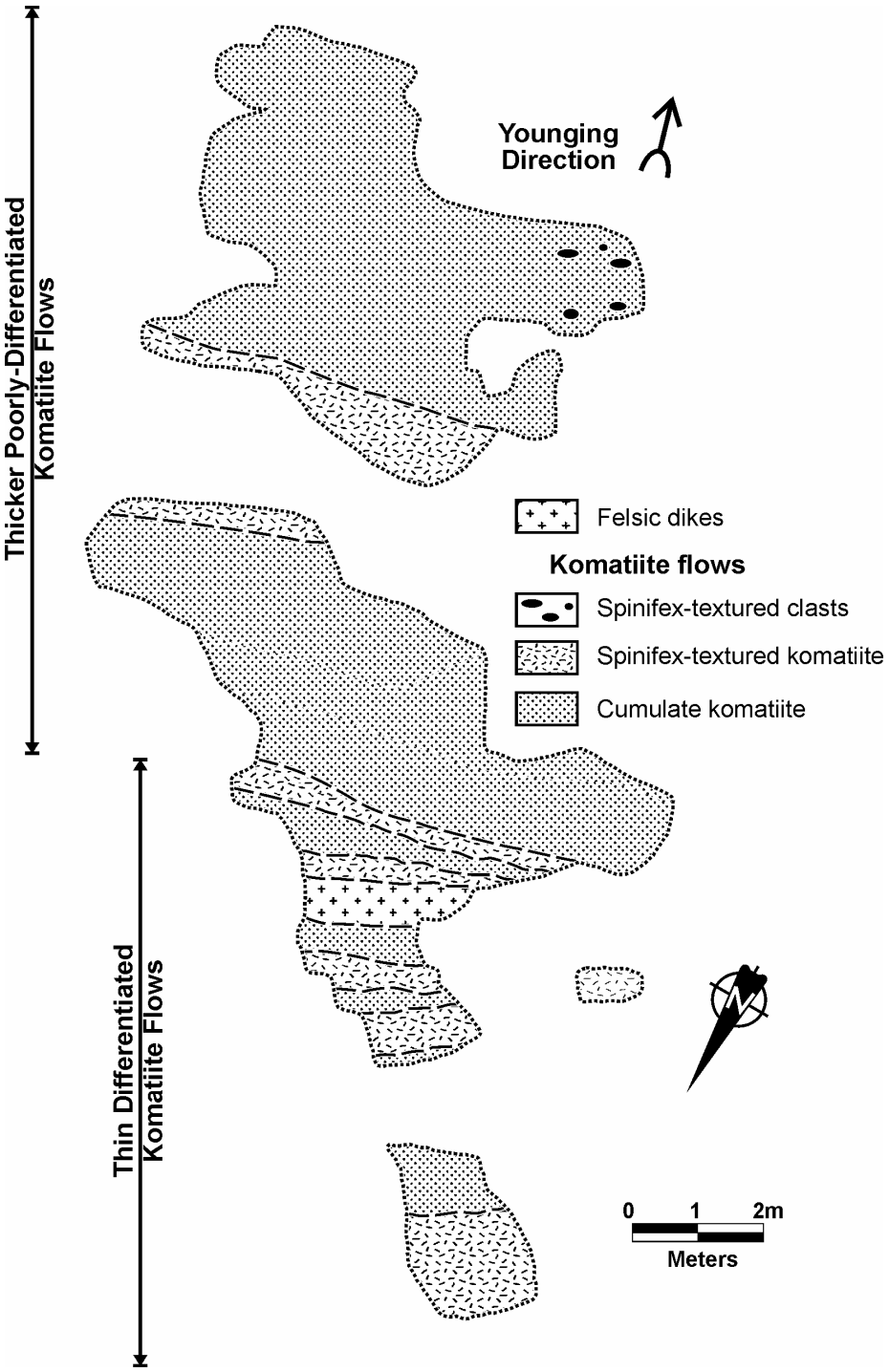

Figure 13. Simplified geological map (by M. Houlé and C. Guilmette) of the Redstone Power Line outcrop, Stop 1.3.

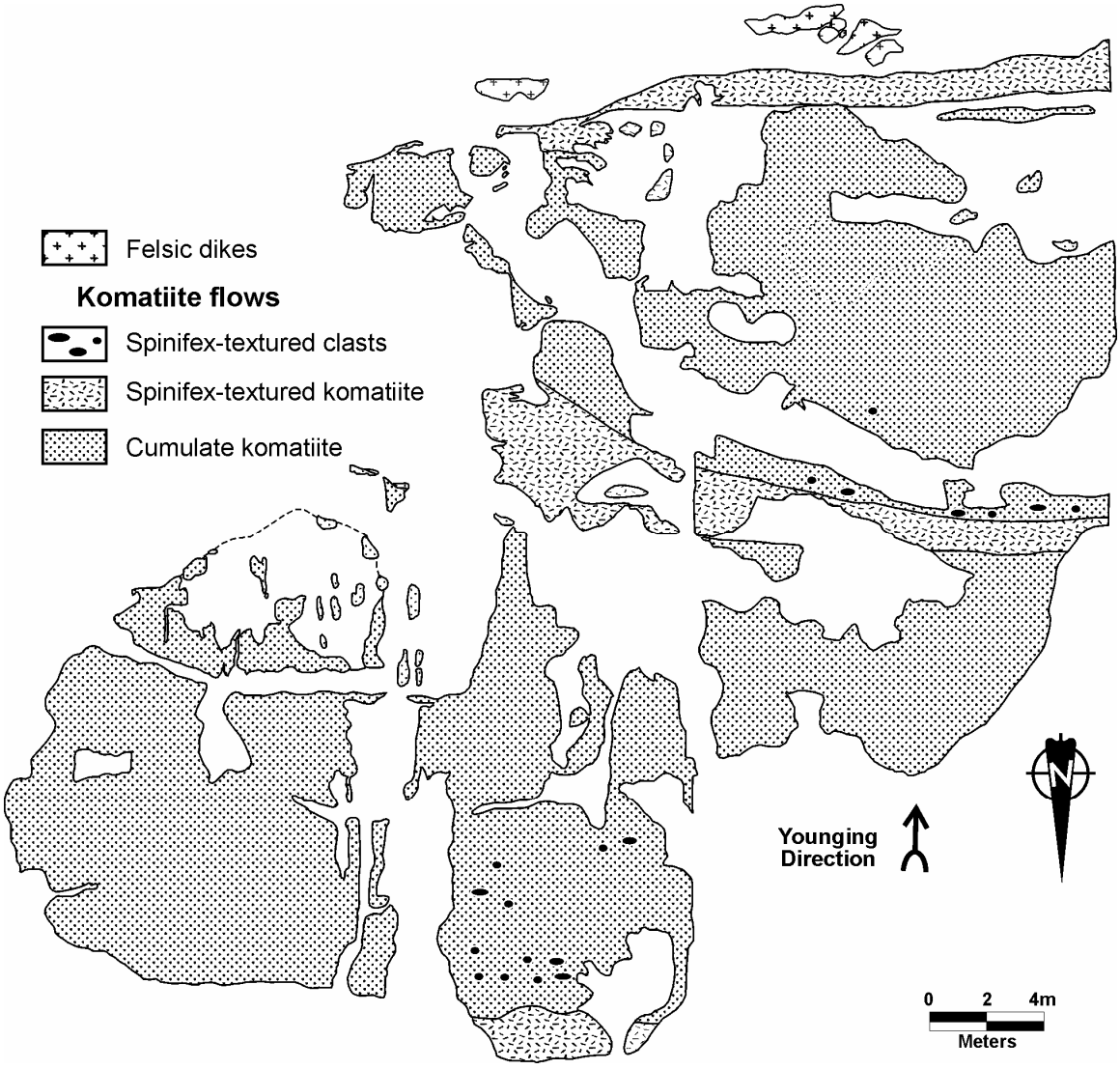

Figure 14. Simplified geological map (by M. Houlé) of the Redstone Pavement I outcrop, Stop 1.4.

STOP 1.5: HART DEPOSIT

These outcrops (Stop 1.5; UTM 5350200mN, 493980mE, Zone 17, NAD 83) are located in the southern part of Eldorado Township along the boundary with Langmuir Township. They are accessible through a gravel road that branches out to the east from the Springer Road approximately 2.5 km after the turn-off for the Redstone Mine road. This stop consists of a series of trenches (5) mechanically stripped and hydraulically cleaned by Liberty Mines Inc. in January 2008, that cross the mineralized zone of the Hart Deposit (Figure 15).

The Hart deposit is a Type I (basal contact), komatiite-associated Ni-Cu-(PGE) deposit hosted within an olivine ortho- to mesocumulate komatiite. The ore zone occurs along the full

200 m strike length of the footwall embayment, where the footwall rocks are composed of sulphide and oxides facies banded iron formation and felsic volcaniclastic rocks. The ore profile is composed of massive sulphides overlain by an envelope of net-textured and disseminated sulphides. Blebby sulphides also occur locally.

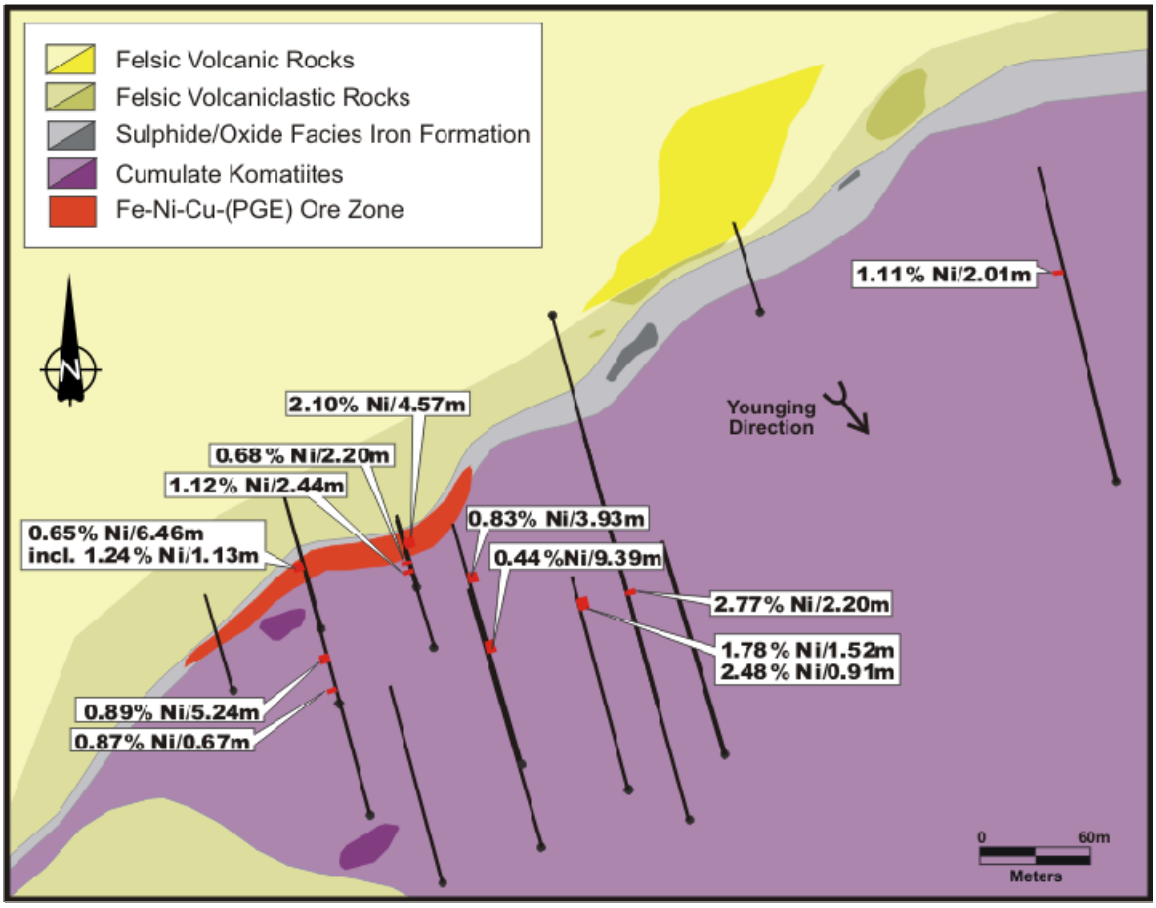

Figure 15. Geology of the Hart Ni-Cu-(PGE) deposit in Eldorado Township, Stop 1.5 (*after* Brereton 2004).

Day 2: Physical Volcanology of Munro Township

by M.G. Houlé, B.R. Berger, B. Moulton, A.D. Fowler and E. Dinel

THE KIDD–MUNRO ASSEMBLAGE FROM KIDD CREEK TO THE QUÉBEC BORDER

The part of the Kidd–Munro assemblage extending from Kidd Township to the Québec border, is well recognized for its mineral endowment, with several VMS deposits such as the giant Kidd Creek Mine, the Potter Zn-Cu deposit, and the Potterdoal deposit, and several komatiite-associated Ni-Cu-(PGE) deposits such as the Alexo Ni-Cu mine, the Kelex, Dundeal and Dundonald South Ni-Cu deposits (Figure 16).

The *Lower Part* of the assemblage is composed predominantly of calc-alkalic intermediate, felsic with rare mafic metavolcanic rocks and U-Pb zircon ages ranging between 2719 and 2716 Ma (Ayer et al. 2002). Volcanic facies are predominantly tuff, lapilli tuff and heterolithic tuff breccia with lesser pillowed and massive flows. These rocks are exposed mainly in three areas: 1) east of the Potter Mine in McCool, Rand and Holloway townships; 2) east of Frederick House Lake in the footwall to the Ni-Cu mineralization in Dundonald Township; and 3) east of the Kidd Creek Mine, intercalated with tholeiitic metavolcanic rocks in Prosser Township. Most of the *Upper Part* of the assemblage is composed of komatiitic and tholeiitic basalt and rhyolite with U-Pb zircon ages ranging between 2716 to 2711 Ma (Bleeker et al. 1999; Ayer et al. 2002; Berger et al. 2007). Tholeiitic mafic metavolcanic rocks represent the major component of the *Upper Part* of the Kidd–Munro assemblage and are composed predominantly of massive and pillowed mafic flows with lesser flow breccia and rare mafic volcaniclastic horizons (i.e., Potter Mine), typical morphologies of most Archean greenstone belts. Komatiitic metavolcanic rocks (komatiites to komatiitic basalts) are composed of classic layered komatiite flows, initially described by Pyke et al. (1973) in Munro Township, that exhibit a lower cumulate zone (B zone) and an upper spinifex zone (A zone), thick differentiated layered komatiite flows (from peridotite to gabbro), and undifferentiated olivine cumulate flows. Tholeiitic felsic metavolcanic rocks (i.e., high-silica rhyolite) are composed of aphyric to densely quartz and feldspar phenocrystic flows, autoclastic breccias, tuff, lapilli tuff, and rare spherulitic flows. Individual spherules within those spherulitic flows could be up to 3 cm in diameter.

This part of the Kidd–Munro assemblage is structurally complex with evidence for a number of folding and faulting events along its roughly 160 km strike length. The southern boundary is in fault contact with younger clastic metasedimentary rocks of the Porcupine assemblage (Bleeker 1999; Berger et al. 2007). This faulted contact is complex in the western part of this segment of the assemblage, suggesting that metavolcanic units are imbricated with metasedimentary units. In the eastern part of the Kidd–Munro assemblage the contact with the Porcupine assemblage corresponds to the Pipestone Fault. Significant portions of the Kidd–Munro stratigraphy are missing, suggesting the Pipestone Fault is most likely a major thrust fault (Berger et al. 2007). Participants will see this contact area along the Croesus Road stop. The northern contact of the assemblage is poorly constrained but is inferred to be a faulted contact with a number of different bounding assemblages along its length and thus differs from the southern contact. Early folding of the Kidd–Munro assemblage is characterized by gently plunging upright folds with axes trending roughly east-west. A late tectonic event generated northwest-striking faults, across which dextral offset is combined with east-side-down vertical movement. Although the movement on each individual fault may be small, the net effect is to expose stratigraphically younger parts of the Kidd–Munro assemblage east of Frederick House Lake.

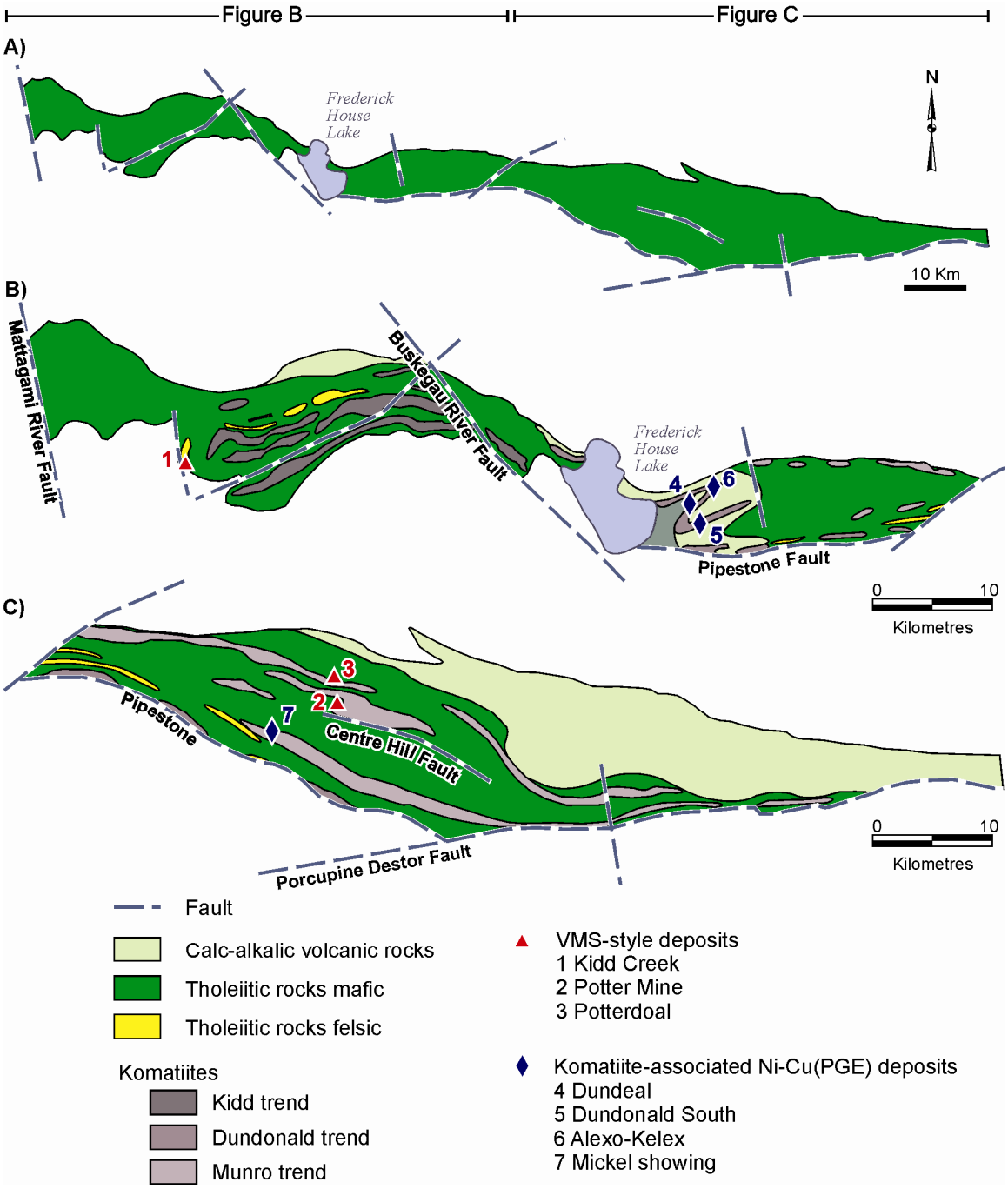

Figure 16. A) Simplified geology of the Kidd–Munro assemblage from the Mattagami River fault to the Porcupine–Destor fault. B) Close-up of the western section of the Kidd–Munro assemblage, showing the distribution of base metals deposits and major lithologies such as komatiite flows/intrusions and tholeiitic rhyolite (high-silica rhyolite). C) Close-up of the eastern section of the Kidd–Munro assemblage, showing the same features as B. (*Modified from* Ayer et al. 2005.)

Reconstruction of the Kidd–Munro volcanic stratigraphy was conducted at local scales within different parts of the assemblage by several workers over several years (Table 4). The first attempts to reconstruct the volcanic stratigraphy of the Kidd–Munro assemblage over most of its strike length was conducted by Barrie (1999) under the Kidd–Munro Extension Project, a collaborative project between the Ontario Geological Survey (OGS), mining industry, and the Geological Survey of Canada (GSC). Recent studies in the past few years are being carried out under the Targeted Geoscience Initiative-(TGI-3), an ongoing collaboration between the GSC, the OGS and the Ministère des Ressources naturelles et de la faune du Québec. As part of this collaboration, the work on the Kidd–Munro project is designed to reassess the Kidd–Munro assemblage and work to date has provided new data, which has been incorporated into the preliminary stratigraphic correlations discussed below.

Table 4. Researchers involved in the reconstruction of the Kidd–Munro volcanic stratigraphy, within the Ontario portion of the Abitibi greenstone belt.

Area	Researcher(s) and Year of Publication
Kidd Creek	Bleeker 1999; DeWolfe 2004
Prosser Township	Berger et al. 2007
Dundonald Township	Davis 1997; Barrie et al. 1999; Houlé et al., in press
Munro Township	Arndt et al. 1977; Johnstone 1987, 1991; Davis 1997

Recent regional mapping, geochronology, stratigraphic and structural interpretations provide for three main correlations along the main part of the Kidd–Munro assemblage: 1) identification of the *Lower Part* of the assemblage; 2) the position of komatiites in at least three different stratigraphic intervals; and 3) the position of tholeiitic rhyolites at two different stratigraphic intervals, both occurring within the *Upper Part* of the assemblage.

In the west, the calc-alkalic metavolcanic rocks in Prosser Township are correlated with the *Lower Part* of the Kidd–Munro assemblage, based on their U-Pb zircon geochronology and stratigraphic facings, which indicate that they consistently underlie the tholeiitic metavolcanic rocks (Berger et al. 2007). A similar stratigraphic succession is observed in the eastern part of the assemblage near the Québec border. In Dundonald and Wilkie townships in the central part of the assemblage, the stratigraphic position of calc-alkalic rocks is less well understood, but they most likely also belong to the *Lower Part*. Widespread hydrothermal alteration in Prosser Township accompanied by mineralized stringers of zinc and copper indicate that these rocks are also prospective hosts for VMS mineralization within the *Lower Part* of the Kidd–Munro assemblage.

Tholeiitic rhyolitic metavolcanic rocks (high-silica rhyolite) occur at two distinct stratigraphic intervals within the *Upper Part* of the Kidd–Munro assemblage. The lowermost horizon occurs predominantly within the western portion of the assemblage and is host to the giant Kidd Creek Cu-Zn VMS deposit. It yields a U-Pb age of 2716.0±0.6 Ma (Bleeker et al. 1999) and has been extended at least 15 km east into Prosser Township (*see* Figure 5) (Berger et al. 2007). This lower rhyolite interval is also interpreted to occur within the eastern section of the Kidd–Munro assemblage, around Munro Township. If true, this correlation implies that much of this lower stratigraphic has been removed in between these areas by thrusting along the Pipestone Fault. The uppermost tholeiitic rhyolite occurs from Clergue to Beatty townships and has a U-Pb age of 2714.3±0.8 Ma (Berger et al. 2007). Widespread hydrothermal alteration is associated with the uppermost high-silica rhyolite, with an age of 2710±1.5 Ma in Wilkie Township (Barrie 1999), but economic base metal mineralization has yet to be found in this area.

Komatiitic metavolcanic rocks (komatiites to komatiitic basalts) occur at three or possibly four stratigraphic intervals within the Kidd–Munro assemblage. The komatiitic rocks occur semi-continuously along the entire strike length of the Kidd–Munro assemblage, but can be subdivided into three major trends: the Kidd trend (from Kidd to Tully townships); the Dundonald trend

(from Dundonald to Munro townships); and the Munro trend (from Clergue to Garrison townships) (*see* Figure 16). The Kidd trend occurs predominately within the western extension of the assemblage where komatiites comprise the footwall to the Kidd Creek deposit and are overlain by the lowermost high-silica rhyolite, yielding a U-Pb age of 2716 Ma. The Dundonald trend occurs predominately within the central section of the assemblage where it is coeval with calc-alkalic rhyolite yielding a U-Pb age of 2717 ± 1.2 Ma (Barrie and Corfu 1999). Komatiitic rocks that probably belong to this trend also occur sporadically along the Pipestone fault at the contact between the Kidd–Munro and the Porcupine assemblages, further suggesting tectonic removal of the lower part of the Kidd–Munro assemblage in the central area. Whether the Kidd and Dundonald trends are correlative is uncertain and further work will be required to verify their stratigraphic positions.

Two stratigraphically distinct komatiitic sequences occur within the Munro trend in the eastern extension of the assemblage. The lower sequence, containing Dee's flow (Arndt 1975) and its probable northern extension, Fred's flow (Arndt et al. 1977), occurs in the southern part of Munro Township. It is underlain by high-silica rhyolite yielding a U-Pb age of 2714 ± 2 Ma (Corfu and Noble 1992). The komatiite sequence containing the Potter Mine (i.e., the Pyke Hill and "Lava Lake" komatiite) is interpreted to be higher in the stratigraphy, based on widespread facing indicators in Munro Township. The known komatiite-associated Ni-Cu-(PGE) deposits occur within the Dundonald trend (e.g., Alexo Mine, the Dundeal and Dundonald South deposits) and the lower sequence of the Munro trend (e.g., the Mickel showing). Interestingly, VMS-style mineralization in the Kidd–Munro assemblage appears to be spatially associated with the upper komatiitic sequence (Kidd Creek: rhyolite-komatiites – Kidd trend; Terminus zone: komatiite – Dundonald trend; and Potter mine: mafic tholeiite-komatiite – Munro trend).

These stratigraphic interpretations are preliminary and future work carried out under TGI-3 and continued mapping by the OGS may result in substantial modification in the future. However, the Kidd–Munro assemblage remains a very attractive exploration target for the discovery of new VMS-style base metal mineralization as well as Ni-Cu komatiite-hosted mineralization, and it is hoped that these interpretations will help in this endeavour.

Geological Setting of Munro Township

Munro Township is located approximately 80 km east of Timmins and covers part of the eastern extension of the Kidd–Munro assemblage (2719-2710 Ma: Ayer et al. 2005). Komatiitic and mafic tholeiitic metavolcanic rocks are dominant, with lesser tholeiitic felsic metavolcanic rocks (FIII rhyolites) present in the southwestern part of the township. Layered ultramafic and mafic sills and dikes (e.g., Center Hill complex, dated at 2706.2 ± 1.2 Ma: Ayer et al. 2005) intruded the Kidd–Munro assemblage and disrupted the volcanic stratigraphy. Clastic metasedimentary rocks of the Porcupine assemblage (2690-2680 Ma: Ayer et al. 2005) are in fault contact (i.e., Pipestone Fault) with the Kidd–Munro assemblage in the southwest portion of Munro Township (Figure 15). The komatiitic and tholeiitic volcanic rocks host many base metal, nickel, asbestos and gold deposits and showings. These include the Potter Mine and Potterdoal Cu-Zn volcanogenic massive sulphide deposits, the komatiite-associated Mickel nickel showing, the Hedman and Munro asbestos mines (peridotite- and dunite-associated chrysotile deposits), Croesus gold mine (tholeiitic basalt flows), and numerous other small gold showings.

The Kidd–Munro assemblage in Munro Township is structurally complex, with evidence for several folding and faulting events. However, the main structure consists of a large northwest-trending syncline with an axial trace in the central part of the township (Péloquin et al. 2005). A minor northwest-trending anticline-syncline pair, of limited extent, also occurs within the western part of Munro Township and in Beatty Township, suggesting more complex fold patterns in the southern limb. Based on Péloquin et al. (2005), the southern limb stratigraphy is composed of

(from base to top): a 200 to 450 m thick sequence of interlayered spherulitic/variolitic felsic and mafic flows (pillowed and massive facies); an approximately 1 km thick sequence of subaqueous basalt flows (massive, pillowed and flow breccias facies); and the 150 m thick tholeiitic Beatty rhyolite (massive, lobe and breccia flow facies), which is intercalated within a 700 m thick subaqueous basaltic sequence (pillowed, massive, pillow breccias and hyaloclastites facies) that has a high magnetic signature. The magnetic basalts are intruded by the layered mafic to ultramafic thoeliitic Munro sill, which hosted the abandoned Munro asbestos mine. It is overlain by a thick sequence of komatiitic lava flows ranging from 200-300 m to 1200-1500 m in thickness.

The komatiitic sequence is composed of variable proportions of massive and olivine spinifex-textured peridotitic komatiite flows intercalated with massive and pyroxene spinifex-textured basaltic komatiite flows. More differentiated flows also occur locally and are composed of massive peridotitic komatiite flows that exhibit upper gabbroic zones overlain by thin olivine spinifex-textured zones. At the base of this komatiite succession, the Mickel Ni-Cu-(PGE) deposit occurs within the differentiated komatiitic Dee's flow at the boundary between Munro and Beatty townships. The mafic metavolcanic rocks have been subdivided into two units, based on their magnetic signature, but are characterized by similar volcanic facies as they are dominated by abundant pillowed flows, with lesser massive flows, and flow breccias.

On the northern limb of the major syncline, facing reversals associated with the McCool syncline and the Potter anticline are observed. The volcanic succession trends southeast-northwest and exposure on the southern limb of the McCool syncline is dominated by ultramafic with lesser mafic volcanic rocks, whereas the northern limb of the McCool syncline is composed of a mix of ultramafic and mafic volcanic rocks and gabbroic intrusions (Figure 18). The southern limb includes the incredible exposures of the Pyke Hill and "Lava Lake" komatiite flows and the Centre Hill layered intrusive complex. The Centre Hill complex is intruded above the Lower Komatiitic Unit and below the Middle Tholeiitic and Upper Komatiitic Unit, defined below. The Potter anticline folded mainly the Middle Tholeiitic and Upper Komatiitic Units, whereas the Lower Komatiittic Unit is cut by the Centre Hill complex. The northern limb includes the tholeiitic Theo's flow and the differentiated komatiitic Fred's flow, described by Arndt in the 1970s (Arndt 1977). Regional geophysical survey patterns, coupled with similar textural and geochemical characteristics of Fred's and Dee's flows, as pointed out by Arndt (1975) and Allen (1986), suggest that those komatiite sequences might be correlative.

Four major faults transect Munro Township subparallel to the stratigraphy (*see* Figure 17): 1) the Pipestone Fault at the Kidd–Munro – Porcupine assemblages boundary; 2) the Munro fault zone centred in the southern part of the township; 3) the Centre Hill fault immediately south of the Centre Hill Complex; and 4) the Warden Hill fault in the area of the Munro Lake sill in the north part of the township.

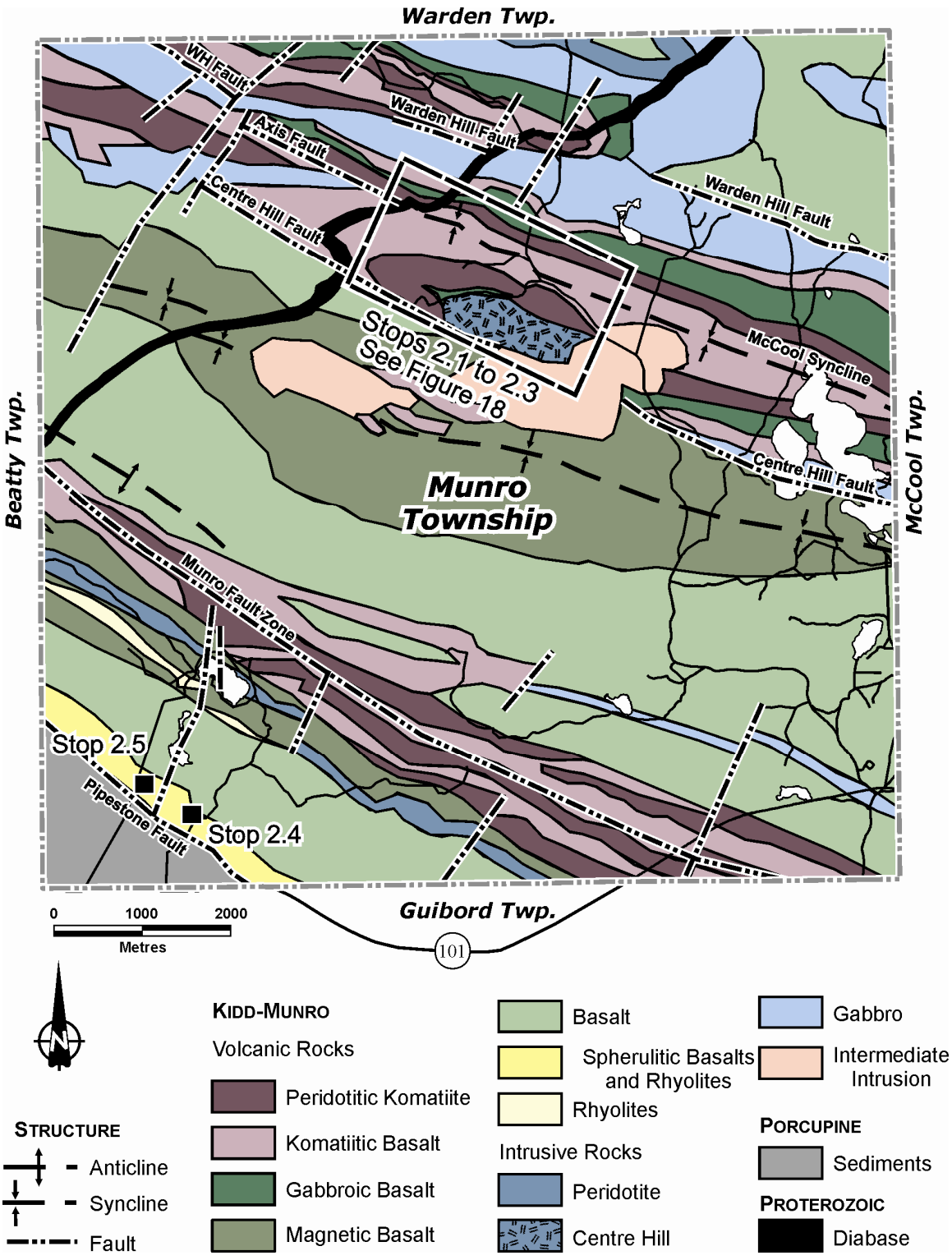

Figure 17. Geology of Munro Township, showing general location of stops for Day 2 (*modified from* Péloquin et al. 2005).

AM: Physical Volcanology of the Potter Mine Area

Potter Mine (477 572 tonnes grading 1.67% Cu; production from 1967-72) is located within the central part of Munro Township, and occurs within the Kidd–Munro assemblage. The Kidd–Munro assemblage also hosts the world-class Kidd Creek Cu-Zn-Ag VMS deposit (>138.7 million tonnes of 2.35% Cu, 6.50% Zn, 0.23% Pb and 89 g/t Ag), located some 80 kilometres to the west, north of Timmins.

The Potter Mine is hosted within a basaltic volcaniclastic deposit intercalated within a komatiitic flow succession (e.g., Gamble 2000) located along the north limb of a northwest-trending anticline (Oliver et al. 1999; Gibson and Gamble 2000; Houlé et al. 2002). The komatiitic-tholeiitic volcanic succession is in contact with the Centre Hill Complex to the south, and is divisible into three lithostratigraphic and chemostratigraphic units, which are, from oldest to youngest: 1) the "Lower Komatiitic Unit"; 2) the "Middle Tholeiitic Unit"; and 3) the "Upper Komatiitic Unit" (*see* Figure 18).

The Lower Komatiitic Unit (LKU) is cut by the ultramafic to mafic Centre Hill Complex intrusion, providing little exposure of komatiite flows in the mine area. They are mainly observed in drill core and occur essentially east of the mine shaft around Pyke Hill. Komatiite flows within the LKU consist of undifferentiated (cumulate/olivine-phyric) to differentiated (cumulate-spinifex) komatiite flows, similar to those observed at Pyke Hill (see description of Stop 2.1).

The Middle Tholeiitic Unit consists of: basaltic volcaniclastic rocks; intact and autobrecciated sills (dykes) of massive quench-textured basalt and komatiite; thin discontinuous deposits of argillaceous and carbonaceous sedimentary rocks; chert; massive sulphide; and lesser komatiitic flows (*see* Figure 18). The Cu-Zn-Co-Ag VMS mineralization occurs as stacked lenses of massive or semi-massive, sub-seafloor replacement deposits within the volcaniclastic deposits, or as massive sulphide lenses (Gibson 1998). The mineralized zones are enveloped by limited semi-conformable black chlorite alteration, characterized by depletion in SiO_2, Na_2O, CaO and MgO, and enrichment in Fe_2O_3 and metals (Gibson 1998). This hydrothermal alteration is currently under investigation by an ongoing MSc project at Laurentian University (S. Préfontaine) in collaboration with the OGS, the GSC and Millstream Mines Ltd., under the Targeted Geoscience Initiative phase 3 (TGI-3). This study will characterize the following aspects of the Potter VMS deposit:

1) the host volcaniclastic units;
2) the alteration facies (mineralogy and composition);
3) the morphology of the alteration facies and their spatial relationship to the deposit and the volcanic stratigraphy; and
4) the mineralogy and geochemistry of the mineralization as well their mechanism(s) of emplacement (seafloor versus sub-seafloor replacement).

Komatiite units within this unit occur as lava flows and sills that exhibit similar textural and morphological facies to those observed within the Lower and Upper komatiitic units. The komatiitic units from the Middle Tholeiitic unit are generally poorly exposed on surface but were intersected in diamond-drill holes.

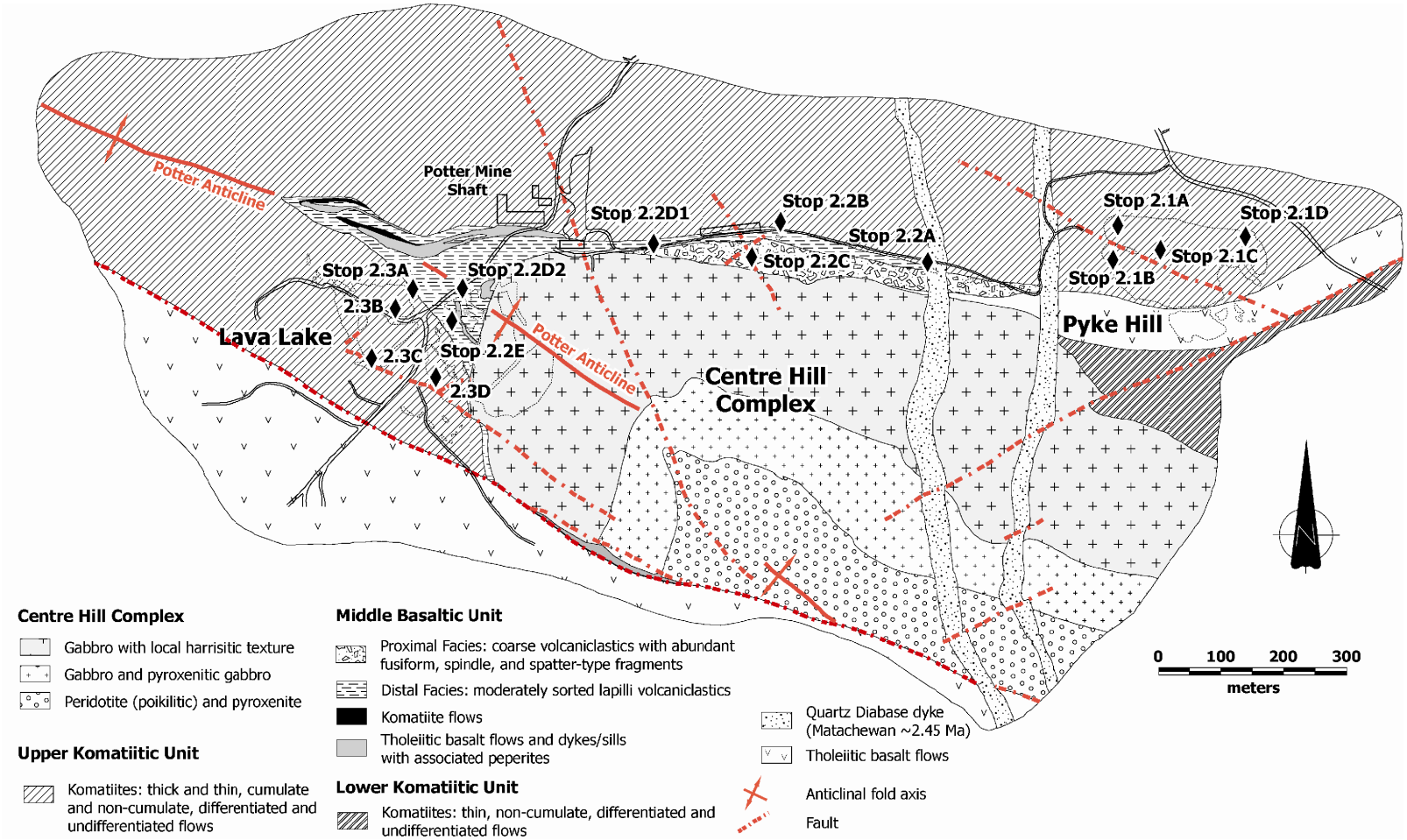

Figure 18. Geology of the Potter Mine property, showing locations of field trip stops 2.1 to 2.3 (*modified from* Oliver et al. 1999, Gamble 2000, and Houlé et al. 2002).

The Upper Komatiitic Unit is relatively well exposed and includes the well-known Pyke Hill (Pyke et al. 1973) and Lava Lake (Arndt 1986) in the Potter Mine area. Those komatiite flows represent one of the best preserved and best exposed sequences of thin differentiated (spinifex-textured) and massive peridotitic komatiite flows in the world. It represents a series of compound flows that exhibit well-developed layering with the lower cumulate zone and the upper spinifex-textured zones. Poorly differentiated, non-cumulate flows also occur, especially within lobate sheet and flattened-pillow morphologies (rather than sheet flows). Immediate to the mine area, komatiite flows are composed of massive to weakly-layered, medium-grained olivine adcumulate to mesocumulate rocks. Peridotitic komatiite flows of the Upper Komatiitic Unit are overlain by basaltic komatiite flows higher in the stratigraphic sequence. The basaltic komatiite flows are poorly exposed and occur as pillowed or massive flows with lesser differentiated flows exhibiting a massive lower olivine-phyric to cumulate zone and an upper pyroxene spinifex-textured zone.

STOP 2.1: KOMATIITE FLOWS: PYKE HILL

Pyke Hill (Figure 19) is located approximately 1 km east-southeast of the Potter Mine, and represents one of the best preserved and best exposed sequences of thin differentiated (spinifex-textured) and massive peridotitic komatiite flows in the world. It represents a series of compound flows. At least 60 flows have been identified over an exposure width of approximately 125 m (Pyke et al. 1973). Individual flows range in thickness from 0.5 to 15 m, averaging approximately 3 m (Pyke et al. 1973). The relative proportions of spinifex-textured “A” zones and cumulate-textured “B” zones vary within individual flows, owing to irregularities along the contact between the zones in response to different rates of cooling. The ratio of Zone A to Zone B averages approximately 2:1 to 1.5:1 at Pyke Hill (Pyke et al. 1973), confirming that this area contains primarily non-cumulate rather than cumulate flows. However, preliminary data indicate that the proportion of A:B zones decreases with increasing thickness. This is consistent with increases in flow thickness allowing for increases in the amount of olivine accumulation: a trend also observed in Western Australia (e.g., Lesher 1989).

Stop 2.1A: Thin differentiated komatiite flows

This stop at Pyke Hill (*see* Figure 19) comprises (from base to top): very thin (~0.75 to 2.5 m) well-differentiated sheet flows; thick (~4 to 12 m) well-differentiated sheet flows; and thin (~3 to 4.5 m) well-differentiated sheet flows. The uppermost section is characterized by thin sheet flows that have conspicuous textural differentiation and represent the komatiite flow archetype described by Pyke et al. (1973), which includes a spinifex-textured “A” zone in the upper part, and a cumulus-textured “B” zone in the lower part of the flow. The A zone unit may be further subdivided into the A1 (fractured upper chill zone / flow top breccia / microspinifex), A2 (randomly oriented spinifex) and A3 (coarse platy spinifex) zones. The B zone may be further subdivided into the B1 (aligned skeletal “hopper” olivine), B2 (medium- to coarse-grained cumulate), B3 (knobby cumulate) and B4 (fine-grained cumulate and basal chill) zones.

Stop 2.1B: Komatiite flow morphologies

The southern part of Pyke Hill (*see* Figure 19, area C: stratigraphically lower) consists of (from base to top): thick (~6.5 to 16 m) differentiated sheet flows; thin (~2.5 to 4.5 m) differentiated sheet flows; thick (~5.5 to 13.5 m) differentiated sheet flows; overlain by thin (~0.75 to 2 m) differentiated sheet flows. Most of the komatiite flows, especially thicker ones, are not as texturally or structural organized as those of area A (Stop 2.1A). Furthermore, within the uppermost section, komatiite flows also occur as thin lobate sheet flows and flattened pillow

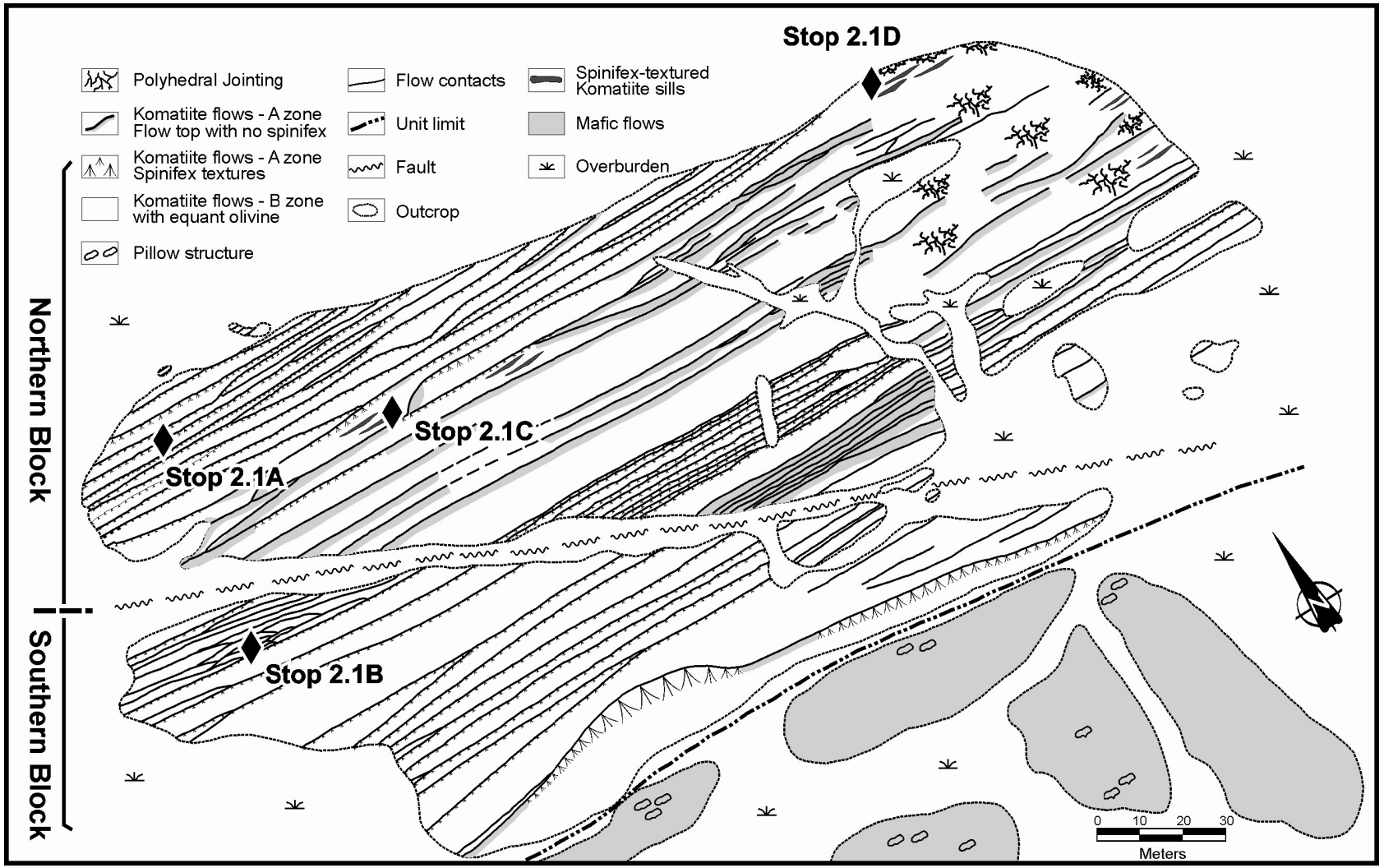

Figure 19. Geology of the Pyke Hill area, showing locations of field trip stops 2.1A to 2.1D (*modified from* Pyke et al. 1973 and Arndt et al. 1977).

facies that exhibit only limited spinifex textures along their cooling margins. However, well-differentiated flows are interlayered within sequences dominated by poorly differentiated flows, indicating that the timing of ponding varied on a flow-by-flow basis. Poorly differentiated, non-cumulate flows, especially those with lobate sheet and flattened-pillow forms (rather than sheet flows) are spinifex textured along their margins and along fractures, indicating rapid crystallization due to extensive hydrothermal cooling and thermally constrained crystallization (Shore and Fowler 1999). Flattened pillows contain shelves that were interpreted by Shore (1996) as molten lava breakouts. However, the thicker parts of some lobate flows exhibit incomplete secondary selvages inside the major external selvages, suggesting that growth may have occurred by progressive inflation. Furthermore, these variations in flow morphologies indicate that the eruption rates waned and waxed through the komatiitic sequence.

Stop 2.1C/D: Spinifex-textured sills

Thin (centimetre-scale) semi-conformable olivine spinifex-bearing sills intrude the cumulate zones of some komatiite flows at Pyke Hill, producing a complex pattern (Figure 20). Euhedral cumulate olivine crystals of the flows immediately adjacent to the contact are coarser than elsewhere. Thin section examination shows that the coarser olivines are composed of olivine crystals that have been overgrown (Photo 1A), obviously during the intrusion of the sills. We interpret this evidence to mean that komatiite flow cumulate materials were somewhat permeable at the time the sills were introduced. In addition, some cumulate olivine crystals of the flows have dendritic overgrowths (Photo 1B) where the dendrites have grown into the sills away from the cooling contacts. This demonstrates that there was a sufficient thermal gradient between the host cumulate and the magma within the sill to promote dendritic growth, and suggests that the host cumulate had undergone cooling prior to introduction of the sills. Hence the sills were intruded into relatively hot unconsolidated cumulate material, which further indicates komatiite growth by inflation (Houlé et al., in press).

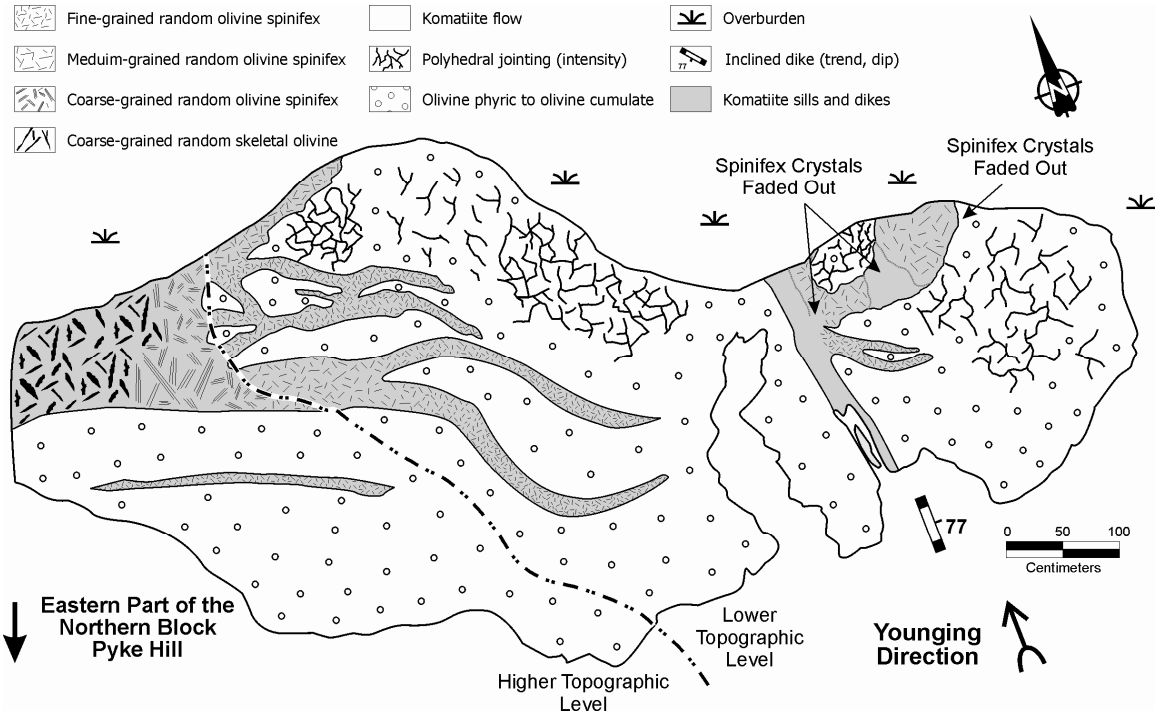

Figure 20. Geological map (*after* Houlé et al., in press) showing olivine spinifex-bearing sills branching out within a komatiite flow at the eastern edge of Pyke Hill, Stop 2.1D.

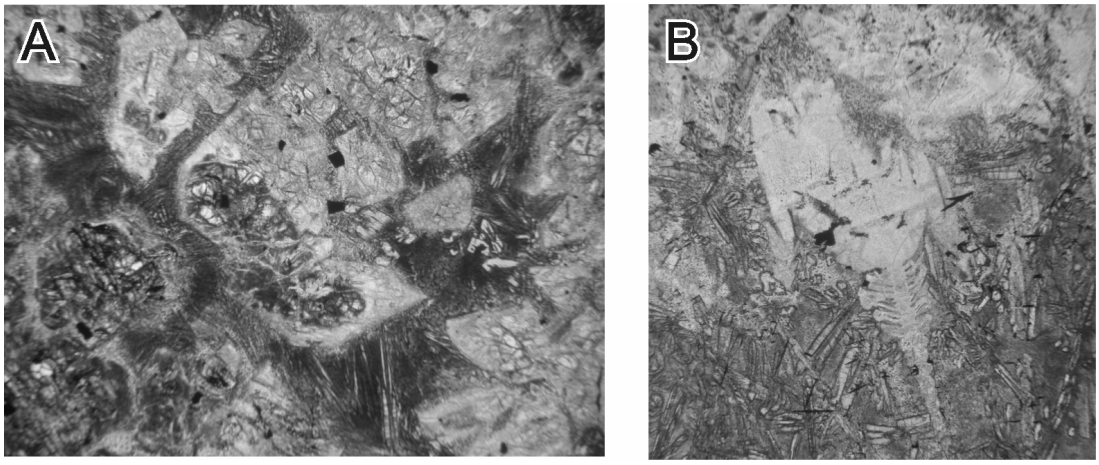

Photo 1. Photomicrographs from Stop 2.1C (*after* Houlé et al., in press). A) Overgrown olivine crystals within the host cumulate at the sill margins (field of view (fov) ~2 mm). B) Olivine crystal with dendritic overgrowth (fov ~2 mm).

STOP 2.2: BASALTIC VOLCANICLASTIC DEPOSITS

The basaltic volcaniclastic deposits were subdivided by Gibson and Gamble (2000) into two main volcanic facies: 1) distal facies that consists of well-bedded, framework-supported lapillistone units that are massive, normal graded, and moderately to well sorted; and 2) proximal facies of massive to poorly bedded, unsorted tuff breccia. (See Figure 18 for locations of stops 2.2A to 2.2D.)

Stop 2.2A: Basaltic volcaniclastic unit

Massive komatiite flows and the basaltic volcaniclastic unit are cross-cut by a quartz diabase dike (Matachewan, ~2.45 Ma).

Stop 2.2B: Thin differentiated komatiite flow

Several spinifex-textured flows overlie the Potter volcaniclastic units. These komatiite flows are similar to flows that will be observed later but that are not as well exposed.

Stop 2.2C: Proximal basaltic volcaniclatic unit

Approximately 500 m east of the Potter Mine area, the basaltic volcaniclastic rocks are massive to poorly bedded, unsorted and consist of globular, irregular “moulded” lapilli that resemble agglutinate (Photo 2C), fluidal bombs (Photo 2D), cored bombs (Photo 2E), blocks (Photo 2F), and armoured lapilli with less than 10% matrix containing fine, plate-like hyaloclastite shards and lapilli (Gibson and Gamble 2000). Accessory fragments of chert, carbonaceous mudstone, argillaceous mudstone, and massive sulphide account for less than 1% of the breccia.

The basaltic volcaniclastic rocks were previously interpreted to have been derived through quench fragmentation and autobrecciation of basaltic flows. However, the lack of basalt flows and in situ hyaloclastite, the abundance of fluidal and cored bombs, armoured lapilli, globular lapilli, and the shear volume of breccia led Gibson and Gamble (2000) to propose an origin through “explosive fragmentation” rather than autobrecciation. The production of large volumes of lapilli-size granules is interpreted to be a product of the rapid eruption of low-viscosity mafic

magma into a water column, where the magma was jetted into the water column, torn apart and quench-fragmented. In this model, massive, poorly sorted volcaniclastic units containing globular, lapilli-size agglutinate and fluidal bombs are interpreted to represent vent-proximal deposits, similar to subaerial fire fountain and spatter rampart deposits. In contrast, well-bedded and well-sorted lapillistone deposits, typical of the mine area, are interpreted as high-particle-concentration mass flow and fall deposits that accumulated within a paleotopographic depression in the underlying komatiitic flow topography (Gibson and Gamble 2000).

Stop 2.2D1/D2: Basaltic and komatiitic sills

Basaltic and komatiitic sills emplaced into the volcaniclastic succession are interpreted by Gibson and Gamble (2000) as high-level synvolcanic intrusions. Evidence for this interpretation includes: 1) their fractured and autobrecciated upper and lower contacts with massive volcaniclastic material, massive sulphide and/or argillite injected along fractures that penetrate the massive sill interior; 2) locally chilled and sharp upper and lower contacts; 3) the development of hyaloclastite along chilled and perlitic-textured sill contacts and the mixing of this hyaloclastite with enclosing argillaceous mudstones and sulphide to form peperite; and 4) a basaltic composition that is identical to the volcaniclastic rocks (Gibson and Gamble 2000).

Stop 2.2E: Distal basaltic volcaniclastic unit

In the immediate mine area, the basaltic volcaniclastic rocks consist of well-bedded (decimetres to metres), framework-supported lapillistone units that are massive, normal graded, and moderately to well sorted (Photos 2A and B). Fragment types include amygdaloidal, globular to angular, plate-like lapilli (<1 to 5 mm) of chloritized sideromelane and occasional armoured lapilli with lesser accessory fragments of olivine-porphyritic basalt, amygdaloidal aphyric basalt and plagioclase microlitic basalt. The matrix, which rarely exceeds 20% by volume of the hyaloclastite units, consists of 1) carbonate; 2) broken crystals of quartz, plagioclase and pyroxene; 3) fine, massive chlorite; 4) carbonaceous sediment; and 5) massive sulphide. Well-bedded, basaltic volcaniclastic units host the massive sulphide mineralization (Gibson and Gamble 2000; Tardif et al. 2000).

STOP 2.3: KOMATIITE FLOWS: “LAVA LAKE”

The “Lava Lake” area (Figure 21: Arndt 1986) is located immediately west of the Centre Hill Complex, approximately 1 km west of Pyke Hill. The “Lava Lake” area is very well exposed at surface, dominated by massive to weakly layered, medium-grained olivine adcumulate rocks and has been previously interpreted to represent an approximately 120 m thick “Lava Lake” that youngs toward the north (Arndt 1986). However, Houlé et al. (2002) suggest, based on geological mapping and drill core logging, that the “Lava Lake” is stratigraphically equivalent to the rocks exposed at Pyke Hill and youngs toward the south. This interpretation is supported by 1) graded bedding in associated volcaniclastites and thin-bedded sediments within the upper part of the Middle Tholeiitic Unit; 2) chilled margin polarities; 3) asymmetric differentiation within flow units; 4) vesicle orientations; 5) fanned platy olivine spinifex; and 6) local asymmetric contacts in spinifex horizons within the komatiitic sequence. The remapping also suggests that the “Lava Lake” includes at least 6 mappable cooling units, and that it represents a series of thick sheet flows emplaced into a shallow depression, or a series of thick sheet flows overlain by a thin lava lake, rather than a thick lava lake. Thus, the Upper Komatiitic Unit in the Potter Mine area is interpreted as sheet-flow facies komatiites that were channelized into a pre-existing depression, flanked by a levee facies represented by the multiple thin undifferentiated to differentiated flows at Pyke Hill.

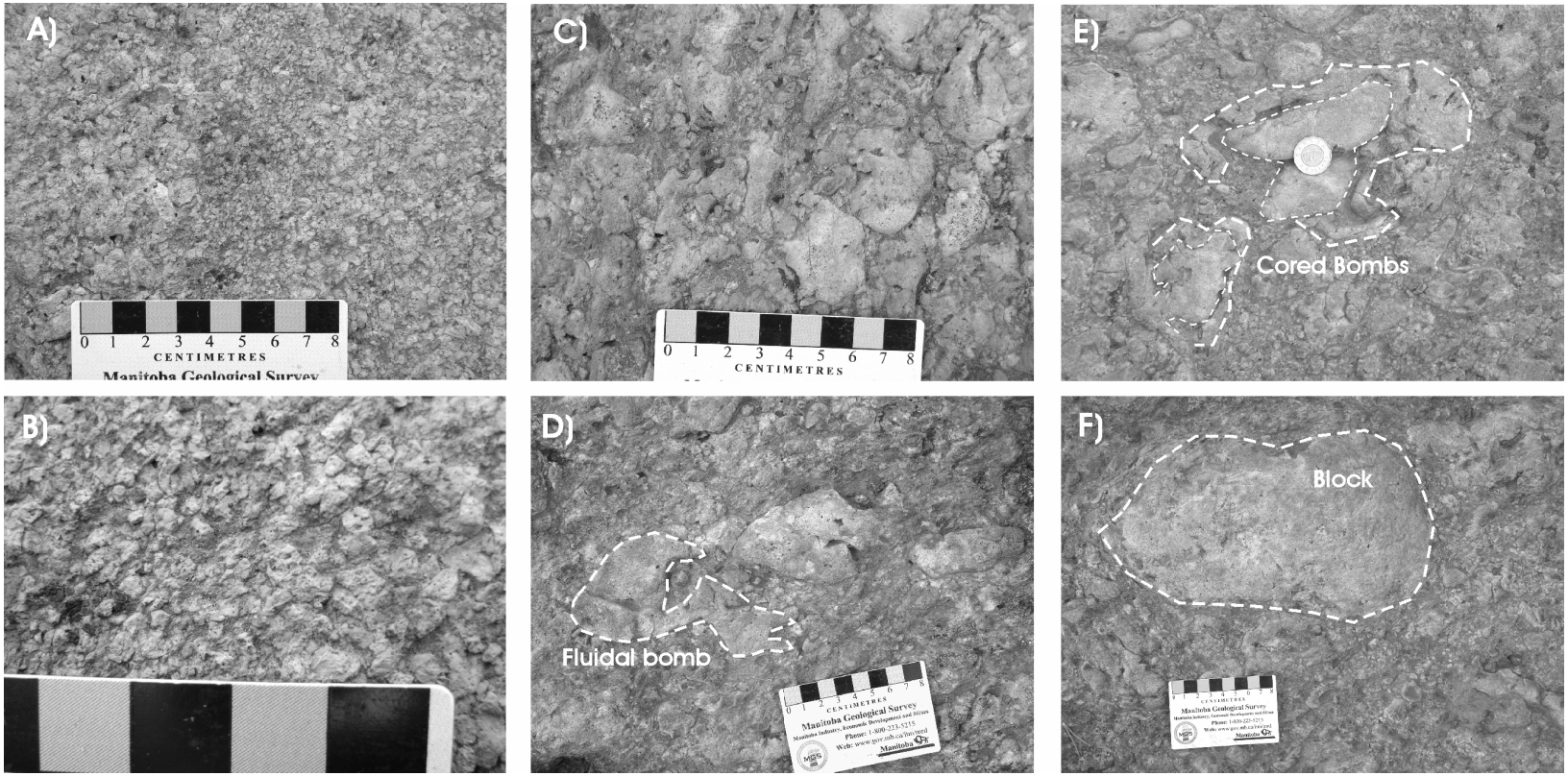

Photo 2. Textures of volcaniclastic rocks of the Middle Tholeiitic Unit at the Potter Mine. A) Framework-supported lapillistone. B) Detail of framework-supported lapillistone. C) "Agglutinate" lapilli. D) Fluidal bombs. E) Cored bombs (for scale, diameter of coin is 28 mm). F) Blocks. (Photos are from stops 2.2C and 2.2E; *from* Péloquin et al. 2005)

Stop 2.3A: Thin komatiite flows

The base of the "Lava Lake" exposure is composed of several thin komatiite flows that exhibit some olivine and pyroxene spinifex-textured zones. Several relatively continuous vesicle-rich horizons are also present within or at the top of individual units. Multiple vesicle-rich horizons are interpreted to result from endogenous growth of these komatiite flows.

Stop 2.3B: Swirling olivine spinifex textures

The middle section of the "Lava Lake" exposure is characterized by the presence of unusual spinifex-textured zones previously interpreted as swirling olivine spinifex veins by Arndt (1986). However, field relationships (i.e., sharp lower contact and gradual upper contact) suggest those unusual zones are probably the result of partial melting and recrystallization of the spinifex-textured zones, due to residual heat from rapidly accumulated flows, as proposed for Honeymoon Well in Western Australia by Gole et al. (1990).

Stop 2.3C: Serpentinization pattern

Toward the upper part, the "Lava Lake" exposure is characterized by intense serpentinization. An irregular network of hierarchized bands of serpentine divides parts of the dunite/peridotite into many irregular and randomly distributed remnants similar to those observed within a serpentinized olivine crystal in thin section.

Stop 2.3D: Columnar jointing

The upper part of the "Lava Lake" exposure is characterized by well-developed columnar jointing.

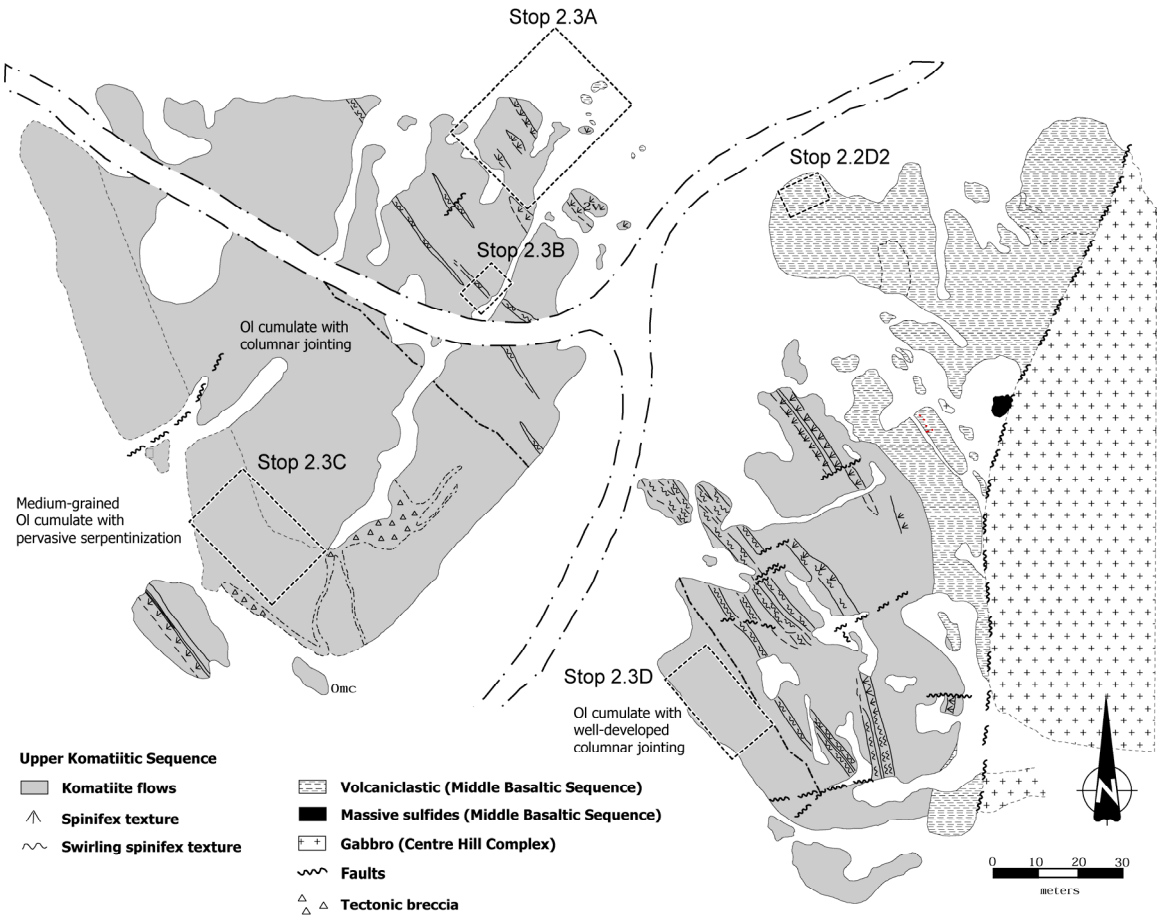

Figure 21. Geology of the "Lava Lake" area, showing locations of field trip stops 2.2D2 and 2.3A to 2.3D (*modified from* Arndt 1986).

Lunch (Core)

Mineralized diamond-drill core from the Potter Cu-Zn-Co-Ag VMS deposit will be on display at the core shack during an extended lunch time, and will be discussed by Dave Gamble, Millstream Mines Ltd.

PM: Physical Volcanology of Mafic and Felsic Volcanic Rocks

STOP 2.4: FELSIC FLOW MORPHOLOGY: CROESUS MINE ROAD OUTCROPS

The Croesus Mine Road rocks are exposed in a series of four main outcrops that stretch over roughly 100 m (UTM 5376811mN, 0555090mE, Zone 17, NAD 27). The first exposed outcrop consists of 0.5-2.5 m long, bulbous, white calc-alkaline rhyolite pods or lobes. The rhyolites have millimetre-scale quartz, sparse plagioclase and pyrite, and often have sericitized and/or epidotized margins. This unit forms an irregular contact with the overlying massive brown-grey chloritized tuff that contains abundant pyrite. This mound of lobate rhyolite best represents a proximal lobe facies.

Roughly 60 m to the north lies the second series of adjacent outcrops (termed South and North outcrops; Figure 22). The base of the exposed section consists of lapilli-tuff-breccia that has many distinguishing features such as perlitic fracturing, jigsaw-fit breccia and a peperitic upper contact. The breccia has a fine-grained chloritized matrix and contains abundant leucocratic and melanocratic fluidal-shaped clasts. The leucocratic fragments are generally ash to lapilli in size, while the melanocratic material is more prominent. There is also melanocratic material that forms fluidal networked-dyke morphology that can be traced for several meters along 1 to 12 cm thick bands. Based on the fluidal morphology, it resembles a deformed spatter deposit in a proximal vent produced by Hawaiian-style fire-fountaining. Michol (2004) has shown that this rock has a hyaloclastite-textured matrix. The upper contact of this unit is irregular due to a peperitic injection of the overlying thin mafic unit.

Approximately 2 m above this mafic unit is another lapilli-tuff breccia that is very similar to the lapilli tuff located below the mafic unit, however within it are brown mesocratic lobes up to 25 cm thick. Individual lobes have a distinct morphology with a layered or banded lower margin that shows vesiculation in the layers towards the core. Laterally, to the northwest, this unit is continuous into the Munro North outcrop, where there are leucocratic nested lobes that appear along a layer roughly 1 m below the irregular contact with the roughly 13 m of overlying basalt.

The variolitic rhyolite is the youngest unit mapped, and also the most ambiguous. Near the base of this unit the varioles are matrix supported and up to 5 cm in diameter. In the basal 8 m of the unit, the varioles increase in size culminating in varioles up to 7 cm in diameter at the coarsest zone. Above this zone, the unit becomes normally graded with an overlying 3 m of varioles up to 7 cm in diameter, overlain in turn by 11 m of varioles grading down to 0.2 cm in diameter. Within the rhyolite, it is common for varioles to impinge on one another, and the upper half of the unit is variole supported. Some of the largest varioles have opaque iron-oxide minerals along their margins and cores. The smaller varioles near the top of the unit show irregular shearing, which defines the apparent lobate features described by Michol (2004). Some do contain spherulites; however, these and the distinctly zoned clasts are uncommon. Columnar joints, up 15 cm on face, are found on the west side of the outcrop.

There are several possibilities for the origin of this rock, the first being that it is coherent lava that has been entirely undercooled creating a quenched glass matrix. This quenched glass produced primary or secondary (through devitrification/alteration) spherulites. The second possibility is that these represent accretionary lapilli in an airfall unit, as suggested by Michol (2004). The third possibility is that the varioles represent spherulites in a pyroclastic deposit. Fowler et al. (2002) considered the textures to be the result of magma mingling.

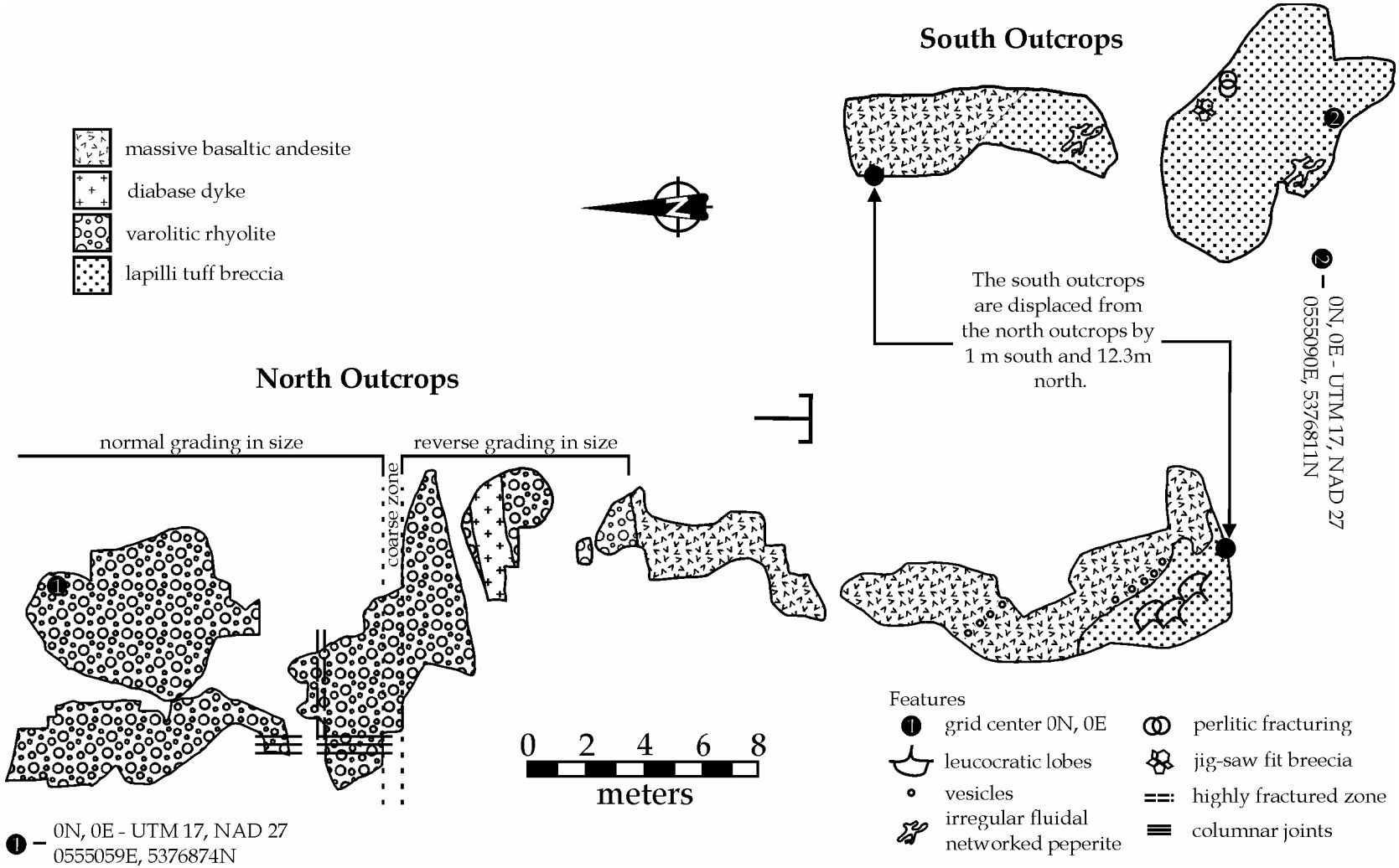

Figure 22. Geological map (by B. Moulton and A. Fowler) of the Croesus Mine Road outcrops 1 and 2, scale is 1:100.)

STOP 2.5: FELSIC FLOW MORPHOLOGY: ASBESTOS MINE ROAD OUTCROPS

The Asbestos Mine Road rocks consist of a series of three main outcrops composed of coherent and fragmental felsic volcanic rocks. Initial work at this locality has been conducted by Dinel and Fowler (unpublished data, 2003) and consisted of detailed geological mapping at a scale of 1:100. It was subsequently re-mapped and re-sampled by B. Moulton.

The first two outcrops (Figure 23: UTM 5377623mN, 0554606mE, Zone 17, NAD 83) consist of rhyolitic lapilli tuff and rhyolitic lapillistone intermixed with minor amounts of massive and autoclastic rhyolite that exhibit a general bedding at 135° with a vertical dip. The rhyolitic lapilli tuff is internally massive. This tuff is interrupted by thin (<0.5 m) bands of rhyolitic lapillistone. In several areas there are significant patches of potentially fines-depleted lapillistone that are up to 2 m thick and 3 m in length of the exposed section, and may represent zones of degassing. In the east portion of the outcrop there is one potential rhyolite lobe measuring roughly 1 m long by 0.5 m in thickness.

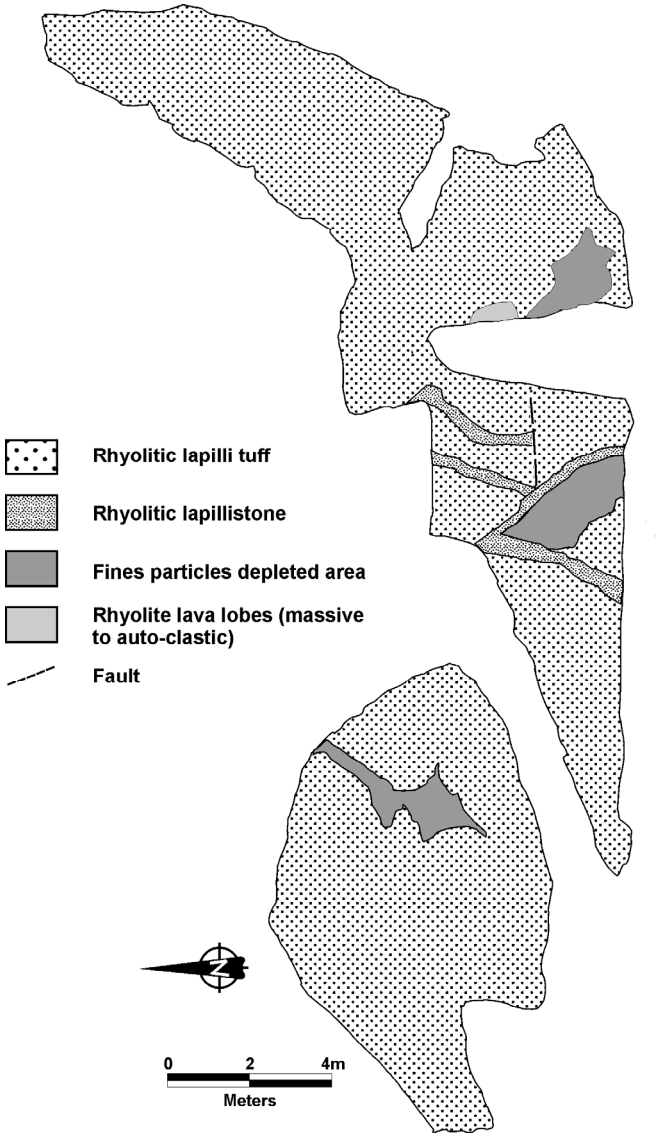

Figure 23. Geological map (by B. Moulton, E. Dinel and A. Fowler) of the Asbestos Mine Road outcrops, Stop 2.5 (first two outcrops).

The third outcrop (Figure 24: UTM 5377630mN, 0554645mE, Zone 17, NAD 83) is approximately 40 m to the east and is comprised almost entirely of rhyolite lobes. These lobes are preserved to varying degrees and internal structure is most evident in the larger of the lobes. These lobes attain a maximum diameter of 4 m. The best preserved lobes contain up to three domains: 1) rhyolitic lapilli tuff containing sub-angular to rounded, less than 1 cm, lapilli of rhyolite auto-clastite within a chloritized matrix; 2) a massive chloritized rhyolite domain containing less than 5% quartz that is in sharp contact with domain 1 and gradationally zoned into domain 3; 3) a massive domain of less than 1 mm varioles (possibly phenocrystic). Zone 3 contains bands of massive coherent rhyolite up to several centimetres in thickness that cut the variolitic material in an irregular fashion. Zone 1 forms the matrix material, while the sharp contact between Zones 1 and 2 defines the lobate morphology. Many of the smaller lobes do not show the complete morphology but consist of an autobreccia lapillistone with a more coherent core. Flow-banding is preserved throughout the lobes, however it is better developed in the massive coherent zone 2. Some lobes contain auto-brecciated cores, indicating that they have rolled over themselves and entrained marginal breccias. These lobes show well developed internal structures typical of the volcanic piles associated with an exogenous dome.

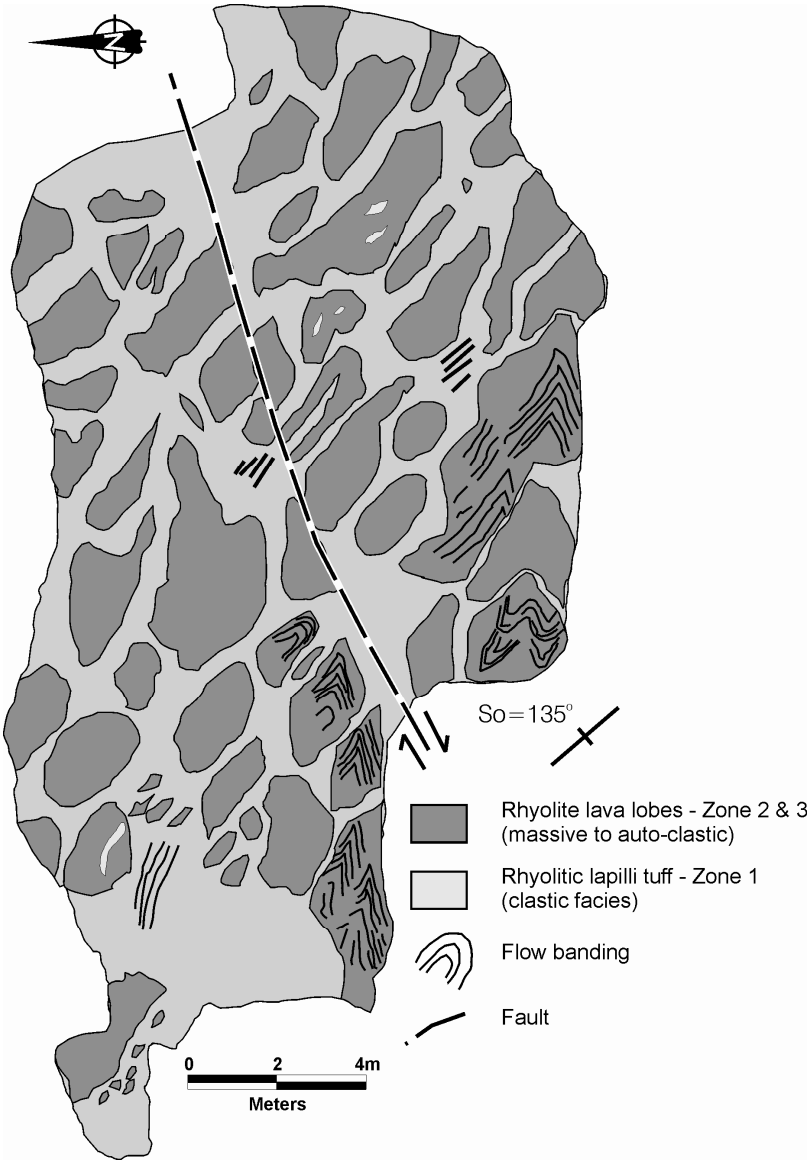

Figure 24. Geological map (by B. Moulton, E. Dinel and A. Fowler) of the Asbestos Mine Road outcrop, Stop 2.5 (third outcrop).

Day 3: Physical Volcanology of the Bartlett Dome

by M.G. Houlé, G. Baldwin and P.C. Thurston

GEOLOGY OF THE BARTLETT DOME

The Bartlett Dome area (Figure 25) is a homoclinal sequence facing eastward, located east of the Kenogamissi batholith and composed of supracrustal metavolcanic and metasedimentary rocks intruded by large felsic intrusions (e.g., Adams pluton, Geikie pluton, and the Kenogamissi batholith) . The volcanic sequence is composed of a lower sequence of mafic and ultramafic volcanic rocks, a central sequence of intermediate to felsic volcanic rocks, and an upper sequence of ultramafic and mafic volcanic rocks (Pyke 1978). Other smaller intrusions, ranging from ultramafic to felsic in composition, are intruded into this volcano-sedimentary succession. Proterozoic diabase dykes observed in the mapped area are attributed to the Abitibi, Sudbury, and Matachewan swarms. The metamorphic grade in the Bartlett Dome is relatively low (mainly greenschist facies) with locally good preservation of primary igneous textures and geological relationships, but locally the rocks are sheared and intensely altered.

DELORO ASSEMBLAGE

Lower Section

The *lower section* of the Deloro assemblage is bound to the west by the Kenogamissi batholith and to the east by the Muskasenda mafic to ultramafic intrusion. It is also present east of the Muskasenda intrusion, in the northern part of Bartlett Township. The lower section is dominated by pillowed mafic metavolcanic rocks, with subordinate massive units and rare felsic metavolcanic rocks. These units are cut by gabbroic dikes and intrusions. New geochronology from a felsic tuff unit within the lowermost part of the succession yielded a U-Pb age of 2728.3 ±1.6 Ma (Houlé, unpublished data) (*see* Figure 25). This new data has resulted in re-interpretation of this part of the sequence to be Deloro assemblage rather the former interpretation of Pacaud assemblage (Ayer et al. 2002).

Upper Section

The *upper section* overlies the *lower section* of the Deloro assemblage in the northern part of the map area, is cut by the Muskasenda intrusion in the southern part of the Bartlett Township, and is overlain to the east by ultramafic metavolcanic rocks of the Tisdale assemblage (*see* Figure 25). It is mostly composed of fragmental metavolcanic rocks of intermediate to felsic composition. Abundant mafic dykes, sills, and small plutons have been intruded into this volcaniclastic sequence.

Intermediate to felsic volcanic rocks are restricted to the eastern part of Bartlett Township. Most of the sequence is entirely composed of volcaniclastic rocks ranging from tuff to pyroclastic breccia. Lapilli-tuff and tuff breccia are prominent facies observed in the intermediate to felsic volcaniclastic rocks. Most of the volcaniclastic rocks do not show well-developed bedding, but, where observed, it is on a scale of tens of metres. Tuff breccias are monomictic to polymictic, matrix-supported and commonly contain 50 to 60% of angular to subrounded clasts up to 1 m long.

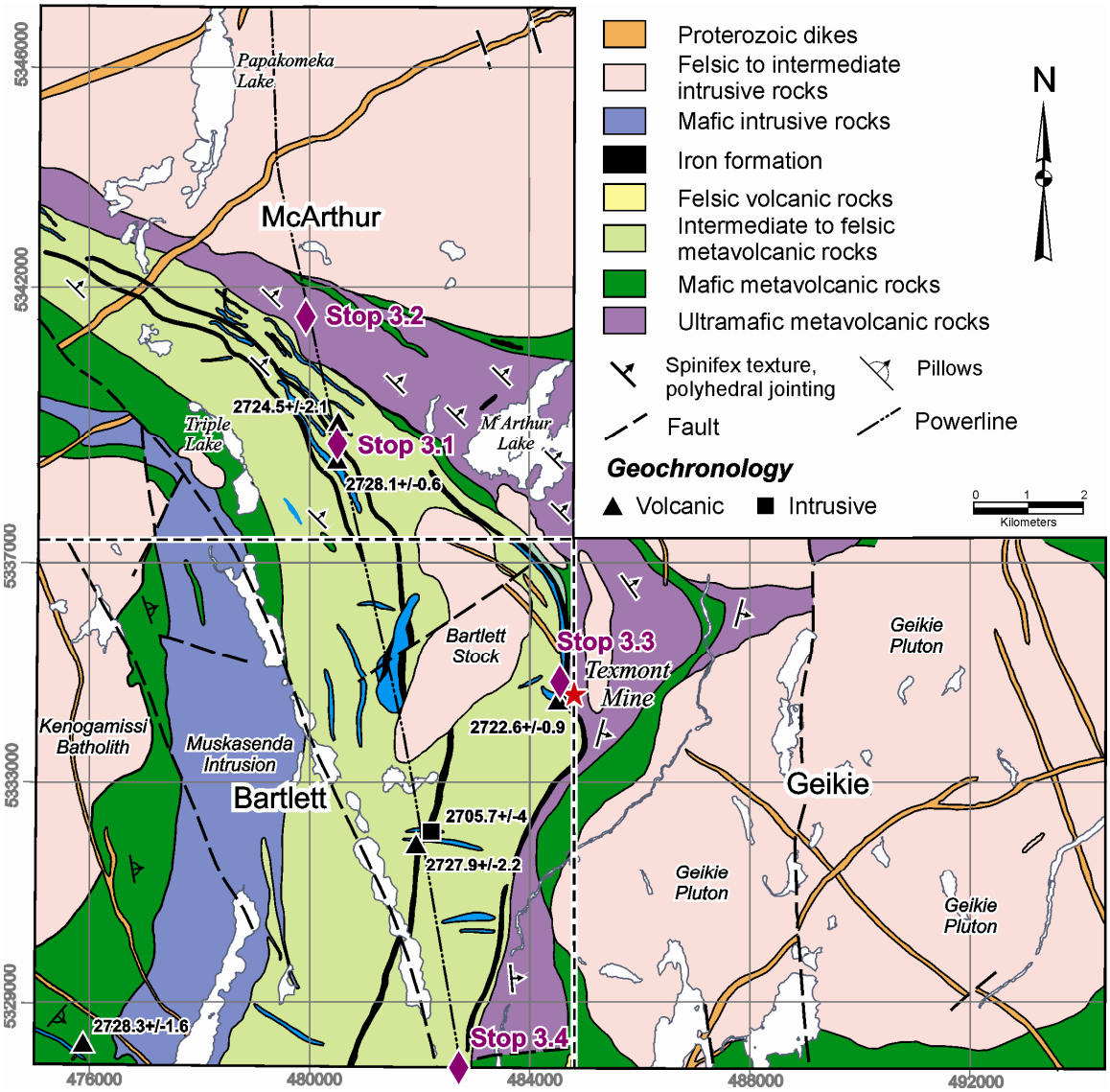

Figure 25. Geology of McArthur, Bartlett and Geikie townships in the Bartlett Dome area, showing locations of stops 3.1 to 3.4. *(modified from* Houlé 2006, Houlé and Solgadi 2007)

Several units of sedimentary rocks are concentrated into three main iron formation horizons intercalated within the intermediate to felsic volcanic rocks. The lower iron formation is a relatively thin (0.5-5 m thick) and discontinuous unit that is magnetite-rich and locally contains red chert (jasper) layers with felsic tuff beds. The middle iron formation (5 to 70 m thick) is interlayered thin magnetite-rich and thicker chert-rich layers and intercalated chert breccia and iron formation conglomerate. The upper iron formation (centimetres to metres thick) is dominantly oxide facies, with lesser carbonate facies and chert breccia, sandstone, siltstone and graphitic and sulphidic argillite with minor chert layers (Houlé 2006; Houlé and Solgadi 2007).

Given the lateral persistence of the Deloro assemblage iron formation units, and their equivalents across the entire Abitibi greenstone belt (AGB), it is important to have constraints on the duration of the depositional interval and hence the significance of the disconformity. For example, on the west side of the Kenogamissi batholith, broadly similar stratigraphy occurs in the Marion Group in the southern part of the Swayze greenstone belt (Heather 2001), interpreted to be correlative with the Deloro assemblage (Ayer et al. 2002). Here, up to three horizons of iron

formation occur within the Marion Group. The basal iron formation is a mix of carbonate and oxide facies, whereas the middle iron formation is chert-rich oxide facies. The third iron formation is only intermittently preserved. van Breemen et al. (2006) obtained U-Pb zircon ages on a rhyolite underlying (2731±2 Ma) and on a rhyolite overlying (2724±2 Ma) the lowermost iron formation. Thus, taking errors into consideration, the iron formation accumulated within 3 to 11 million years. Thurston et al. (submitted) considered this sedimentary interface zone (SIZ) and its associated disconformity to be of regional significance. To constrain the duration of the SIZ deposition in the Bartlett Dome area, 120 km to the northeast, we have undertaken U-Pb zircon dating of a number of units in the Deloro assemblage (Houlé, unpublished data). The ages (Figure 26) include 2728.1 ±1.6 Ma from a felsic tuff immediately underlying the middle iron formation in McArthur Township; 2724.5 ±2.1 from a heterolithic debris flow immediately overlying the middle iron formation in McArthur Township; and 2722.6 ±0.9 Ma from a felsic lapillistone immediately underlying the uppermost iron formation in Bartlett Township. The latter sample also corresponds to the immediate footwall rocks of the Texmont nickel mine (discussed below). Based on this new geochronology, a better defined time constraint has been established for the deposition of AGB iron formations. This also has implications for this SIZ regionally, as the felsic volcanic rocks underlying the Deloro middle iron formation collectively yield a U-Pb age of 2727 Ma (i.e., average of 2727.9±2.2, 2727.4±1, 2727±7, and 2731±2 Ma), and felsic volcanic rocks overlying this iron formation yield a U-Pb age of 2724 Ma (i.e., average of 2724.1 ±3.7, 2724±2, 2724.6±0.8, 2723.1±1.3, and 2724±2 Ma) (Ayer et al. 2002, 2005; van Breeman 2007). Despite some of this U-Pb data having lower precision and overlap in error, the more precise data indicates the middle iron formation was regionally deposited by slow sedimentation over an interval of 3 to 4 million years.

TISDALE ASSEMBLAGE

The Tisdale assemblage in the Bartlett Dome area overlies the upper part of the Deloro assemblage and is intruded to the east by the Geikie pluton. It is dominated by ultramafic and mafic metavolcanic rocks with rare felsic metavolcanic rocks. Fine- to medium-grained gabbro dykes intruded both ultramafic and mafic metavolcanic rocks.

Ultramafic volcanic rocks are confined to two stratigraphic intervals in the Bartlett Dome area (*see* Figure 25). Both komatiitic sequences are dominated by *sensu stricto* komatiite flows with subordinate komatiitic basalt flows. Ultramafic flows were recognized in this area, but the "classical" komatiite flows with all internal subdivisions as defined by Pyke et al. (1973) were not found in this area. Instead, the komatiite flows are mainly sheet flows that exhibit a lower olivine cumulate or olivine-phyric zone and an upper zone of randomly oriented olivine spinifex textured, or flattened pillowed flows. Thicker komatiite flows are generally characterized by cumulate texture comprised of olivine pseudomorphs. Polysuturing defined by polygonal jointing is common to most of the komatiites mapped as lava flows. Locally, spinifex-textured veins intrude ultramafic flows.

Massive and pillowed mafic metavolcanic rocks are generally poorly exposed, but outcrop as highly strained, folded and amphibolitized units in proximity to the Geikie pluton.

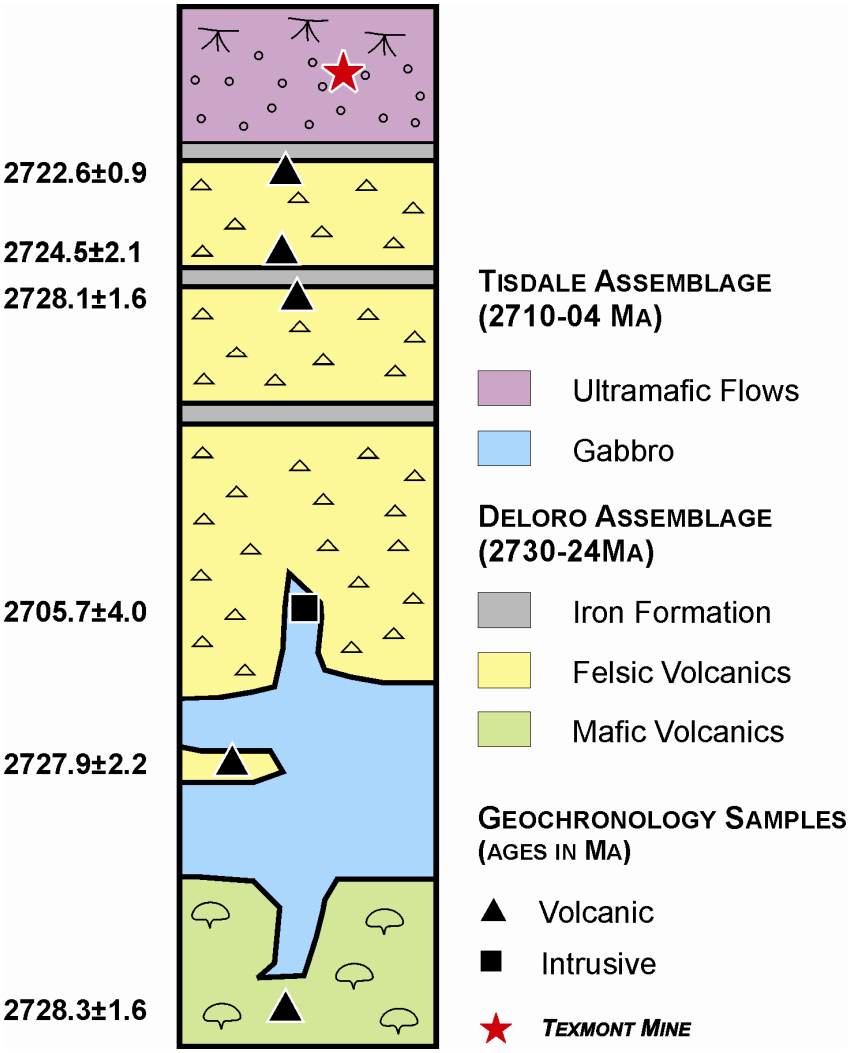

Figure 26. Stratigraphic column and U-Pb geochronological ages (Houlé, unpublished data) for the Bartlett Dome area.

AM: Deloro–Tisdale Assemblage Transect in McArthur Township

STOP 3.1: SEDIMENTARY INTERFACE ZONE (SIZ) IN MCARTHUR TOWNSHIP

The iron formation at the McArthur Power Line location (Figure 27) is one of the best locations to examine the contact relationship between the Deloro and the Tisdale assemblages as it represents semi-continuous exposures of a submarine unconformity. Furthermore, the duration of deposition of this middle iron formation is constrained by new geochronology collected in 2006 and 2007 under the Targeted Geoscience Initiative (TGI-3). The underlying felsic volcanics yielded a U-Pb age of 2728.1 ±1.6 Ma (*see* Figures 25 and 26), whereas felsic volcanic rocks directly overlying the iron formation yielded a U-Pb age of 2724.5 ±2.1 Ma (Houlé, unpublished data). The exposures on the power line consist of, from base to top: felsic volcanics; basal sulphide facies banded iron formation (BIF); silicate-facies-bearing BIF; oxide facies BIF; heterolithic debris flow; and oxide-sulphide facies BIF.

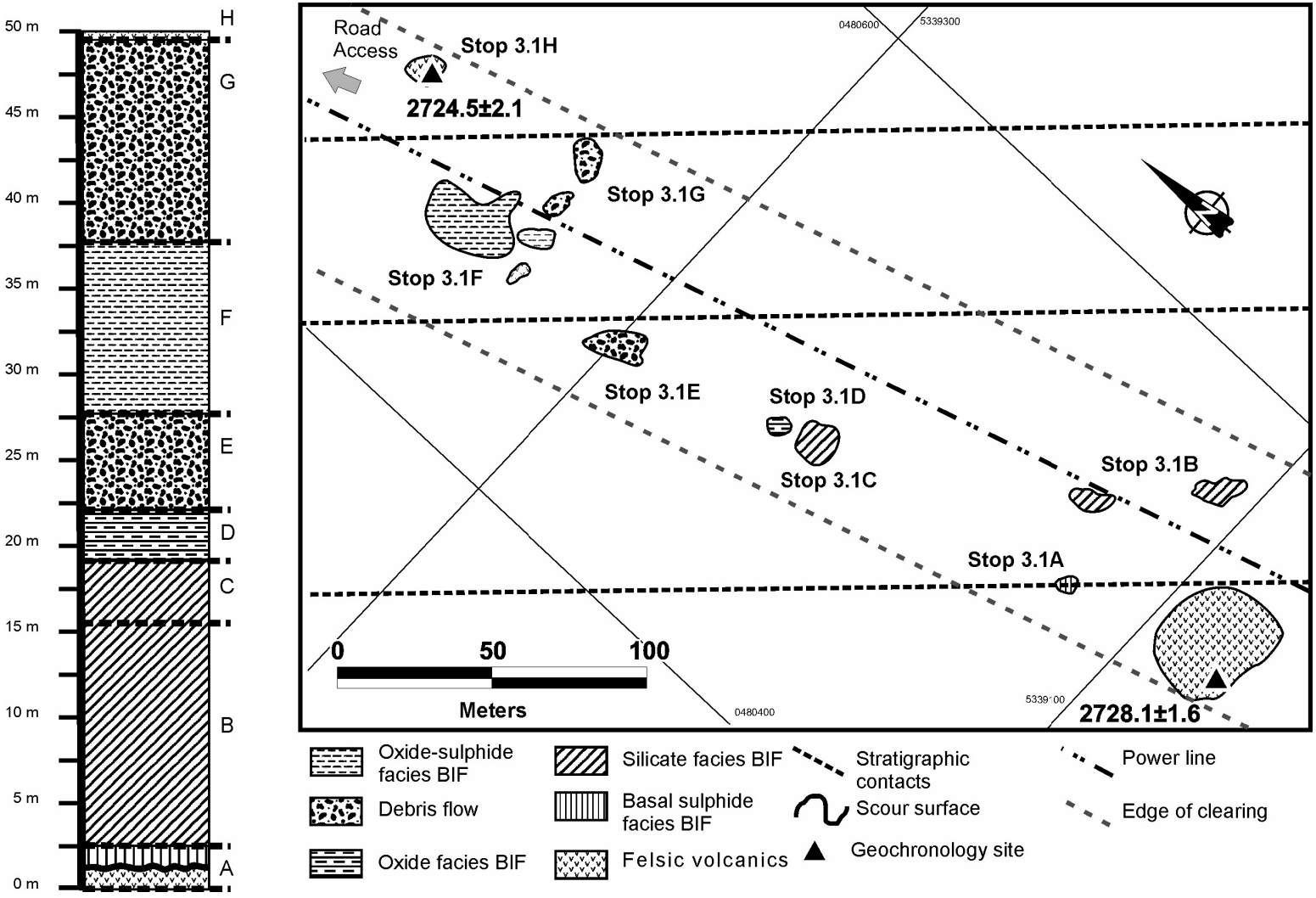

Figure 27. Geology and stratigraphic column (by G. Baldwin) of the Power Line outcrops (stops 3.1A to 3.1G) in McArthur Township, Bartlett Dome area.

Stop 3.1A: Basal sulphide facies BIF

This stop consists of felsic volcaniclastic rocks and the overlying basal sulphide BIF that marks the beginning of the volcanic hiatus during which this iron formation was deposited (*see* Figure 27). The upper surface of the felsic volcanic unit is somewhat undulose and is interpreted as a wavy, scoured surface based on termination of individual laminae. No apparent angularity is observed between bedding trends in the volcanic rocks and the iron formation. Iron formation at this location consists of heavily rusted sulphide facies iron formation, comprising pyritic layers less than 1 cm thick intercalated with chert layers (crystalline silica with a sugary texture) up to 4.75 cm thick. In thin section, this iron formation was found to consist solely of pyrite and quartz, which suggests the chert may be a primary precipitate, in contrast to the chert in the other units in this section.

Stop 3.1B: Silicate facies BIF

This outcrop consists of silicate facies BIF and is separated from the basal sulphide facies by a gap of about 22 m in the section (*see* Figure 27). It demonstrates a number of changes in the type of iron formation deposited. This unit consists of centimetre- or meter-scale alternations of silicate, oxide (magnetite) and sulphide facies material. In contrast to Stop 3.1A, all chert from this outcrop and higher in the stratigraphy is interpreted to be silicified ash, based on petrographic observation. Some units within this outcrop in fact appear to be extensively silicified pillows, now largely silica with minor muscovite. The upper chert units in this outcrop still exhibit relict ash textures resulting from a lower intensity of silification. Iron-rich layers generally consist of oxides (magnetite) and sulphides (pyrite). However, several discrete layers of green iron-silicate are found throughout the outcrop and are locally up to 10 cm thick. Fine layers of siderite have also been observed in thin sections of samples from this outcrop, indicating a full range of iron mineral facies at this outcrop.

Stop 3.1C/D: Silicate facies to oxide facies BIF

These two outcrops mark the upper part of the silicate facies BIF and its transition to an oxide facies BIF. The lowermost outcrop of these exposures (*see* Figure 27, outcrop 3.1C) contains a series of discrete iron silicate layers, each generally thicker than any other BIF layer observed at this locality. Following a 4 m gap in exposure, the silicate facies BIF are no longer observed, and approximately 0.4 m up-stratigraphy, sulphide minerals are no longer seen (outcrop 3.1D). Outcrop 3.1D is solely oxide facies BIF, therefore outcrop 3.1D marks the lowermost occurrence of the exclusively oxide facies BIF at this locality. The lower part of the oxide BIF unit is dominated by chert layers with minor oxide (magnetite) layers. These chert layers exhibit small flame structures along the contact between thick chert layers and thin (mm scale) oxide layers separating them, and are interpreted as syn-sedimentary deformation. This indicates a sufficient pre-lithification history to allow for water to escape between soft sediment layers. Like the cherts in Stop 3.1B, cherts here contain significant amounts of fine-grained muscovite, indicating the possibility of a silicified ash. Outcrop 3.1C/D at this stop consists of a more oxide-rich BIF, with the uppermost bands marking a return of sulphide facies BIF.

Stop 3.1E: Heterolithic debris flow

This outcrop consists of unbedded, ungraded heterolithic tuff breccia with clasts of mixed origin. On the basis of these attributes, this tuff breccia is interpreted as debris flows formed via multiple

sources, indicated by the heterolithic nature of this unit. The lowermost unit is an unbedded, ungraded tuff breccia, about 1.6 m thick, containing quartz-phyric felsic volcanic clasts, as well as minor clasts of sulphides. This debris flow is overlain by close to 4 m of sulphide and oxide facies BIF. Sawn slabs and thin sections reveal parts of this "BIF" are chert breccia consisting of angular chert fragments in an iron mineral matrix. Above the BIF/ chert breccia, another debris flow is found, this one containing chert clasts and other features that suggest that the underlying BIF was an errosional source for this particular debris flow.

Stop 3.1F: Oxide-sulphide facies BIF

There is an exposure gap of about 32 m between Stops 3.1E and 3.1F. However, regional mapping (Houlé 2006) indicates the gap is underlain by felsic volcanic rock. Due to the limited exposure, this lithology has not been included in the composite stratigraphic section for this locality. This particular felsic volcanic does not contain any visible fragments, and is massive, gray, and quartz-rich. It is uncertain whether this is a flow or volcanogenic sediment. Above this volcanic interruption, BIF deposition recurs, with the iron formation being dominated by oxides (magnetite) and sulphides (pyrite). Chert represents an estimated 50% of the bands counted, however the chert bands are considerably thicker than the iron layers. The chert layers range up to 15 cm in thickness, while iron-rich layers are either poorly defined in thickness or are much thinner (generally <1 cm in thickness), sometimes clustering into millimetre-scale alternations of chert-oxide to form pseudo-thick layers of iron oxides. Lower in the stratigraphy at this stop, thin layers of unsilicified ash are found, similar to the upper stratigraphy of Stop 3.1B. This is not observed in higher stratigraphy; however extensive syn-sedimentary folding is seen with only local disturbance of bedding.

Stop 3.1G: Heterolithic debris flow

This uppermost unit of the SIZ in this section (about 10 to 12 m thick) contains two more debris flows. No clasts are observed, at the base of the first debris flows but, near the top, several plagioclase-phyric and sulphide clasts are visible. Following a 2 m gap, sulphide-oxide-silicate facies iron formation is observed, characterized by thick layers of sulphide facies iron formation. Between two of these sulphide-bearing layers is a 40 cm medium-grained mass flow, which is largely equigranular except for a couple of chert grains near the top of the layer. Above this layer the remainder of the section is dominated by oxide and chert facies BIF. The thicker chert layers contain coarse magnetite grains dispersed within the layer, indicating the possibility of silicification of iron formation precursors. The scour at the top of this section is inferred to be the top of the iron formation at this location.

Stop 3.1H: Felsic volcaniclastic rocks

Above the iron formation are quartz-phyric heterolithic fragmental volcanic rocks. These rocks bear minor sulphides, and have been dated at 2724.5 ± 2.2 (Houlé, unpublished data). The relatively large error is considered to be the result of inheritance, with the inclusion of slightly older zircons, but this age correlates well with others that occur regionally above the middle iron formation horizons (Ayer et al. 2005; van Breemen et al. 2006) and a more precise age of 2722.6 ± 0.9 Ma in the felsic volcanic unit immediately underlying the uppermost iron formation at Texmont (Houlé, unpublished data).

STOP 3.2: KOMATIITE FLOWS AT SERPENTINE MOUNTAIN

The Serpentine Mountain area contains some of the most spectacular exposures of komatiitic rocks, in terms of their degree of preservation of cooling and crystallization features. Numerous flows have been identified on seven outcrops through a thick sequence of komatiites, exposed over a distance of approximately 350 m (Figure 28, inset). Individual flows range in thickness from 1 to at least 8 m; however, the exact number of flows within the sequence and the maximum thickness are uncertain because of the thick overburden that masks much of the outcrop. None of the komatiitic flows have the well-organized textural internal zonation of those documented at Pyke Hill. Generally, the flows contain only fine-grained to coarse-grained random olivine spinifex zones that overlie their olivine cumulate zones. All seven outcrops contain sub-concordant spinifex-textured sills that cross-cut their host olivine cumulate. Two specific areas will be visited during this field trip - outcrops 3.2A and 3.2B (*see* Figure 28, inset) - because they have abundant and magnificent spinifex-textured sills.

Stop 3.2A: Komatiite flows with spinifex-textured sills

A detailed map was made by the authors of a manually stripped and cleaned outcrop that contains several komatiite sills (*see* Figure 28). The host differentiated flow is at least about 6 m thick and is composed of an olivine cumulate zone, overlain by a spinifex-textured zone, which in turn is overlain by a flow-top breccia having characteristic polyhedral jointing.

The olivine meso- to orthocumulate is composed of equant, 0.05 to 0.1 cm diameter, euhedral and subhedral crystals of altered olivine. The contact between the spinifex zone and cumulate zone of the komatiite is sharp. The approximately 1.5 m thick olivine spinifex zone is composed of unoriented blades that tend to decrease in size toward the stratigraphic top. Within this zone, the spinifex blades are up to 21 cm in length. Some of the blades are preferentially oriented normal to the flow top. Overlying the spinifex zone, a 20 cm thick breccia having a gradational contact with the spinifex zone was observed. Field observation and petrography suggest that the breccia is a flow-top breccia overprinted by a non-penetrative tectonic fabric. Some rounded clasts (5 to 30 cm in length) having centimetre-scale margins are found in the spinifex zone, and more rarely in the cumulate zones.

Conformable and semi-conformable spinifex-textured komatiite sills intrude the cumulate zone of the host flow. The sills range from 3 to 24 cm in thickness and are bordered by conspicuous centimetre-scale grey layers that stand out in relief against the light-green-colored cumulate rocks. These layers vary from 0 to 2 cm in thickness and are composed of equant olivine crystals. Spinifex textures within the sills are composed of blades of altered olivine approximately 1 to 5 mm in thickness, ranging in length from 0.5 to 4 cm and are oriented at relatively high angles to the intrusive contacts. They occur as individual crystals or “booklets” of crystals and their distribution is non-uniform and asymmetric with respect to upper and lower sill contacts. Sills can have their larger spinifex crystals near their stratigraphic top, middle or base.

Stop 3.2B: Thick spinifex-textured sill

The host flow at this stop is an olivine cumulate (at least 4 m thick) cut by several spinifex-textured sills that range from 0.02 to 1.5 m in thickness, with the thinner ones occurring lower within the flow. In this outcrop, the thinner komatiite sills are quite similar to the sills previously described at Stop 3.2A. However, the thick komatiite sill here is very different and exhibits an extreme textural variation and complexity, having spinifex olivine zones organized with respect to its contacts.

This komatiite sill exhibits a more complex textural variation (Figure 29) than a typical spinifex-textured zone of a komatiite lava flow. The sill is composed of, from base to top: a roughly 45 cm thick, coarse, random spinifex zone; a roughly 70 cm thick, very coarse, aligned platy spinifex zone; and a medium-grained, roughly 35 cm thick random spinifex zone. The lower margin of the komatiite sill is largely obscured by deformation, however, locally platy 0.5 cm long olivine crystals are aligned parallel to the sill contact. The overlying coarse random spinifex zone consists of dendritic, platy, and fan-shaped olivine crystals that are up to 20 cm in length and approximately 0.5 cm wide. The aligned platy spinifex zone has crystals over 30 cm in length and about 0.01 cm wide, which are organized into sheaves. Locally it contains decimetre-scale patches of the coarse random spinifex olivine. The lower boundary is sharp and has a wavy geometry that appears to be related to the termination of the fan-shaped sheaves of olivine crystals. The overlying random spinifex zone is composed of bladed olivine crystals that are up to 2 cm long and about 0.01 cm wide. This zone also contains decimetre- to metre-scale blocks of host rock olivine cumulate material in sharp contact with the spinifex-textured sill interior.

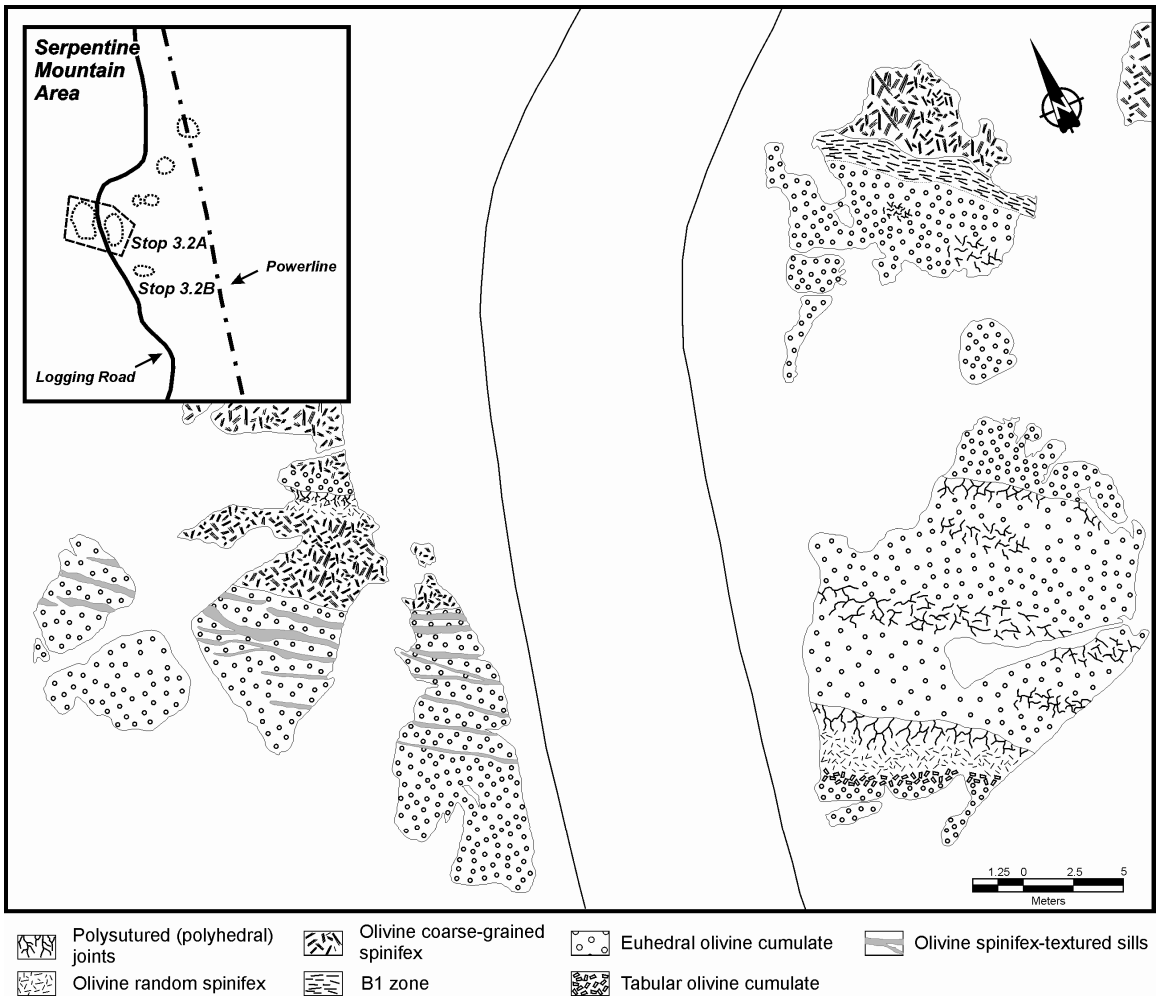

Figure 28. Geology of Stop 3.2A at Serpentine Mountain in McArthur Township (*modified after* Atkinson 1999; Houlé et al., in press).

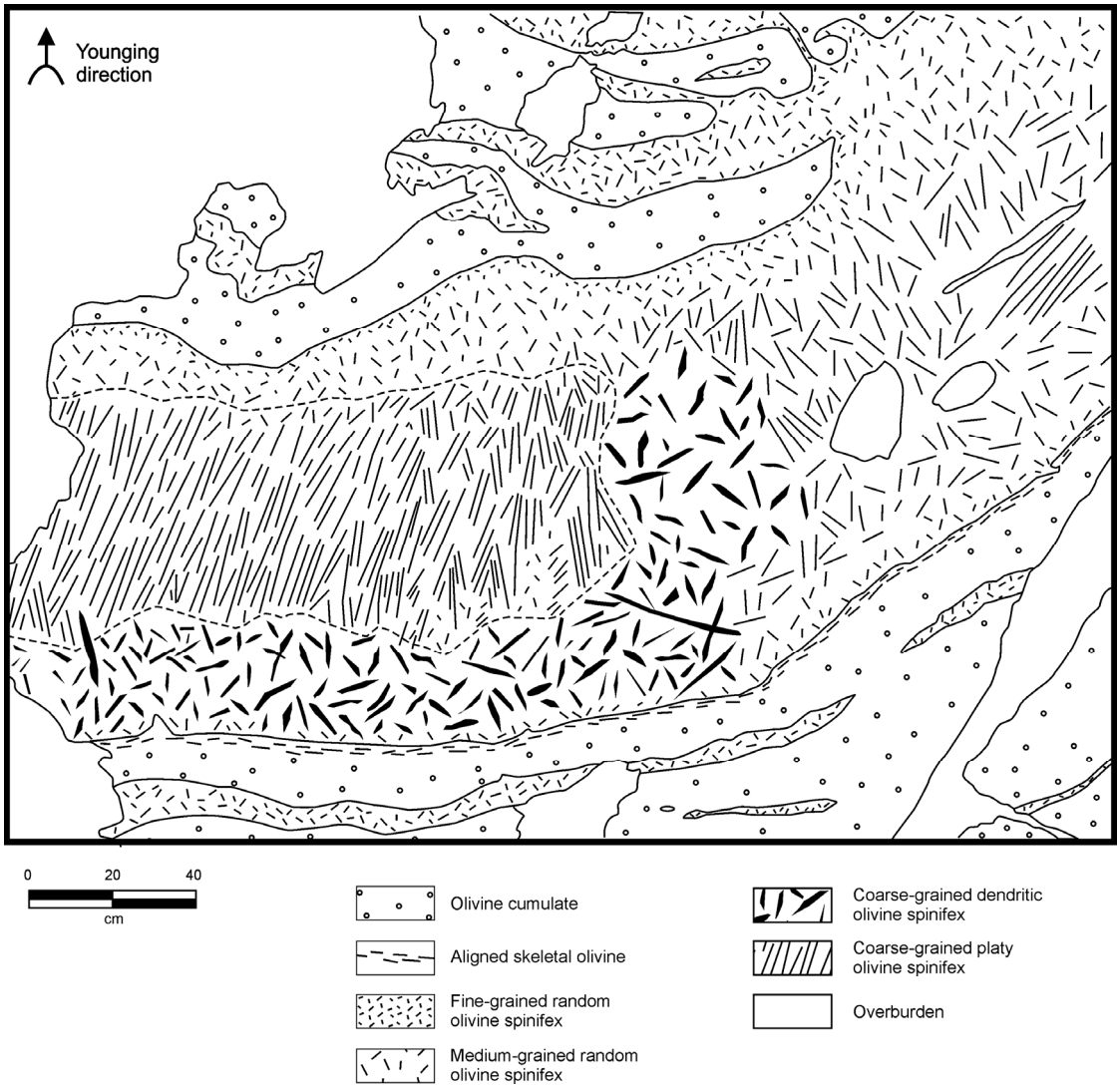

Figure 29. Detailed geological map of Stop 3.2B at Serpentine Mountain, McArthur Township (Houlé et al., in press).

Lunch

PM: Insights from Bartlett and English Townships

STOP 3.3: DELORO–TISDALE ASSEMBLAGES CONTACT AT THE TEXMONT MINE

The Texmont Mine has historic resources reported at 3.19 Mt grading 0.92% Ni (Leigh 1971, but not NI 43-101 compliant). It is located at the boundary between Geikie and Bartlett townships, about 35 km south of Timmins. It is a Type II (Mt. Keith-style), komatiite-associated Ni-Cu-(PGE) deposit, where the Fe-Cu sulphide mineralization occurs as disseminated and blebby sulphides within a thick cumulate komatiite flow. The hanging wall of the deposit is composed of numerous thin differentiated komatiite flows (spinifex/cumulate), whereas the footwall rocks consist of iron formation and felsic volcanic rocks of the Deloro assemblage.

After discovery in 1951, the Texmont Mine underwent several drilling programs and underground development until it ceased limited production in 1972. In 2006, Fletcher Nickel Inc. started an exploration program to determine the size and grade of the remaining ore at the former mine, and the potential for increasing the mineral reserves.

Stop 3.3A: Upper iron formation

Iron formation at the Texmont Mine site (Figure 30, Stop 3.3A2) is part of the upper iron formation within the Deloro assemblage in the Bartlett Dome area. It has been studied in a series of bush outcrops around the site, and rough correlations have been carried out leading to the interpretation that it consists of two relatively thin iron formations.

The lower iron formation at this locality is best exposed as a breccia of white, tabular chert clasts in an outcrop south of the old bunkhouse site. The matrix of this chert breccia is dominantly magnetite with some sulphide clasts as well. This outcrop is correlated with outcrops in and north of the road entering the mine site, which consists of mixed carbonate and oxide facies BIF with two thin (5 cm and 20 cm, respectively) layers of chert breccia within relatively undisturbed BIF (only seen in the outcrop in the clearing to the north of the road).

The upper iron formation at this locality is found south of the road (also behind the old bunkhouse) approximately 30 m down-dip of the chert breccia of the lower iron formation . It overlies plagioclase-phyric sulphidized felsic volcaniclastic rocks. In this area the BIF is mixed oxide-sulphide facies iron formation with high levels of supergene weathering in sulphide layers. On the north side of the road, to the left of the old headframe, another outcrop consists of carbonate facies iron formation with black chert, possibly of hydrothermal origin.

Stop 3.3B: Komatiite flows of the Tisdale assemblage

The base of the Tisdale assemblage is exposed on the Texmont Mine site. Here, after a small gap in the exposure, several outcrops of cumulate komatiite occur just above the iron formation outcrops seen at the previous stop (3.3A).

The komatiites outcrop in low, flat surfaces that exhibit well-preserved cumulate textures locally intermixed with variable degrees of serpentinization, talcose alteration, and carbonatization of the ultramafic rocks. Small outcrops containing 2 to 5 cm randomly oriented blades of olivine spinifex-textureed komatiites were mapped in this area by Pyke (1975).

Nickel mineralization at this site has been divided into six lenses, referred to as “A” Zone, “B” Zone, “C” Zone, “D” Zone, South Zone, and North Zone, within a thick unit of komatiite cumulate (Coad 1979). The South Zone is defined by numerous surface diamond-drill holes and also by underground drilling (Pyke 1978). This second largest ore zone is locally exposed at surface and Fletcher Nickel Inc. have recently improved the exposure the South Zone by mechanical stripping and cleaning.

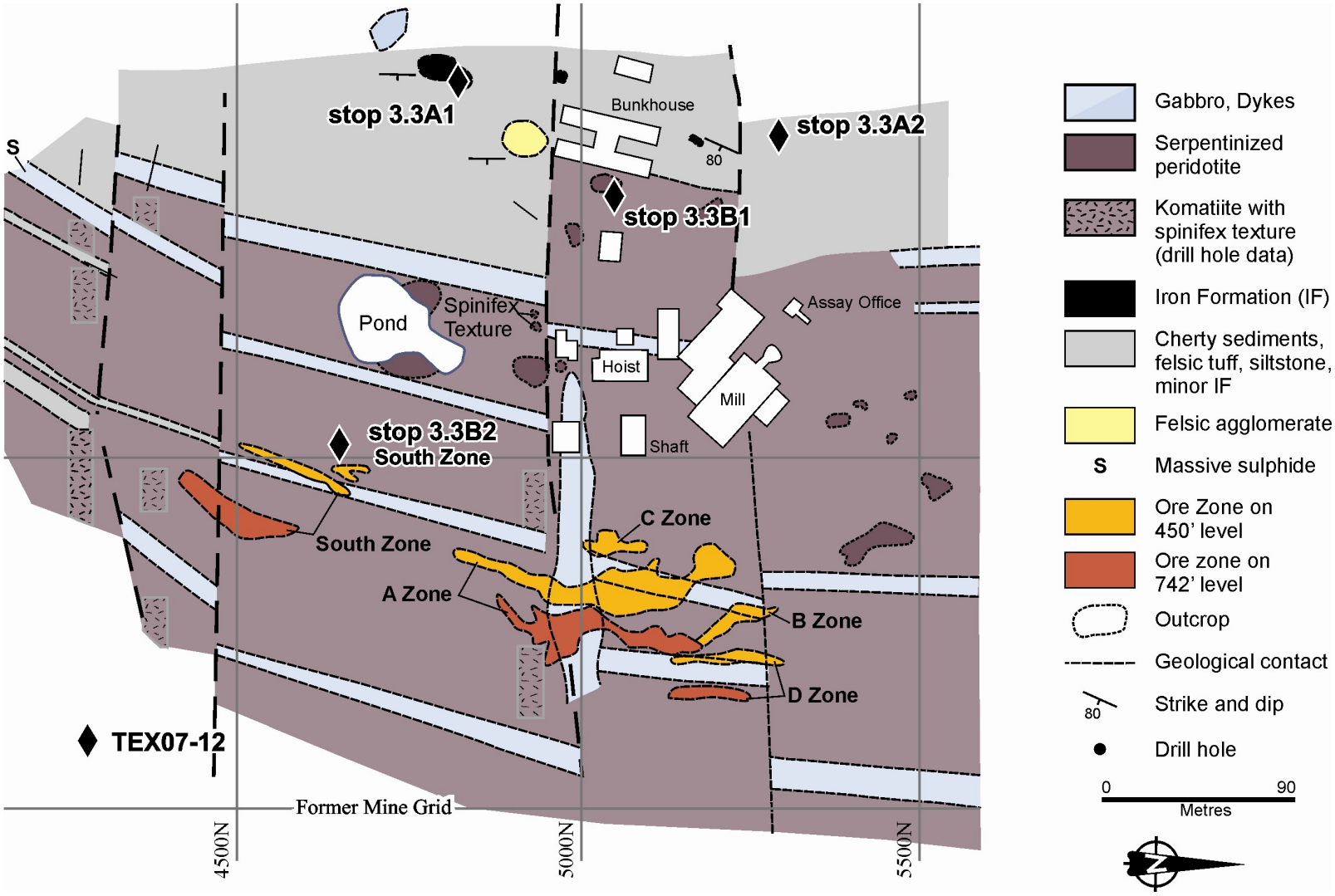

Figure 30. Geology of the former Texmont Mine near the Bartlett–Geikie township boundary, showing the surface expression of several orebodies from two different levels (450' and 742' level) and locations of stops 3.3A and 3.3B (*after* Pyke 1978a; Coad 1979).

STOP 3.4: ENGLISH TOWNSHIP: SUBMARINE UNCONFORMITY

This outcrop is the discovery outcrop for research on the relationship between the contact of the Deloro and Tisdale assemblages This series of outcrops represents a section through the upper iron formation unit of the Deloro SIZ, and supports the contention of a disconformable contact between the two assemblages. This stop will consist of examination of all rock types in the section described below, with several stations from the base to the top of the unit over a short distance (Figure 31).

Important features in this series of exposures that contribute to the notion of a disconformable contact between the Deloro and Tisdale assemblages are:

- The transition from chert breccia to wacke and chert (Stop 3.4B) indicates that the chert breccia was syn-sedimentary (van Kranendonk 2006).
- The transition from bedded chert to chert breccia (Stop 3.4B) clearly indicates the provenance of chert within chert breccias.
- The scoured contact between the wacke-conglomerate unit (Stop 3.4F) and the overlying rhyolitic fragmental unit (Stop 3.4G) is a local-scale unconformity of possible regional importance (Thurston et al. 2007)
- The upward transition from andesitic and rhyolitic fragmental units (Stop 3.4A) represents the end of relatively normal volcanism, succeeded by a volcanic hiatus with direct precipitation of hydrothermal chert.
- The presence of a mass flow unit sourced from a hydrothermal breccia (Stop 3.4A) indicates that the period of volcanic hiatus was already well underway prior to the deposition of bedded chert and chert breccia.

Stop 3.4A: Felsic to intermediate flows

Coherent rhyolitic and andesitic flows and fragmental units totaling roughly 95 m in thickness are poorly exposed in several small outcrops.

Stop 3.4B: Chert breccia

This stop comprises approximately 3 m of a unit consisting mainly of silicic volcanic clasts and chert. The subrounded to angular clasts range from 4 to 45 cm within an iron-rich matrix that consists dominantly of carbonate with minor magnetite, sulphide, and iron silicates. This unit, based on its unbedded, ungraded nature, appears to be a debris flow (McPhie et al. 1993). The angular nature of the clasts and the cherty nature of some clasts suggest that the largely volcanic source included hydrothermal chert and iron minerals similar to those described by van Kranendonk (2006).

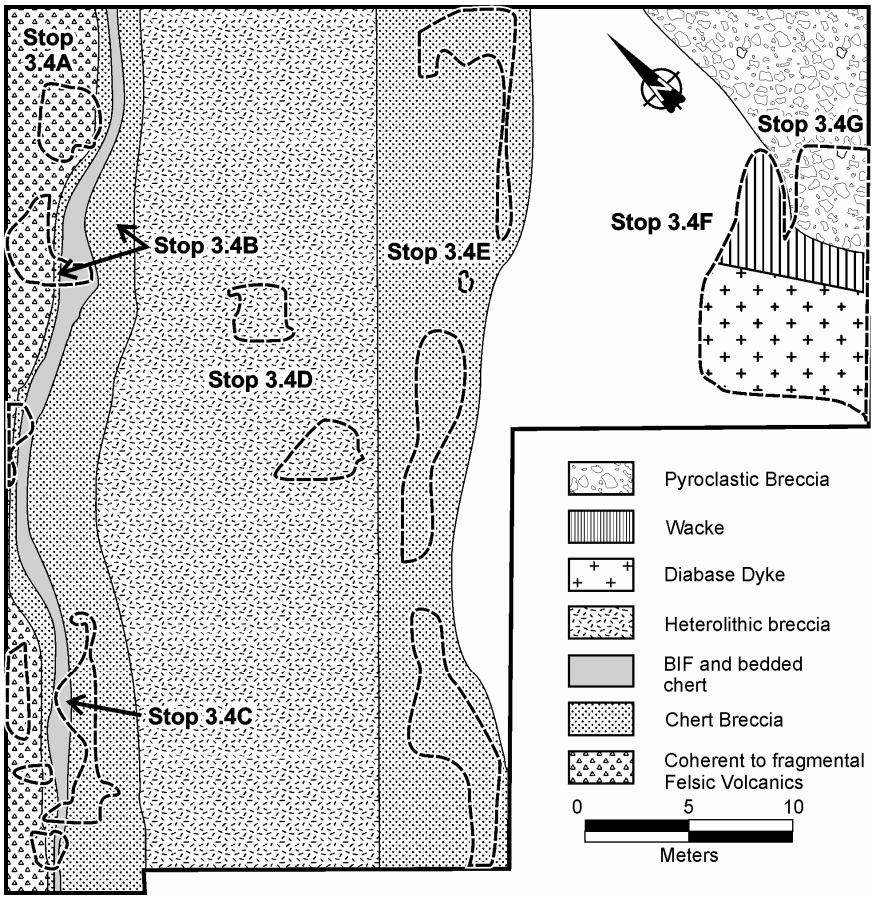

Figure 31. Geological map (by G. Baldwin) of the sedimentary interface zone (SIZ) exposed in English Township, Bartlett Dome area, and locations of stops 3.4A to 3.4G.

Photo 3. Transition from chert breccia upward to bedded chert illustrating the syn-sedimentary nature of the production of chert breccia (from Stop 3.4B).

Stop 3.4C: Bedded chert and BIF

This stop examines bedded chert with bed thicknesses ranging from approximately 1 to 10 cm with intercalations of pyritic wacke less than 1 cm thick, forming a unit about 3 m thick. The unit includes about 30% classic oxide facies iron formation. It grades upward into minor lenses of chert breccia consisting of centimetre-scale chert fragments in a cherty matrix. Some syn-depositional slump folds are observed. Some lenses of chert breccia are observed overlain by wacke and bedded chert. No evidence of a precursor felsic tuff or wacke is present in this chert unit, leading to the conclusion that here the chert represents the product of precipitation (van den Boorn et al. 2007). The lower and upper portions of this unit are chert breccias in a dominantly iron carbonate matrix. Chert clasts are tabular and up to 5 cm long. The lower chert breccia is approximately 30 cm thick, and is in direct contact with an overlying BIF layer. The upper chert breccia is thicker (approximately 1.5 m) and contains clasts, up to 50 cm thick, of volcanic origin near the top of the unit.

Stop 3.4D: Heterolithic pyroclastic breccia

A 6 to 8 m thick unit of heterolithic, unbedded, ungraded pyroclastic breccia, dacitic to andesitic in bulk composition, with subangular fragments of varying rock types, including minor sulphide clasts and inter-fragment quartz infilling is investigated at this stop.

Stop 3.4E: Chert breccia

A roughly 4 m unit of unbedded, non-graded chert breccia consisting of angular chert fragments up to 10 to 15 cm by 1 to 2 cm, in a matrix consisting of magnetite, biotite, quartz and feldspar is exposed at this stop. Based on the occurrence of this style of brecciation enclosed within the bedded cherts and wackes, we interpret this breccia to represent syn-sedimentary dewatering (see Krapez et al. 2003; van Kranendonk 2006).

Stop 3.4F: Pebble conglomerate and wacke

This stop examines exposures of 3 m of conglomerate interbedded with wacke beds a few centimetres thick. Clasts are dominated by chert fragments. The wacke consists of bright green amphibole, garnet, quartz and feldspar. The upper part of the unit displays the erosional truncation of several beds, overlain by a heterolithic rhyolitic pyroclastic breccia.

Stop 3.4G: Pyroclastic breccia

A 10 to 15 m thickness of rhyolitic pyroclastic breccia is exposed at this stop, consisting of uniform feldspar-phyric fragments displaying variable amounts of vesicularity and phenocryst content. The unit is unbedded and non-graded and is thus interpreted as a debris flow.

References

Allen, R.L. 1986. Petrology and chemistry of a komatiite sill and Fe-Ni-Cu sulfide mineralization, Munro and Beatty townships, Ontario; unpublished MSc thesis, Queen's University, Kingston, Ontario, 108p.

Arndt, N.T. 1975. Ultramafic rocks of Munro Township and their volcanic setting; unpublished PhD thesis, University of Toronto, Toronto, Ontario, 296p.

Arndt, N.T. 1977. Thick, layered peridotite-gabbro lava flows in Munro Township, Ontario; Canadian Journal of Earth Sciences, v. 14, p. 2620-2637.

Arndt, N.T. 1986. Differentiation of komatiite flows; Journal of Petrology, v.27, p.279-301.

Arndt, N.T. 1986. Spinifex and swirling olivines in komatiite lava lake, Munro township, Canada; Precambrian. Research, v. 34, p. 139-155.

Arndt, N.T., Naldrett, A.J. and Pyke, D.R. 1977. Komatiitic and Fe-rich tholeiitic lavas of Munro Township, northeastern Ontario; Journal of Petrology, v.18, p.319-369.

Atkinson, B.T. 1999. Geology and mineral potential of the Serpentine Mountain area, Timmins; *in* Summary of Field Work and Other Activities 1999, Ontario Geological Survey, Open File Report 6000, p.13-1 to 13-8.

Ayer, J.A., Amelin, Y., Corfu, F., Kamo, S.L., Ketchum, J.W.F., Kwok, K. and Trowell, N. 2002. Evolution of the southern Abitibi greenstone belt based on U-Pb geochronology: autochthonous volcanic construction followed by plutonism, regional deformation and sedimentation; Precambrian Research, v.115, p.63-95.

Ayer, J.A., Chartrand, J.E., Grabowski, G.P.B., Josey, S., Rainsford, D.R.B. and Trowell, N.F. 2006. Geological compilation of the Cobalt–Temagami area, Abitibi greenstone belt; Ontario Geological Survey, Preliminary Map P.3581, scale 1:100 000.

Ayer, J.A., Dubé, B., Goodfellow, W.D., Ross, P.-S., Bleeker, W., Taylor, B.E., Peter, J.M., Grunsky, E.C., Hillary, B., Thurston, P.C., Berger, B.R., Houlé, M.G., Beakhouse, G.P., Trowell, N.F., Snyder, D.B., McNicoll, V.J., Keating, P., Percival, J.A., Mercier-Langevin, P., Lauzière, K., Paradis, S.J., Goutier, J., Dion, C., Pilote, P., Legault, M., Monecke, T., Dumont, R., Brouillette, P., Gosselin, P. and van Breemen, O. 2007. The Abitibi greenstone belt: update of the Precambrian Geoscience Section program, the Targeted Geoscience Initiative III Abitibi and Deep Search projects; *in* Summary of Field Work and Other Activities 2007, Ontario Geological Survey, Open File Report 6213, p.3-1 to 3-44.

Ayer, J.A., Thurston, P.C., Bateman, R., Dubé, B., Gibson, H.L., Hamilton, M.A., Hathway, B., Hocker, S.M., Houlé, M.G., Hudak, G., Ispolatov, V.O., Lafrance, B., Lesher, C.M., MacDonald, P.J., Péloquin, A.S., Piercey, S.J., Reed, L.E. and Thompson, P.H. 2005. Overview of results from the Greenstone Architecture Project: Discover Abitibi Initiative; Ontario Geological Survey, Open File Report 6154, 175p.

Bandyayera, D., Rhéaume, P., Doyon, J. and Sharma, K.N.M. 2004. Géologie de la région du lac Hébert ; Ministère des Ressources naturelles et de la Faune du Québec, RG 2003-07, 57p.

Barr, E. 2005. Porcupine Joint Venture internal report.

Barrie, C. T., Naldrett, A.J. and Davis, D.W. 1990. Geochemical constraints on the genesis of the Montcalm gabbroic complex and Ni-Cu deposit, western Abitibi Subprovince, Ontario; Canadian Mineralogist, v.28, p.451-474.

Barrie, C.T. and Corfu, F. 1999. The Kidd–Munro Extension Project: results of U-Pb geochronology for Year 1; *in* Summary of Field Work and Other Activities 1998, Ontario Geological Survey, Miscellaneous Paper 169, p.74-81.

Barrie, C.T. 1998. The Kidd–Munro Extension Project: Year 2 Report (unpublished report).

Barrie, C.T. 1999. The Kidd–Munro Extension Project: Year 3 Report (unpublished report).

Barrie, C.T. and Davis, D.W. 1990. Timing of magmatism and deformation in the Kamiskotia–Kidd Creek area, western Abitibi Subprovince, Canada; Precambrian Research, v.46, p.217-240.

Barrie, C.T., Corfu, F., Davis, P.C., Coutts, A.C. and MacEachern, D. 1999. Geochemistry of the Dundonald komatiite-basalt suite and genesis of Dundeal Ni deposit, Abitibi Subprovince, Canada; Economic Geology, v.94, p.845-866.

Bateman, R. and Bierlein, F.P. 2006. On Kalgoorlie (Australia), Timmins–Porcupine (Canada), and factors in intense gold mineralization; Ore Geology Reviews, v.32, p.187-206.

Bateman, R., Ayer, J., Dubé, B. and Hamilton, M.A. 2005. The Timmins–Porcupine gold camp, northern Ontario: the anatomy of an Archaean greenstone belt and its gold mineralization: Discover Abitibi Initiative; Ontario Geological Survey, Open File Report 6158, 90p.

Benn, K. and Peschler, A. P. 2005. A detachment fold model for fault zones in the Late Archean Abitibi greenstone belt; Tectonophysics, v.400, p.85-104.

Berger, B., Ayer, J., McNicoll, V.J. and Bleeker, W. 2007. The Kidd–Munro Project: stratigraphy of the Kidd–Munro assemblage in Prosser Township and area based on geology, geochemistry and new geochronology; *in* Summary of Field Work and Other Activities 2007, Ontario Geological Survey, Open File Report 6213, p.5-1 to 5-8.

Bickle, M.J., Nisbet, E.G. and Martin, A. 1994. Archean greenstone belts are not oceanic crust; Journal of Geology, v.102, p.121-138.

Bleeker, W. 1999. Structure, stratigraphy and primary setting of the Kidd Creek volcanogenic massive sulphide deposit: a semiquantitative reconstruction; Economic Geology Monograph, v.10, p.71-122.

Bleeker, W., Parrish, R.R. and Sager-Kinsman, S. 1999. High-precision U-Pb geochronology of the late Archean Kidd Creek deposit and surrounding Kidd volcanic complex; Economic Geology Monograph, v.10, p.43-69.

Bohlke, J.K. 1988. Carbonate-sulphide equilibria and "stratabound" disseminated epigenetic gold mineralization: a proposal based on examples from Alleghany, California, U.S.A.; Applied Geochemistry, v.3, p.499-516.

Born, P. 1995. A sedimentary basin analysis of the Abitibi greenstone belt in the Timmins area, northern Ontario, Canada; unpublished PhD dissertation thesis, Carleton University, Ottawa, Ontario, 489p.

Brereton, W.E. 2004. A report to NI 43-101 Standards on the Timmins area nickel properties of the Legendary Ore Mining Corporation to be acquired by Canadian Arrow Mines Ltd., Ontario, Canada; MPH Consulting Ltd., unpublished report, 70p.

Brisbin, D.I. 1997. Geological setting of gold deposits in the Porcupine gold camp, Timmins, Ontario; unpublished PhD thesis, Queen's University, Kingston, Ontario, 52p.

Butler, H.R. 2007. Technical (geological) report on the Texmont and Bartlett-English properties: Bartlett, Geikie, English, and Zavitz townships, porcupine Mining Division, Ontario, Canada; Fletcher Nickel Inc., unpublished report, 75p.

Catuneanu, O. 2003. Sequence stratigrapy of clastic systems; Geological Association of Canada, Short Course Notes, v.16, 248p.

Chown, E.H., Daigneault, R., Mueller, W. and Mortensen, J.K. 1992. Tectonic evolution of the northern volcanic zone, Abitibi belt, Québec; Canadian Journal of Earth Sciences, v.29, p.2211-2225.

Coad, P.R. 1979. Nickel sulphide deposits associated with ultramafic rocks of the Abitibi belt and economic potential of mafic-ultramafic intrusions; Ontario Geological Survey, Study 20, 84p.

Cole, G. 2007. Mineral resource estimation for the Redstone Nickel Mine in Ontario, Canada, Report prepared for Liberty Mines Inc; SRK Consulting Inc., unpublished report, 89p.

Corfu, F. and Noble, S.R. 1992. Genesis of the southern Abitibi greenstone belt, Superior Province, Canada: evidence from zircon Hf isotope analyses using a single filament technique; Geochimica et Cosmochimica Acta, v.56, p.2081-2097.

Corfu, F., Krogh, T.E., Kwok, Y.Y. and Jensen, L.S. 1989. U-Pb geochronology in the south-western Abitibi greenstone belt, Superior Province; Canadian Journal of Earth Sciences, v.26, p.1747-1763.

Daigneault, R., Mueller, W.U. and Chown, E.H. 2004. Abitibi greenstone belt plate tectonics: a history of diachronic arc development, accretion and collision; *in* Eriksson, K.A., Altermann, W., Nelson, D.R., Mueller, W., Catuneanu, O. and Strand, K. (eds.), The Precambrian Earth: Tempos and Events, Developments in Precambrian Geology, Amsterdam, Elsevier, p.88-103.

Davis, P.C. 1997. Volcanic stratigraphy of the late Archean Kidd–Munro assemblage in Dundonald and Munro townships and genesis of associated nickel and copper-zinc volcanogenic massive sulfide deposits, Abitibi greenstone belt, Ontario, Canada; unpublished MSc thesis, University of Alabama, Tuscaloosa, Alabama, 201p.

DeWolfe, Y.M. 2004. Volcanic reconstruction of the Archean north rhyolites, Kidd Creek Mine, Timmins Ontario, Canada; unpublished MSc thesis, Laurentian University, Sudbury, Ontario, 149p.

Dimroth, E., Imreh, L., Goulet, N. and Rocheleau, M. 1983. Evolution of the south-central segment of the Archean Abitibi belt, Quebec. Part II: Tectonic evolution and geomechanical model; Canadian Journal of Earth Sciences, v.20, p.1355-1373.

Dimroth, E., Imreh, L., Rocheleau, M. and Goulet, N. 1982. Evolution of the south-central part of the Archean Abitibi belt, Quebec. Part I: Stratigraphy and paleogeographic model; Canadian Journal of Earth Sciences, v.19, p.1729-1758.

Dinel, E. 2007. Structural, geochemical and host rock control on gold mineralization in tholeiitic volcanic rock of the Tisdale assemblage, Timmins, Ontario: the Hoyle Pond mine and the Vipond V10b unit; unpublished PhD thesis, University of Ottawa, Ottawa, Ontario, 282p.

Dinel, E., Fowler, A.D., Ayer, J., Still, A., Tylee, K. and Barr, E., in press. Litho-geochemical and stratigraphic controls on gold mineralization within the meta-volcanic rocks of the Hoyle Pond Mine, Timmins, Ontario; Economic Geology.

Dubé, B., Mercier-Langevin, P., Hannington, M.D., Lafrance, B., Gosselin, G. and Gosselin, P. 2007. The LaRonde Penna world-class Au-rich volcanogenic massive sulfide deposit, Abitibi, Québec: mineralogy and geochemistry of alteration and implications for genesis and exploration; Economic Geology, v.102, p.633-666.

Dubé, B., Mercier-Langevin, P., Hannington, M.D., Davis, D.W. and Lafrance, B. 2004. Le gisement de sulfures massifs volcanogènes aurifères LaRonde, Abitibi, Québec : altération, minéralisation, genèse et implications pour l'exploration; Ministère des Ressources naturelles, de la Faune et des Parcs, Québec, MB 2004-03, 122p.

Dubé, B., Williamson, K. and Malo, M. 2003. Gold mineralization within the Red Lake Mine trend; example from the Cochenour–Willans Mine area, Red Lake, Ontario, with new key information from the Red Lake Mine and potential analogy with the Timmins Camp; *in* Geological Survey of Canada, Current Research no. 2003-C21, 15p.

Duke, J.M. 1986. Petrology and economic geology of the Dumont Sill: an Archean intrusion of komatiitic affinity in northwestern Québec;Geological Survey of Canada, Economic Geology Report, v.35, 56p.

Dunbar, W.R. 1948. Structural relations of the Porcupine Ore deposits (Ontario); *in* Canadian Ore Deposits, Canadian Institute of Mining and Metallurgy, Montréal, v.1, p.442-456.

Ferguson, S.A., Buffman, B.S.W., Carter, O.F., Griffis, A.T., Holmes, T.C., Hurst, M.E., Jones, W.A., Lane, H.C. and Longley, C.S. 1968. Geology and ore deposits of Tisdale Township; Ontario Department of Mines, Geological Report 58, 177p., accompanied by Map 2075, scale 1"=1000'.

Fowler, A.D., Berger, B., Shore, M., Jones, M.I. and Ropchan, J. 2002. Supercooled rocks: development and significance of varioles, spherulites, dendrites and spinifex in Archaean volcanic rocks, Abitibi Greenstone belt, Canada; Precambrian Research, v.115, p.311-328.

Fowler, A.D., Jensen, L.S. and Péloquin, S.A. 1987. Varioles in Archean basalts: products of spherulitic crystallization; Canadian Mineralogist, v.25, p.275-289.

Franklin, J.M., Gibson, H.L., Jonasson, I.R. and Galley, A.G. 2005. Volcanogenic Massive Sulfide Deposits; Economic Geology, 100th Anniversary Volume, p.523-560.

Galley, A.G., Pilote, P. and Davis, D.W. 2003. Gold-related, subvolcanic, Mooshla intrusive complex, Bousquet mining district, Quebec; *in* Program with Abstracts, Geological Association of Canada–Mineralogical Association of Canada, Joint Annual Meeting, 2003, v.28.

Gamble, A.P.D. 2000. Geology of the Potter Cu-Zn-Co-Ag VMS mineralization and exploration progress report to March 31, 2000 at Millstream Mines Ltd. Potter Mine Exploration project; Dave Gamble Geoservices Inc., 80p.

Gibson, H.L. 1989. The mine sequence of the central Noranda volcanic complex: geology, alteration massive sulphide deposits and volcanological reconstruction; unpublished PhD thesis, Carleton University, Ottawa, Ontario, 715p.

Gibson, H.L. 1998. A petrographic and geochemical study of the Potter Mine and interpretation on its volcanic environment, Munro Township, Ontario; unpublished report, Millstreams Mines Ltd.

Gibson, H.L. and Gamble, A.P.D. 2000. A reconstruction of the volcanic environment hosting Archean seafloor and subseafloor VMS mineralization at the Potter Mine, Munro Township, Ontario, Canada; *in* Volcanic Environments and Massive Sulfide Deposits, Centre for Ore Deposit Research, University of Tasmania, Hobart, Tasmania, CODES Special Publication 3, p.65-66.

Gibson, H.L. and Watkinson, D.H. 1990. Volcanogenic massive sulphide deposits of the Noranda Cauldron and shield volcano, Quebec; *in* Rive, M., Verpaelst, P., Gagnon, Y., Lulin, J.-M., Riverin, G. and Simard, A. (eds.), The Northwestern Quebec Polymetallic Belt: A Summary of 60 Years of Mining Exploration, Canadian Institute of Mining and Metallurgy, Special Volume 43, p.119-132.

Giovenazzo, D. 2000. Section 3B – Minéralisation nickelifères dans le secteur La Motte-Vassan : La mine Marbridge ; Ministère des Ressources naturelles du Québec, MB 2000-09, p.73-75.

Gole, M.J., Barnes, S.J. and Hill, R.E.T. 1990. Partial melting and recrystallization of Archean komatiites by residual heat from rapidly accumulated flows; Contributions to Mineralogy and Petrology, v.105, p.704-714.

Good, D.J. 1989. Platinum group element distribution in the Kanichee intrusion, District of Nipissing; Ontario Geological Survey, Open File Report 5705, 42p.

Good, D.J. and Crocket, J.H. 1999. Geology of the Mann intrusive complex and evidence for Pt-rich hydrothermal platinum-group elements; Economic Geology Monograph, v.10, p.613-625.

Goodwin, A.M. 1965. Mineralized volcanic complexes in the Porcupine–Kirkland Lake–Noranda region, Canada; Economic Geology, v.60, p.955-971.

Goodwin, A.M. 1979. Archean volcanic studies in the Timmins–Kirkland Lake–Noranda region of Ontario and Quebec; Geological Survey of Canada, Bulletin 278, 51p.

Goutier, J. 1997. Géologie de la région de Destor ; Ministère des Ressources naturelles du Québec, RG 96-13, 37p.

Goutier, J. and Melançon, M. 2007. Compilation géologique de la Sous-province de l'Abitibi (version préliminaire) ; Ministère des Ressources naturelles et de la Faune, Québec, échelle 1/500 000, http://www.mrn.gouv.qc.ca/mines/geologie/geologie-projets.jsp.

Goutier, J., Rhéaume, P. and Davis, D.W. 2004. Géologie de la région du lac Olga (32F/14) ; Ministère des Ressources naturelles et de la Faune, RG 2003-09, 40p.

Graton, L.C., McKinstry, H.E. and others 1933. Outstanding features of Hollinger geology; *in* The Transactions of the Canadian Institute of Mining and Metallurgy and of the Mining Society of Nova Scotia, v.36, p.1-21.

Griffis, A.T. 1962. A geological study of the McIntyre Mine; The Canadian Mining and Metallurgical Bulletin, v.55, p.76-83.

Hall, L.A.F. and Smith, M.D. 2002. Precambrian geology of Denton and Carscallen townships, Timmins West area; Ontario Geological Survey, Open File Report 6093, 75p.

Hall, L.A.F., MacDonald, C.A. and Dinel, E.R. 2003. Precambrian geology of Deloro Township; Ontario Geological Survey, Preliminary Map P.3528, scale 1: 20 000.

Hart T.R., Gibson, H.L. and Lesher, C.M. 2004. Trace element geochemistry and petrogenesis of felsic volcanic rocks associated with volcanogenic Cu-Zn-Pb sulfide deposits; Economic Geology, v.99, p.1003-1013.

Hathway, B., Hudak, G.J. and Hamilton, M.A. 2005. Geological setting of volcanogenic massive sulphide mineralization in the Kamiskotia area: Discover Abitibi Initiative; Ontario Geological Survey, Open File Report 6155, 81p.

Hawke, D.R. 1982. Geology and geochemistry of the kanichee ultramafic intrusion; unpublsihed MSc thesis, Laurentian University, Sudbury, Ontario, 87p.

Heather, K.B. 1998. New insights on the stratigraphy and structural geology of the southwestern Abitibi greenstone belt: implications for tectonic evolution and setting of mineral deposits in the Superior Province; *in* The First Age of Giant Ore Formation: Stratigraphy, Tectonic and Mineralization in the Late Archean and Early Proterozoic, Toronto, Prospectors and Developers Association of Canada Annual Convention, Toronto, Abstracts Volume, p.63-101.

Heather, K.B. 2001. The geological evolution of the Archean Swayze greenstone belt, Superior Province, Canada; unpublished PhD thesis, Keele University, United Kingdom, 370p.

Heather, K.B., Shore, G.T. and van Breemen O. 1995. The convoluted "layer-cake": an old recipe with new ingredients for the Swayze greenstone belt, southern Superior Province; *in* Current Research 1995-C, Geological Survey of Canada, p.1-10.

Hodgson, C.J. 1983. The structure and geological development of the Porcupine camp - a re-evaluation; *in* The Geology of Gold in Ontario, Ontario Geological Survey, Miscellaneous Paper 110, p.211-225.

Houlé, M.G. 2006. Geological and mineral potential of McArthur Township in the Bartlett Dome, Abitibi greenstone belt; *in* Summary of Field Work and Other Activities 2006, Ontario Geological Survey, Open File Report 6192, p.6-1 to 6-14.

Houlé, M.G. and Hall, L.A.F. 2007. Geological compilation of the Shaw Dome area, northeastern Ontario; Ontario Geological Survey, Preliminary Map P.3595, scale 1:50 000.

Houlé, M.G. and Solgadi, F. 2007. Geological and mineral potential of Bartlett and Geikie townships in the Bartlett dome, Abitibi greenstone belt; *in* Summary of Field Work and Other Activities 2007, Ontario Geological Survey, Open File Report 6213, p.7-1 to 7-15.

Houlé, M.G., Gibson, H.L., Lesher, C.M., Davis, P.C., Cas, R.A.F., Beresford, S.W. and Arndt, N.T., in press. Komatiitic basalt sills and multi-generational peperite at Dundonald Beach, Abitibi greenstone belt, Ontario: implications for komatiite volcanic-subvolcanic architecture and seafloor-subseafloor nickel sulfide distribution; Economic Geology.

Houlé, M.G., Fowler, A.D., Préfontaine, S. and Gibson, H.L. 2006. Endogenous growth in komatiite lava flows: evidence from spinifex-textured sills at Pyke Hill and Serpentine Mountain, western Abitibi greenstone belt, Ontario; *in* Program with Abstract, GAC-MAC Annual Meeting, Montréal, Québec.

Houlé, M.G., Hall, L.A.F. and Tremblay, E. 2004. Precambrian geology of Eldorado and Adams townships; Ontario Geological Survey, Preliminary Map P.3542, scale 1:20 000.

Houlé, M.G., Lesher, C.M., Gibson, H.L. and Sproule, R.A. 2002. Recent advances in komatiite volcanology in the Abitibi greenstone belt, Ontario; *in* Summary of Field Work and Other Activities 2002, Ontario Geological Survey, Open File Report 6100, p.7-1 to 7-19.

Hurst. M.E. 1935. Vein formation at Porcupine, Ontario; Economic Geology, v.30, p.103-127.

Ispolatov, V.O., Lafrance, B., Dubé, B., Hamilton, M.A. and Creaser, R.A. 2005. Geology, structure, and gold mineralization, Kirkland Lake and Larder Lake areas (Gauthier and Teck townships): Discover Abitibi Initiative; Ontario Geological Survey, Open File Report 6159, 170p.

Jackson, S.L. and Fyon, J.A. 1991. The western Abitibi Subprovince in Ontario; *in* Geology of Ontario, Ontario Geological Survey, Special Volume 4, Part 1, p.405-482.

Jackson, S.L., Fyon, J.A. and Corfu, F. 1994. Review of Archean supracrustal assemblages of the southern Abitibi greenstone belt in Ontario, Canada: products of micro-plate interactions within a large-scale plate-tectonic setting; Precambrian Research, v.65, p.183-205.

Jensen, L.S. and Langford, F.F. 1985. Geology and petrogenesis of the Archean Abitibi belt in the Kirkland Lake area, Ontario; Ontario Geological Survey, Miscellaneous Paper 123, 130p.

Johnstone, R.M. 1991. The geology of the northwestern Black River–Matheson area, District of Cochrane; Ontario Geological Survey, Open File Report 5785, 288p.

Johnstone, R.M. 1987. Geology of the Stoughton–Roquemare Group, Beatty and Munro townships, northeastern Ontario; unpublished MSc thesis, Carleton University, Ottawa, Ontario, 325p.

Ketchum, J., Ayer, J., van Breemen, O., Pearson, N.J., O'Reilly, S.Y. and Becker, J.K., in press. Pericratonic crustal growth of the southwestern Abitibi subprovince, Canada; Economic Geology.

Krapez, B., Barley, M.E. and Pickard, A.L. 2003. Hydrothermal and resedimented origins of the precursor sediments to banded iron formation: sedimentological evidence from the Early Palaeoproterozoic Brockman supersequence of Western Australia; Sedimentology, v.50, p.979-1011.

Lafrance, B., Davis, D.W., Goutier, J., Moorhead, J., Pilote, P., Mercier-Langevin, P., Dubé, B., Galley, A.G. and Mueller, W.U. 2005. Nouvelles datations isotopiques dans la portion québécoise du Groupe de Blake River et des unités adjacentes ; Ministère des Ressources naturelles et de la Faune du Québec, RP 2005-01, 9p.

Lafrance, B., Moorhead, J. and Davis, D.W. 2003. Cadre géologique du camp minier de Doyon-Bousquet-Laronde ; Ministère des Ressources naturelles, de la Faune et des Parcs du Québec, ET 2002-07, 43p., 1 map.

Lafrance, B., Mueller, W.U., Daigneault, R. and Dupras, N. 2000. Evolution of a submerged composite arc volcano: volcanology and geochemistry of the Normetal volcanic complex, Abitibi greenstone belt, Quebec, Canada; Precambrian Research, v.101, p.277-311.

Leigh, O.E. 1971. Texmont Mine Ltd., Bartlett and Geikie townships property; *in* Statement of Material Facts, filed with Ontario Securities Commission February 29, 1972, AFRO# 63.2951, NTS 42 A/11, assessment file AFRI# 42A11NE0056.

Lesher, C.M. 1989. Komatiite-associated nickel sulphide deposits; Reviews in Economic Geology, v.4, p.44-101.

Lesher, C.M., Goodwin, A.M., Campbell, I.H. and Gorton, M.P. 1986. Trace-element geochemistry of ore-associated and barren, felsic metavolcanic rocks in the Superior Province, Canada; Canadian Journal of Earth Sciences, v.23, p.222-237.

Lowe, D.R., Byerly, G.R. and Heubeck, C. 1999. Structural divisions and development of the west-central part of the Barberton Greenstone Belt; *in* Lowe, D.R. and Byerly, G.R. (eds.), Geologic Evolution of the Barberton Greenstone Belt, South Africa, Geological Society of America, Special Paper 329, p.37-82.

McPhie, J., Doyle, M. and Allen, R. L. 1993. Volcanic textures: a guide to the interpretation of textures in volcanic rocks; Centre for Ore Deposit and Exploration Studies, University of Tasmania, Hobart, Tasmania, 197p.

Mercier-Langevin, P., Dubé, B., Hannington, M.D., Davis, D.W. and Lafrance, B. 2004. Contexte géologique et structural des sulfures massifs volcanogènes aurifères du gisement LaRonde, Abitibi ; Ministère des ressources naturelles, de la Faune et des Parcs du Québec, ET 2003-03, 49p.

Mercier-Langevin, P., Dubé, B., Hannington, M.D., Davis, D.W., Lafrance, B. and Gosselin, G. 2007a. The LaRonde Penna Au-rich Volcanogenic Massive Sulfide Deposit, Abitibi Greenstone Belt, Quebec: Part I. Geology and Geochronology; Economic Geology, v.102, p.585-609.

Mercier-Langevin, P., Dubé, B., Hannington, M.D., Richer-Lafleche, M. and Gosselin, G. 2007b. The LaRonde Penna Au-rich volcanogenic massive sulfide deposit, Abitibi greenstone belt, Quebec: Part II. Lithogeochemistry and paleotectonic setting; Economic Geology, v.102, p.611-631.

Miall, A.D. 1994. Sequence stratigraphy and chronostratigraphy: problems of definition and precision in correlation, and their implications for global eustasy; Geoscience Canada, v.21, p.1-26.

Michol, K. 2004. Volcanology of the Croesus Mine area, Munro Township, Abitibi, Ontario; unpublished BSc thesis, University of Ottawa, Ottawa, Ontario, 78p.

Ministère de l'Énergie et des Ressources and Ontario Geological Survey 1984. Lithostratigraphic map of the Abitibi Subprovince; Ontario Geological Survey and Ministère de l'Énergie et des Ressources, Québec, Map 2484 and DV 83-16, scale 1:500 000.

Mitchum, R. M., Jr. 1977. Seismic stratigraphy and global changes of sea level: Part 11. Glossary of terms used in seismic stratigraphy; Memoir, American Association of Petroleum Geologists, 1977, Issue 26, p.205-212.

Mortensen, J.K. 1993. U-Pb geochronology of the eastern Abitibi Subprovince. Part 1: Chibougamau–Matagami–Joutel region; Canadian Journal of Earth Sciences, v.30, p.11-28.

Mueller, W. 1991. Volcanism and related slope to shallow marine volcaniclastic sedimentation: an Archean example, Chibougamau, Quebec, Canada; Precambrian Research, v.49, p.1-22.

Mueller, W.U. and Mortensen, J.K. 2002. Age constraints and characteristics of subaqueous volcanic construction, the Archean Hunter Mine Group, Abitibi greenstone belt; Precambrian Research, v.115, p.119-152.

Oliver, J.L., Rebagliati, C.M. and Haslinger, R.J. 1999. Summary exploration report - Potter Mine property, Munro Township, Ontario for the HDG Potter Exploration Limited Partnership of Hunter Dickinson Group Inc. and Millstream Mines Limited; Hunter Dickinson Group Inc., unpublished company report, p.1-1 to 11-3.

Péloquin, A.S., Houlé, M.G. and Gibson, H.L. 2005. Geology of the Kidd–Munro assemblage in Munro Township, and the Tisdale and Lower Blake River assemblages in Currie Township: Discover Abitibi Initiative; Ontario Geological Survey, Open File Report 6157, 94p.

Pickard, A.L., Barley, M.E. and Krapez, B. 2003. Deep-marine depositional setting of banded iron formation: sedimentological evidence from interbedded clastic sedimentary rocks in the early palaeoproterozoic Dales Gorge member of Western Australia; Sedimentary Geology, v.170, p.37-62.

Pilote, P. 2006. Métallogenie de l'extrémité est de la sous-province de l'Abitibi; *in* Pilote, P. (ed.), Le camp minier de Chibougamau et le parautochtone Grenvillien : métallogénie, métamorphisme et aspects structuraux, Livret-guide d'excursion B1, Geological Association of Canada, 138p.

Pyke, D.R. 1978a. Geology of the Redstone River area, District of Timiskaming; Ontario Division of Mines, Geological Report 161, 75p. Accompanied by Map 2363 and Map 2364, scale 1:31 680.

Pyke, D.R. 1978b. Geology of the Peterlong Lake area, districts of Timiskaming and Sudbury; Ontario Geological Survey, Report 171, 53p.

Pyke, D.R. 1982. Geology of the Timmins area, District of Cochrane; Ontario Geological Survey, Report 219, 141p.

Pyke, D.R., Naldrett, A.J. and Eckstrand, A.P. 1973. Archean ultramafic flows in Munro Township, Ontario; Geological Society of America Bulletin, v.84, p.955-978.

Rhys, D.A. 2003. Report on January-February 2003 structural studies of the Hoyle Pond Mine, Timmins, Ontario, Porcupine Joint Venture; unpublished company report, 36p.

Robert, F. 2000. World-class greenstone belt deposits and their exploration; *in* 31st International Geological Congress, August 2000, Rio de Janeiro, Brasil, Vol. de Presentaciones, CD-ROM, doc. SG304a, 4p.

Robert, F. and Poulsen, K.H. 1997. World-class Archaean gold deposits in Canada: an overview; Australian Journal of Earth Sciences, v.44, p.329-351.

Robert, F. 2003. Giant gold deposits of the Abitibi greenstone belt; *in* Western Australia Gold Giants and Global Gold Giants, M.Sc. Short Course, Perth, Western Australia, February 6-7, 2003, p.81-90.

Robert, F. and Brown, A.C. 1986. Archean gold-quartz veins at the Sigma mine, Abitibi greenstone belt, Québec. Part I: Geologic relations and formation of the vein system; Economic Geology, v.81, p.578-592.

Roberts, R.G. and Morris, J.H. 1982. The geologic setting of the Upper Beaver mine, Kirkland Lake District, Ontario: a copper-gold deposit in mafic volcanic rocks, *in* Hodder, R.W. and Petruk, W. (eds.), Geology of Canadian Gold Deposits, Canadian Institute of Mining and Metallurgy, Special Volume 24, p.73-82.

Ropchan, J.R., Luinstra, B., Fowler, A.D., Benn, K., Ayer, J., Berger, B., Dahn, R., Labine, R. and Amelin, Y. 2002. Host-rock and structural controls on the nature and timing of gold mineralization at the Holloway Mine, Abitibi Subprovince, Ontario; Economic Geology, v.97, p.291-309.

Sanborn-Barrie, M., Skulski, T. and Parker, J. 2001. Three hundred million years of tectonic history recorded by the Red Lake greenstone belt, Ontario; *in* Current Research Part C19, Geological Survey of Canada, p.1-19.

Saumur, B.-M. 2005. The variolitic intermediate lobate breccia of the V10B flow unit (Vipond Formation, Abitibi greenstone belt): a detailed study at the Fire-tower outcrop, Schumacher Ontario; unpublished BSc thesis, University of Ottawa, Ottawa, Ontario, 69p.

Scott, C.R., Mueller, W.U. and Pilote, P. 2002. Physical volcanology, stratigraphy and lithogeochemistry of an Archean volcanic arc: evolution from plume-related volcanism to arc rifting of SE Abitibi greenstone belt, Val-d'Or, Canada; Precambrian Research, v.115, p.223-260.

Shore, M. 1996. Cooling and crystallization of komatiite flows; unpublished PhD thesis, University of Ottawa, Ottawa, Ontario, 211p.

Shore, M. and Fowler, A.D. 1999. The origin of spinifex texture in komatiites; Nature, v.397, p.691-693.

Simony, P.S. 1964. Geology of northwestern Timagami area, District of Nipissing; Ontario Department of Mines, Geological Report 28, 30p.

Sproule, R.A., Lesher, C.M., Ayer, J.A., Thurston, P.C. and Arndt, N.T. 2004. Nd isotope geochemistry of 2750–2701 Ma komatiitic rocks in the Abitibi greenstone belt, Canada; Geological Association of Canada–Mineralogical Association of Canada, Annual Meeting, St. Catherines, Ontario.

Sproule, R.A., Lesher, C.M., Houlé, M.G., Keays, R.R., Ayer, J.A. and Thurston, P.C. 2005. Chalcophile element geochemistry and metallogenesis of komatiitic rocks in the Abitibi greenstone belt, Canada; Economic Geology, v.100, p.1169-1190.

Stone, W.E., Crocket, J.H., Fleet, M.E. and Larson, M.S. 1996. PGE mineralization in Archean volcanic systems: geochemical evidence from thick, differentiated mafic-ultramafic flows, Abitibi greenstone belt, Ontario, and implications for exploration; Journal of Geochemical Exploration, v.56, p.237-263.

Tardif, N.P., Gibson, H.L., Whitehead, R.E.S., MacDonald, C.A. and Gamble, A.P.D. 2000. Subaqueous fire-fountaining, hyaloclastite and massive sulphide mineralization; presentation, Ontario Prospectors Association, Northeastern Ontario Mines and Minerals Symposium, April 18-19, Kirkland Lake, Ontario.

Thériault, R.D. and Fowler, A.D. 1996. Gravity driven and in situ fractional crystallization processes in the Centre Hill Complex, Abitibi Subprovince, Canada: evidence from bilaterally-paired cyclic units; Lithos, v.39, p.41-55.

Thompson, P.H. 2005. A new metamorphic framework for gold exploration in the Timmins–Kirkland Lake area, western Abitibi greenstone belt: Discover Abitibi Initiative; Ontario Geological Survey, Open File Report 6162, 104p.

Thurston, P.C., Ayer, J. and Goutier, J. 2007. New stratigraphic and structural influences on development of structure and related base metal mineralization in the Abitibi greenstone belt; *in* Abstracts Volume, Prospectors and Developers Association of Canada, 75th Annual Meeting, Toronto, Ontario, March 4-7.

Thurston, P.C., Ayer, J.A., Goutier, J. and Hamilton, M.A., in press. Depositional gaps in Abitibi greenstone belt stratigraphy: a key to exploration for syngenetic mineralization; Economic Geology.

Trudel, P. 1978. Géologie de la région de Cléricy ; Ministère des richesses naturelles (Québec); report DP-598, 149 p.

Vaillancourt, C., Pickett, C.L. and Dinel, E. 2000. Precambrian geology, Timmins West – Bristol and Ogden townships; Ontario Geological Survey, Preliminary Map P.3436, scale 1:20 000.

van Breemen, O., Heather, K.B. and Ayer, J. 2006. U-Pb geochronology of the Neoarchean Swayze sector of the southern Abitibi greenstone belt; *in* Current Research 2006-F1, Geological Survey of Canada, p.1-32.

van den Boorn, S.H.J.M., van Bergen, M.J., Nijman, W. and Vroon, P.Z. 2007. Dual role of seawater and hydrothermal fluids in Early Archean chert formation: evidence from silicon isotopes; Geology, v.35, p.939-942.

van Kranendonk, M.J. 2006. Volcanic degassing, hydrothermal circulation and the flourishing of early life on Earth: a review of the evidence from c. 3490-3240 Ma rocks of the Pilbara Supergroup, Pilbara Craton, Western Australia; Earth-Science Reviews, v.74, p.197-240.

Zhang, Q.-Z., Machado, N., Ludden, J.N. and Moore, D.M. 1993. Geotectonic constraints from U-Pb ages for the Blake River Group, the Kinojévis Group and the Normétal mine area, Abitibi, Québec; *in* Program with Abstract, Geological Association of Canada–Mineralogical Association of Canada Annual Meeting, p.A114.

Metric Conversion Table

Conversion from SI to Imperial			Conversion from Imperial to SI		
SI Unit	*Multiplied by*	*Gives*	*Imperial Unit*	*Multiplied by*	*Gives*
		LENGTH			
1 mm	0.039 37	inches	1 inch	**25.4**	mm
1 cm	0.393 70	inches	1 inch	**2.54**	cm
1 m	3.280 84	feet	1 foot	**0.304 8**	m
1 m	0.049 709	chains	1 chain	20.116 8	m
1 km	0.621 371	miles (statute)	1 mile (statute)	**1.609 344**	km
		AREA			
1 cm^2	0.155 0	square inches	1 square inch	**6.451 6**	cm^2
1 m^2	10.763 9	square feet	1 square foot	**0.092 903 04**	m^2
1 km^2	0.386 10	square miles	1 square mile	2.589 988	km^2
1 ha	2.471 054	acres	1 acre	0.404 685 6	ha
		VOLUME			
1 cm^3	0.061 023	cubic inches	1 cubic inch	**16.387 064**	cm^3
1 m^3	35.314 7	cubic feet	1 cubic foot	0.028 316 85	m^3
1 m^3	1.307 951	cubic yards	1 cubic yard	0.764 554 86	m^3
		CAPACITY			
1 L	1.759 755	pints	1 pint	0.568 261	L
1 L	0.879 877	quarts	1 quart	1.136 522	L
1 L	0.219 969	gallons	1 gallon	**4.546 090**	L
		MASS			
1 g	0.035 273 962	ounces (avdp)	1 ounce (avdp)	28.349 523	g
1 g	0.032 150 747	ounces (troy)	1 ounce (troy)	**31.103 476 8**	g
1 kg	2.204 622 6	pounds (avdp)	1 pound (avdp)	**0.453 592 37**	kg
1 kg	0.001 102 3	tons (short)	1 ton (short)	**907.184 74**	kg
1 t	1.102 311 3	tons (short)	1 ton (short)	**0.907 184 74**	t
1 kg	0.000 984 21	tons (long)	1 ton (long)	**1016.046 908 8**	kg
1 t	0.984 206 5	tons (long)	1 ton (long)	**1.016 046 90**	t
		CONCENTRATION			
1 g/t	0.029 166 6	ounce (troy)/ ton (short)	1 ounce (troy)/ ton (short)	34.285 714 2	g/t
1 g/t	0.583 333 33	pennyweights/ ton (short)	1 pennyweight/ ton (short)	1.714 285 7	g/t

OTHER USEFUL CONVERSION FACTORS

	Multiplied by	
1 ounce (troy) per ton (short)	31.103 477	grams per ton (short)
1 gram per ton (short)	0.032 151	ounces (troy) per ton (short)
1 ounce (troy) per ton (short)	20.0	pennyweights per ton (short)
1 pennyweight per ton (short)	0.05	ounces (troy) per ton (short)

Note: Conversion factors which are in bold type are exact. The conversion factors have been taken from or have been derived from factors given in the Metric Practice Guide for the Canadian Mining and Metallurgical Industries, published by the Mining Association of Canada in co-operation with the Coal Association of Canada.

ISSN 0826-9580 [print]
ISBN 978-1-4249-6866-4 [print]

ISSN 1916-6117 [online]
ISBN 978-1-4249-6867-1 [PDF]